SYNTHESIS OF THE CONFORMATIONALLY CONTROLLED β–TURN MIMETIC TORSION BALANCE CORE SCAFFOLD

by

Alyssa B. Lypson

B.S. in Biochemistry and Psychology, Allegheny College, 2009

Submitted to the Graduate Faculty of

The Dietrich School of Arts and Sciences in partial fulfillment

of the requirements for the degree of

Master of Science in Organic Chemistry

University of Pittsburgh

2018

UNIVERSITY OF PITTSBURGH

DIETRICH SCHOOL OF ARTS AND SCIENCES

This dissertation was presented

by

Alyssa B. Lypson

It was defended on

January 5, 2018

and approved by

Dennis Curran, PhD, Distinguished Service Professor of Chemistry and Bayer Professor

Seth Horne, PhD, Associate Professor

Dissertation Advisor: Craig S. Wilcox, PhD, Professor

SYNTHESIS OF THE CONFORMATIONALLY CONTROLLED

β-TURN MIMETIC TORSION BALANCE CORE SCAFFOLD

Alyssa B. Lypson, M.S.

University of Pittsburgh, 2018

The molecular torsion balance concept was applied to a new conformationally controlled scaffold to accurately evaluate pairwise amino acid interactions in an antiparallel β-sheet motif. The scaffold's core design combines (*ortho*-tolyl)amide and o,o,o′-trisubstituted biphenyl structural units to provide a geometry better-suited for intramolecular hydrogen bonding. The aim of this study was to develop synthetic methods for the core scaffold and to conduct a preliminary investigation into the improved sequence alignment on upper and lower aromatic rings to promote hydrogen bond formation at the correct distance and antiparallel orientation.

TABLE OF CONTENTS

LIST OF TABLES

LIST OF FIGURES

LIST OF SCHEMES

LIST OF ABBREVIATIONS

Ac	acetyl
ACN	acetonitrile
Ala	alanine
Bn	benzyl
Boc	*tert*-butyloxycarbonyl
[bmim]BF_4	1-butyl-3-methylimidazolium tetrafluoroborate
DBU	1,8-diazabicyclo[5.4.0]undec-7-ene
DCM	dichloromethane
DMF	*N,N'*-dimethylformamide
DMS	dimethylsulfate
DMSO	dimethyl sulfoxide
EI	electron ionization
equiv	equivalents
ESI	electrospray ionization
Et	ethyl
Fmoc	9-fluorenylmethyloxycarbonyl
Gly	glycine
HOBt	1-hydroxybenzotriazole
HRMS	high resolution mass spectrometry
IR	infrared spectroscopy
LRMS	low resolution mass spectrometry
Me	methyl
MS	mass spectrometry
NMR	nuclear magnetic resonance
NOESY	nuclear overhauser effect spectroscopy
Ph	phenyl
Py	pyridine
Q-TOF	quadrupole time-of-flight
ROESY	rotating-frame nuclear overhauses effect correlation spectroscopy
rt	room temperature
SPhos	2-dicyclohexylphosphino-2',6'-dimethoxybiphenyl
TBS-Cl	*tert*-butyldimethylsilyl chloride
TFA	trifluoroacetic acid
THF	tetrahydrofuran
TLC	thin layer chromatography

1.0 INTRODUCTION

1.1 INTRODUCTION TO THE TORSION BALANCE

The concept of a "molecular torsion balance" was introduced in 1994 to describe a tool to examine molecular interactions present in biomolecules.[1] Like a protein folding model, the torsion balance has two configurations. These configurations represent the folded and unfolded states of a protein, and are distinguishable in the original example because of the presence of a gently restricted aryl-aryl bond rotation ($\Delta G^{\ddagger}$ = 14 kcal·mol^{-1}; Figure 1).[1] The original molecular torsion balance featured an asymmetrical top half attached to the bottom half's Tröger's base moiety. The flexibility of the dibenzodiazocine unit allows the needed self-adjustment of distances required to permit attractive non-covalent interactions. The barrier to interconversion separates the conformations into two distinct thermodynamic states with lifetimes that allow for a direct measurement of their ratio by ^{1}H NMR spectroscopy. Intramolecular forces and solvent effects are identified by any deviation of the 1:1 ratio between the two states. The first generation torsion balance in Figure 1 has been utilized to investigate the benzene dimer edge-to-face, aryl- and alkyl-CH-π interactions, and the hydrophobic effect.[1] A second generation balance was later implemented to measure noncovalent interactions in water.[2,3]

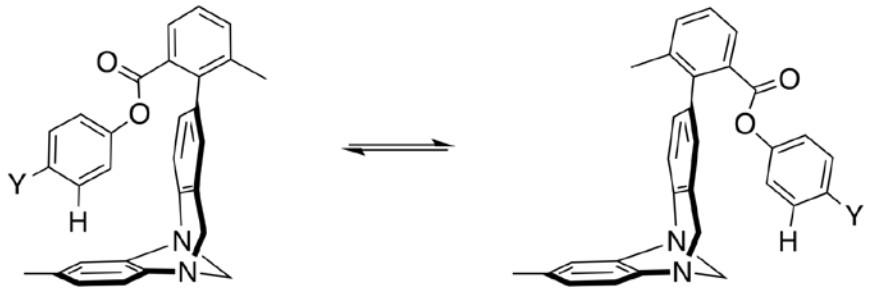

Figure 1. Folded (left) and unfolded (right) conformational states of the first-generation torsion balance.

1.2 DESIGN OF THE CONFORMATIONALLY CONTROLLED TORSION BALANCE PERTINENT TO PEPTIDES

Enzyme and drug-receptor binding rely upon many inter- and intramolecular interactions. Efforts have been made to design secondary protein mimetic structures, such as antiparallel β-sheet mimics[4] that accurately model protein folding.[5-7] Gellman's β-hairpin motif was developed to measure the folding and stability of β-sheets in water. This study provided valuable NMR data to relate the thermodynamic parameters between two conformational states.[5] Nowick and coworkers utilize the incorporation of natural and synthetic amino acids to generate a protein folded state of a β-sheet.[6] Several other studies designed to probe structural aspects of β-motifs, reveal their flexibility by integrating peptidomimetics into β-hairpins and β-sheets.[8]

A peptide torsion balance hybrid (Figure 2) was developed by the Wilcox group to investigate the pair-wise amino acid interactions in anti-parallel orientation of a β-sheet, as well as, short β-strand stability with changes in amino acids.[9] In this case, the dibenzodiazocine torsion balance scaffold was not useful. Modeling indicated that the scaffold did not have the correct

shape to (1) match the ends of an anti-parallel β-sheet and to (2) achieve the configuration required for intramolecular peptidomimetic hydrogen bond formation.

The two-state nature of folding, as shown in Figure 2, was imposed by the restricted rotation around an aryl-nitrogen bond.[10,11] This core structure was developed to mimic a β-turn, and thus allow us to acquire data for implementation in molecular recognition and protein folding models.

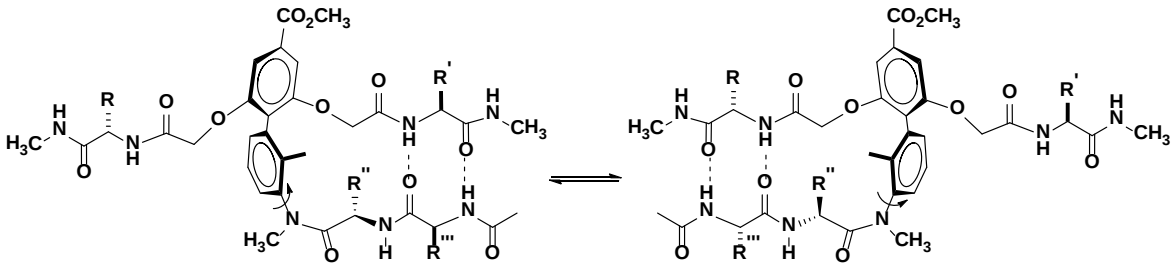

Figure 2. Example of two conformations of the β-turn mimetic torsion balance. The R groups are different and each represents an amino acid side chain.

This design featured the substitution of an *o,o,o'*-trisubstituted biphenyl as our established torsion balance structural unit with an incorporated (*ortho*-tolyl)amide unit. Thus, both the aryl-aryl[11] and N-aryl[10] bonds are sites for bond restriction. Although *ortho*-substituents are mostly responsible for the biaryl bond restriction, the incorporation of m*eta*-substituents are also known to offer a rotational restriction due to a buttressing effect.[11a,b] The *ortho* substituent is well-known to constrain rotation about the N-aryl bond.[10,12] This was reported by Mislow for acyclic and cyclic (*ortho*-tolyl)amides[10] and the Curran group for their study on *o*-haloanilide atropisomers.[11]

Thus, selected protein models were derived from small manipulations of the torsion balance side chains to realize the difference in energies of the pair-wise amino acid interactions. The two *ortho* sites of the top aromatic ring of the biaryl structure were altered to investigate

intramolecular hydrogen bonds and salt-bridge effects (1) by attaching *different amino acids* on each side or (2) by attaching side chains of *different chain lengths*.

Both 1D and 2D NMR analysis indicated the presence of intramolecular hydrogen bonding and salt-bridge formation, in addition to solvent effects. Hydrogen bonding was promoted in toluene-d8.[9] ^{1}H NMR and EXSY experiments were used to calculate the torsion balance rotational barriers. The aryl-aryl bond between the upper and lower halves of the peptide hybrid torsion balance was determined to have a rotational barrier of 35.7 kcal·mol^{-1} at 418 K.[9] The N-aryl bond rotational barrier was calculated to be 20.9 kcal·mol^{-1} at 343 K, while that of the neighboring N-CO bond was only 17 kcal·mol^{-1} at 298 K.[9] Because of the large rotational barrier for the aryl-aryl bond, it was obvious that the rotation of the N-aryl bond was to be responsible for the conformational switch of the balance. Although the scaffold has the overall shape necessary to match with the ends of an anti-parallel β-sheet, further investigation of the torsion balance structure was necessary.

The goal of this project is to study the structure of the previously synthesized balance more closely. Specifically, we planned to investigate the alignment of the *o*-methylene ether side chains of the top half of the balance to promote hydrogen bonding. Modeling suggests that 90˚ (relative to the plane of the aromatic ring) is the best angle to provide alignment. Thus, we proposed the incorporation of bromine atoms *ortho* to the aryl ether and *o*-methylenes. Subsequent 1D and 2D NMR experiments can be utilized to determine if additional intramolecular hydrogen bonding occurs between the amino acids of the torsion balance. The torsion balances of interest are shown in Figure 3.

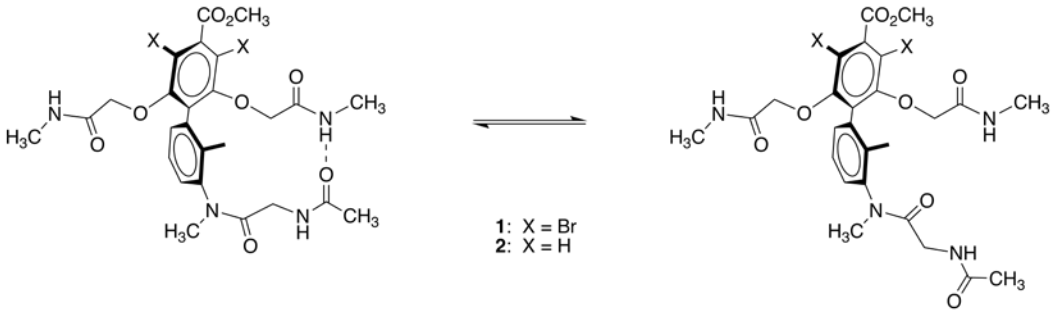

Figure 3. The conformationally controlled β-turn mimetic torsion balance target (**1**) and control analog (**2**). An example of one possible intramolecular hydrogen bonding pattern is shown in the folded state (left).

The structure of **1** and **2** differ by the presence of bromines on the top ring of **1**. Torsion balance **2** was determined to be the best control for the study to evaluate conformational effects from the bromines alone. We hypothesize that **1** will form a stronger hydrogen bond than **2**. This study describes the synthesis toward targets **1** and **2**.

1.3 CONFORMATIONAL RESTRICTION OF SYNTHETIC DRUG TARGETS

Structure-based drug design is often modeled after proteins and enzymes that participate in metabolic and/or cell signaling pathways that relate to disease. Pharmaceuticals are envisioned to inhibit, restore, or modify the structure and behavior of disease-related proteins and enzymes. Protein fragments can be generated synthetically to mimic a protein system as exact copies, or as structurally modified derivatives, by incorporation of nonproteinogenic amino acid residues or by alteration of peptide backbone; however, several challenges have been faced in the area of peptide therapeutics, such as poor bioavailablility, proteolytic stability, and difficult cellular uptake.[13-24] 3D structure elucidation is necessary for the development of new pharmaceuticals and is most

often derived from X-ray crystallography and 2D NMR studies. Such data can provide valuable insights to the significance and nature of a given protein binding event. Structure-based drug design (SBDD) has been successful by incorporating the structural and conformational features of peptides that are necessary for biological activity.

The target protein's well-defined "hotspot", or binding pocket, is linked to a disease-triggering pathway through its interaction with a small molecule or with a second protein or protein substructure. In SBDD, the goal is to optimize ligand structure to fit complementarily in a given binding pocket to disrupt the interaction responsible for the undesired biological cascade. The ligand-enzyme conformational complementarity is crucial for adequate potency and selectivity in synthetic drug targets. Computational methods are relied upon for lead discovery and optimization through applying preferences from the Protein Data Base (PDB) and Cambridge Structural Database (CSD); however, predicting unbound ligand conformation is difficult for structures with rotatable bonds. The guiding principles of Lipinski's small molecule approach to drug discovery are insufficient given the challenge of developing drugs against advanced PPI target classes. Yet, thoughtful consideration of substrate design can ensure conformational stability. Minimizing entropic barriers to intermolecular binding and to constraining intramolecular interactions, within the protein itself, lead to potential benefits such as increased selectivity and potency.

A 2014 investigation by La Plante and coworkers[16] uses a conformational control approach to design hepatitis C polymerase inhibitors. The study was designed to illuminate the effects of the molecular shape and mutual adaptions required to form and maintain bioactivity of a ligand-enzyme pocket binding event. Initially a structural hinge was developed to form a class of diamides that would mimic the reported bioactive conformation; however, 2D NMR studies indicated that additional optimization of the diamide structure was needed. Substitution of the benzimidazole

unit with a more lipophilic indole was verified by 2D NMR analysis to realize their goal. Figure 4 (reproduced from the literature)[16] shows the constrained torsion angles and their folding preferences, as determined from 2D ROESY data. This work indicates how NMR-guided conformational restrictions and scaffold replacements are valuable strategies in drug design.

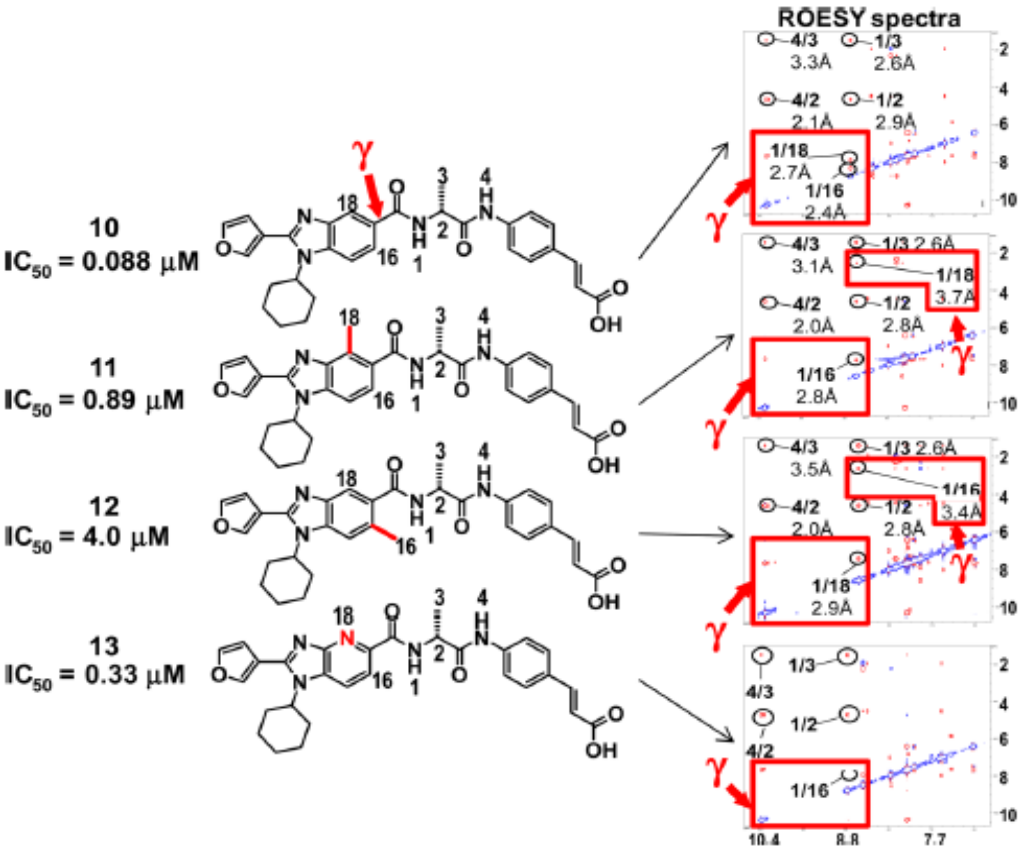

Figure 4. Structures, inhibition activities, and NMR ROESY data for La Plante's redesign of the initial diamide series towards the development of hepatitis C virus polymerase inhibitors (reprinted from the literature).[16] The ROESY data indicates the hydrogen bond distance information and subsequent conformational preference. Copyright (2012) Elsevier Ltd., Canada.

Recent studies on anti-cancer therapeutics report on XIAP, an inhibitor family of interest with recent applications of novel strategies[25-29] for conformational control between a globular protein and a continuous epitope, such as a β-turn. The binding of tetrapeptide AVPI from Smac

to XIAP blocks the XIAP-Caspase 9 interaction that prevents cellular apoptosis.[25] Strategies for conformational restriction have been imposed on the AVPI tetrapeptide through a bicyclic ring system that fuses the heterocycle of Pro to the neighboring Val to form a second ring.[26-27] Monfardini and coworkers[28] developed a strategy to identify inhibitors against XIAP by identifying the anchoring residue (Ala of AVPI) from the bound motif; however, synthetic analogues designed by docking studies exhibited limited potency. With the goal of improving drug-like properties of lead compounds, Pellechia[29] applied fragment-based design methods to XIAP, where virtual screening was again based on Ala of AVPI. Small fragments displaying weak binding interactions were identified by 2D NMR spectroscopy. The optimization of the resulting hit fragment generated a structure with a dissociation constant (K_D) of 2.5 μM, compared to 0.58 μM for XIAP-AVPI interaction,[30] and with enhanced human plasma stability and permeability over the AVPI peptide.[29]

For a given binding event, the conformation generally observed is that of a low energy state. Alternatively, the free ligand may assume lower energy conformations outside of the binding pocket. Such conformational constraints[13-24] can be imposed to control configurational propensity of the unbound ligand to reflect the stability of its bound state, such as the *cis*-amide preference over the *trns* conformation. Cyclized amides, sulfonamides, and intramolecular hydrogen-bonded motifs have been installed to satisfy this requirement for mineralocorticoid receptor (MR) antagonists and for poly ADP-ribose polymerase (PARP) inhibitors as anti-cancer targets. Lotesta[31] installed sulfonamide and lactam units to investigate Asn-770 binding for assessment of *cis*-amide mimetics in synthetic non-steroidal antagonists of MR. PARP inhibitors designed by Wang and coworkers[32] engage gly active site residues with an intramolecular hydrogen-bonded motif in place of the *cis*-amide requirement of other PARP inhibitors.

In addition to mimicking *cis*-amide structures, sulfonamides are attractive for controlling molecular architecture in nuclear receptor modulators over linear amides, as recently shown for PPARγ partial agonism[33] and for the induced-fit binding model to nuclear receptor RORγ[34]. Other examples of conformational control exploit the axial preference of the α-substituent in biaryl systems for kinase inhibitors[35] or the methyl effect, as done in biphenyl amide inhibitors of p38 kinase from GSK[36].

Furthermore, the utility of various tools and methods measuring propensities of intra- and intermolecular interactions applied to SDBB, serves to enhance conformation to its preferred state.[37] Given the additional factors influencing drug design, such as substrate flexibility and solvation, quantified energetic contributions as determined by conformational analysis, must be considered for successful SBDD.

2.0 SYNTHESIS OF THE TORSION BALANCE

2.1 RETROSYNTHETIC ANALYSIS

The primary target for our synthesis of a conformationally controlled β-turn mimetic torsion balance is depicted in Scheme 1 as biaryl amide **3**. The scaffold was initially designed with the same versatility of the original *β*-turn mimetic torsion balance (Figure 2) by allowing for independent amino acid couplings at three orthogonally protected positions. Yet, the synthesis of any hexa-substituted benzenoid target is challenging.

In this project, two alternate routes to the balance were examined. Our first experiments were guided by the retrosynthetic plan presented in Scheme 1. This plan was directed toward asymmetrical torsion balance analog **3**. This target has orthogonally protected side chains at positions a, b, and c. The pathway was based on installment of two different upper side chains before the aryl coupling to give an asymmetrical balance (Scheme 1). In contrast, the second retrosynthetic analysis discussed here features addition of the upper side chains after the aryl coupling to form a symmetrical biaryl core of the balance (Scheme 2).

2.1.1 Retrosynthetic analysis of the asymmetrical torsion balance.

Scheme 1. Retrosynthetic pathway to the asymmetrical β-turn mimetic torsion balance.

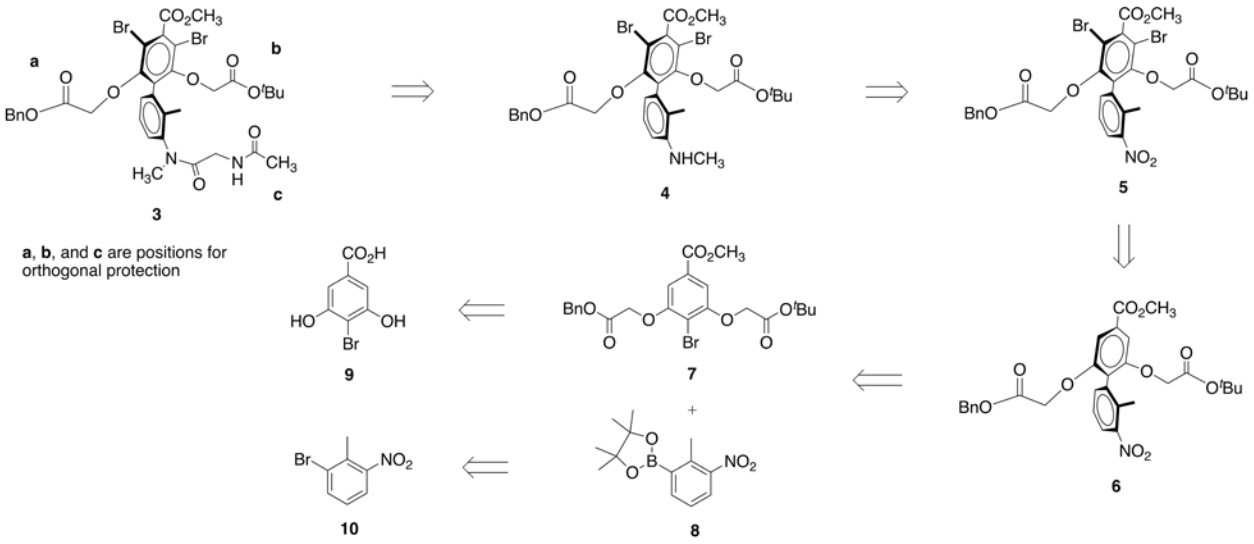

The retrosynthesis of **3** involved an amide coupling of biaryl toluidine **4** with the Fmoc-protected glycine chloride derivative,[38] before subsequent deprotection and acylation. N-methylation of the primary aniline from the reduced nitro group of **5** was proposed to produce **4**. We envisioned that a Suzuki-Miyaura cross-coupling between bromide fragment **7** and boronic ester **8**, followed by dibromination would afford asymmetrical biaryl **6**. The retrosynthetic pathway for fragment **7** involved Fischer esterification[39] of commercially available 4-bromo-3,5-dihydroxybenzoic acid **9** prior to its treatment of two Williamson aryl ether synthetic protocols[40] to attach differential acetoxy side chains. This synthesis, though not completed, remains of interest to us. However, our central question regarding the effect of bromination on conformation could be answered more quickly using the simpler, symmetrical balance **11**.

2.1.2 Retrosynthetic analysis of the symmetrical torsion balance.

Scheme 2. Retrosynthesis of the symmetrical β-turn mimetic torsion balance.

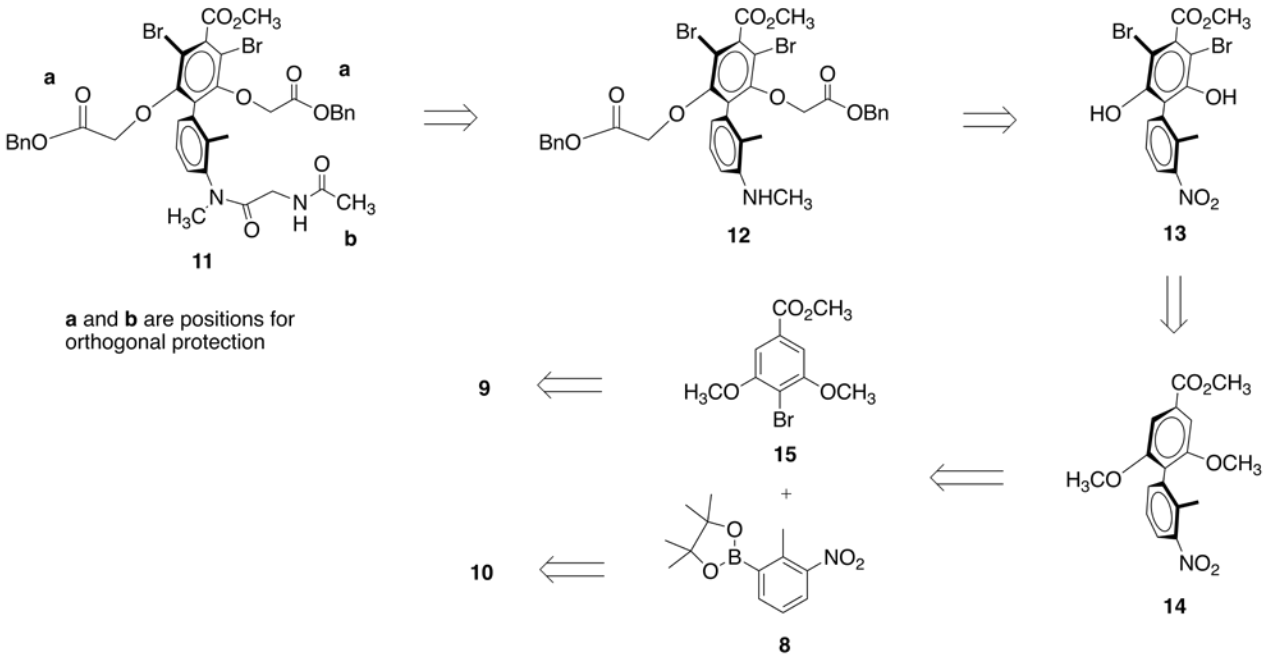

Synthesis of symmetrical biaryl amide **11** was expected to proceed via an amide coupling of biaryl toluidine **12** with Fmoc-protected glycine chloride[38] analog, before subsequent deprotection and acylation. We envisioned nitro group reduction would readily give the primary aniline derivative needed to prepare **12** by N-methylation, preceded by Williamson aryl ether synthesis conditions.[40] To obtain biaryl **13**, we proposed the dibromination of the upper ring after Fischer esterification[39] and after methoxy group cleavage of the Suzuki-Miyaura cross-coupling[41] product **14**. Bromide **15** was readily accessible from the methylation of commercially available 4-bromo-3,5-dihydroxybenzoic acid **9**. Boronic ester **8** was prepared via Miyaura boration reaction of commercially available 2-bromo-6-nitrotoluene **10**.[42]

2.2 STUDIES DIRECTED TOWARD SYNTHESIS OF THE ASYMMETRICAL TORSION BALANCE

2.2.1 Synthesis of coupling fragment bromide 7.

Scheme 3 depicts the synthesis of the coupling fragment bromide **7**.[9] Fischer esterification[39] of commercially available 4-bromo-3,5-dihydroxybenzoic acid **9** afforded methyl benzoate **16** in 99% yield. Ether **17** was synthesized by Williamson aryl ether synthesis[40] on **16** with 1 equiv of commercially available *t*-butyl bromoacetate in 35% yield. The asymmetrical product **17** was separated from the symmetrical ether **17** via flash column chromatography. The Williamson aryl ether synthesis protocol was again utilized to generate coupling fragment **7**. The product was afforded by coupling **18** with commercially available benzyl bromoacetate in a suitable 80% yield of **7**.

Scheme 3. Synthesis of coupling fragment bromide **7**.

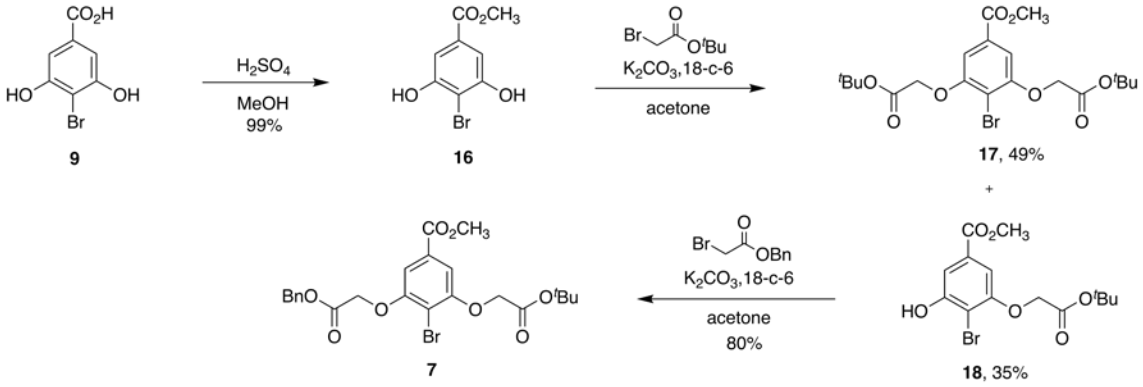

2.2.2 Synthesis of arylboronic ester coupling fragment 8.

Synthesis of the second coupling fragment, boronic ester **8**, was the next challenge to be addressed before forming the core of the torsion balance. Commerically available 2-bromo-6-nitrotoluene **10** was subjected to Miyaura boration conditions[42] with bis(pinacolato)diboron used as the boron nucleophile (Scheme 4). Nitrotoluene **8** was chosen as the starting material, rather than its methylated aniline derivative,[9] due to the amine incompatibility with the bromination step that would later be employed (Scheme 6). A similar procedure using additional 1,1'-bis(diphenylphosphino)ferrocene (dppf) in dioxane also gave boronic ester **8** but with significantly lower yield.[42b]

Scheme 4. Miyaura boration of nitrotoluene **10**.

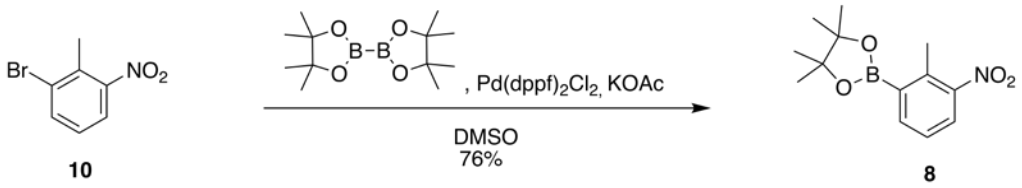

2.2.3 Steps towards the synthesis of asymmetrical biaryl 5.

With both coupling fragments in hand, we next turned our attention to the Suzuki-Miyaura cross-coupling[41] to give biaryl ether **6**, which we then planned to brominate to afford the dibromo-biaryl **5**. We proposed that the coupling step should be done before bromination because of the coupling fragments exhibiting a total of three *ortho*-substituents and a *meta*-substituent; dibromination of **7** would not only increase the difficulty of the coupling reaction due to the presence of two additional *meta*-substituents but also decrease the yield because of competing

cross-couplings reactions. In addition, cleavage of *t*-butyl ester could be observed due to its sensitivity to high temperatures if longer reaction times needed to be employed. Treatment of fragments **7** and **8** with tris(dibenzylideneacetone)dipalladium(0) ($Pd_2(dba)_3$) in toluene accompanied by Buchwald's SPHOS® ligand[41] afforded **6** with a yield of 34%.

Scheme 5. Suzuki-Miyaura cross-coupling of fragments **7** and **8**.

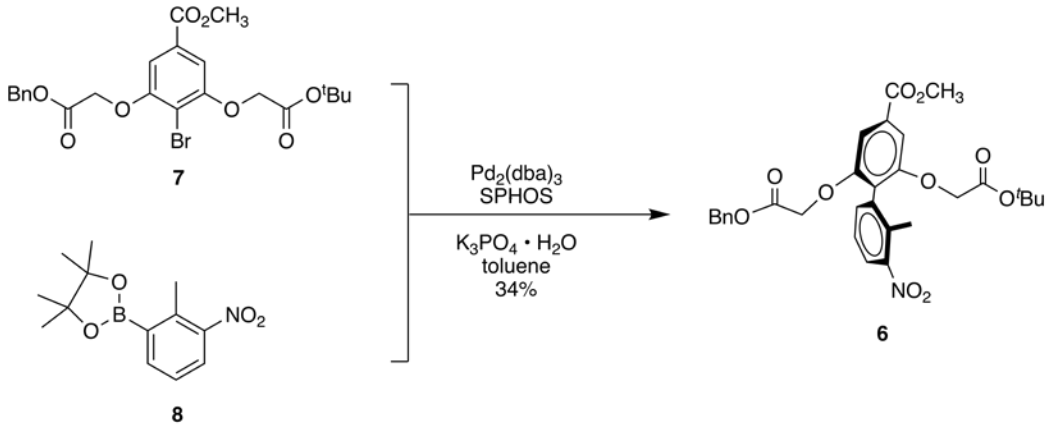

Now that biaryl ether **6** was constructed, dibromination *ortho* to the side chains was the next goal towards the core of the torsion balance. Scheme 6 summarizes our attempts to produce the dibromo-biaryl **5** from **6**. It is difficult to predict where bromination will occur in this molecule due to the competing demands of electronic and steric effects. In fact, no dibromination product (**5**) was isolated. Employment of substitution reaction conditions, entries 1-4, resulted in decomposition and cleavage of the *t*-butyl ester, indicated by the formation of *t*-butyl alcohol in ^{1}H NMR spectra.[43] Addition of sodium acetate to suppress acidity by creating a buffer system was ineffective to form biaryl **5**, even at increased reaction times. This may be due to the steric hindrance of the bulky side chains as well as the inductively less activating effects of the α-benzyloxycarbonyl ethers.

Scheme 6. Attempted dibromination of asymmetrical precursor **6.**

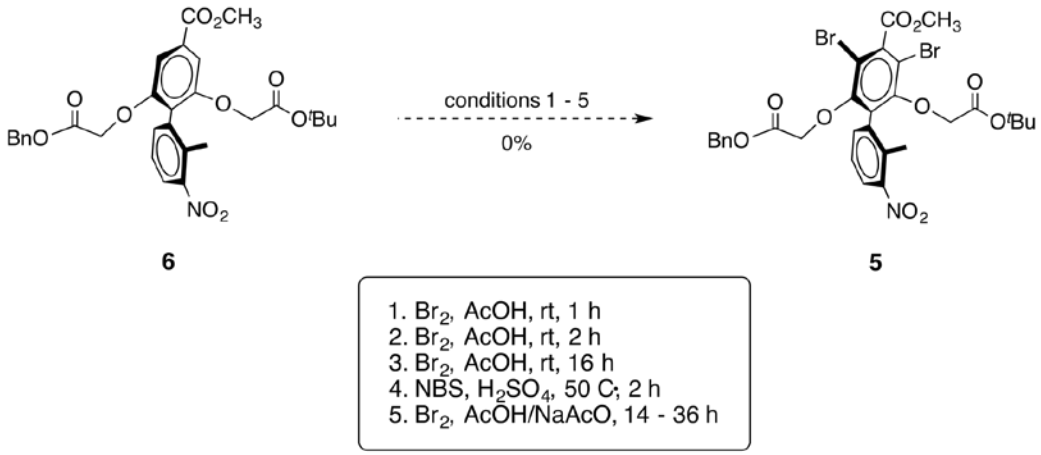

2.2.3.1 Model reactions for dibromination.

In order to probe the stability of our substrate under acidic conditions and investigate other methodology to dibrominate **6**, the symmetrical bromide fragment analog **19** was used for model bromination reactions (Table 1). Starting material and/or monobromination product **20** were observed in all entries. These results strengthen our argument that steric and electronic effects are mostly responsible for the poor reactivity of our substrate, as previously stated. With the exception of entries 3, 7, and 8, formation of *t*-butyl alcohol was observed by ^{1}H NMR of the crude product.[43] Only the procedure in Entry 3 provided dibromination product **21**.

Table 1. Results of model bromination reactions to test substrate stability under acidic conditions.

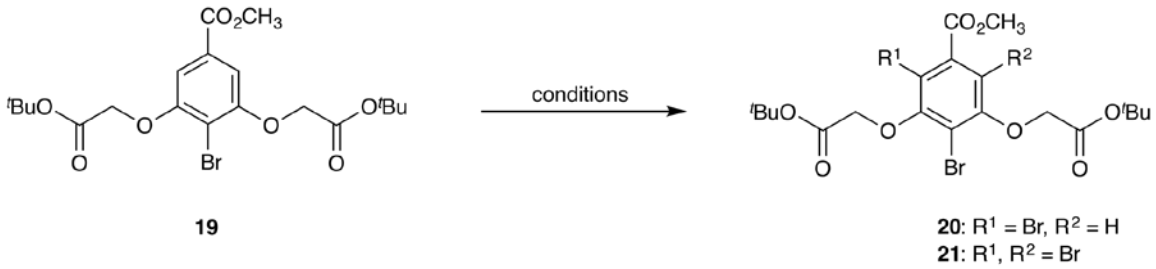

19

20: R^1 = Br, R^2 = H
21: R^1, R^2 = Br

Entry	Conditions[a]	Yield[b]
1	Br_2, AcOH, 3 h	0%[c]
2	Br_2, AcOH, 30 min	0%[c]
3	Br_2, AcOH/NaOAc, 24 h	29%
4	Br_2, AcOH/NaOAc, 3 days	0%[c]
6	Br_2, DCM, 1 h	0%[c]
7	NBS, DCM, 2 days	0%
8	NBS, $Pd(OAc)_2$, AcOH, 6 h	0%
9	NBS, $Pd(OAc)_2$, AcOH, 80 ˚C, 12 h	0%[c]

[a]Reaction scale based on 0.22 mmol; all reactions were run at room temperature except entry 9. [b]Isolated yield of **21**; recovered material also included **20** and starting material; [c]cleavage of *t*-butyl group observed by ^{1}H NMR.

Finally, the asymmetrical coupling fragment **7** was subjected to the entry 3 conditions described above (Scheme 7). The experiment revealed evidence (^{1}H NMR and HRMS) of bromination occurring on the aryl ring of the benzyl ester to afford product **22** (21% yield).

Scheme 7. Bromination of asymmetrical coupling fragment bromide **7**.

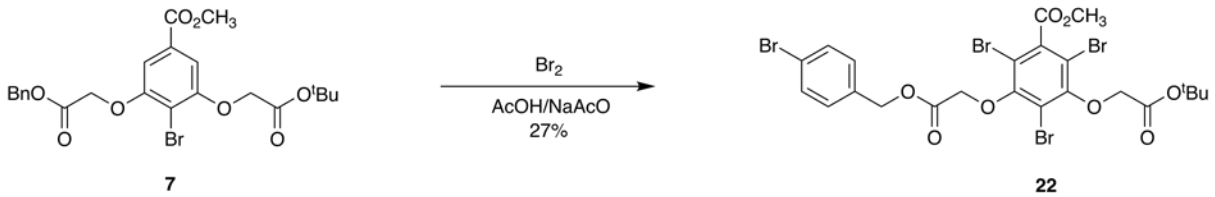

2.3 PREPARATION OF THE SYMMETRICAL BIARYL CORE OF THE TORSION BALANCE

We learned from the above experiments that the dibromination of **6** was very slow, and would not be easily achieved without simultaneous bromination of the benzyl ester (similar to Scheme 7). Furthermore, we learned that the *t*-butyl ester was sensitive to the bromination conditions (Table 1). Therefore, we turned to a modified synthetic route to meet our goal (Scheme 1).

This pathway of the conformationally controlled β-turn mimetic torsion balance began with preparation of the biaryl core of the balance. This involved cross-coupling bromide **15** and boronic ester **8** using the same conditions for the Suzuki-Miyaura reaction as before to give **14** with a good yield of 74% (Scheme 8). The increase in percent yield (from 34% in Scheme 5) is most likely due to the less sterically hindered methoxy side chains of **14** than the bulky side chains of coupling fragment **7**.

Scheme 8. Successful Suzuki-Miyaura cross-coupling of fragments **15** and **8**.

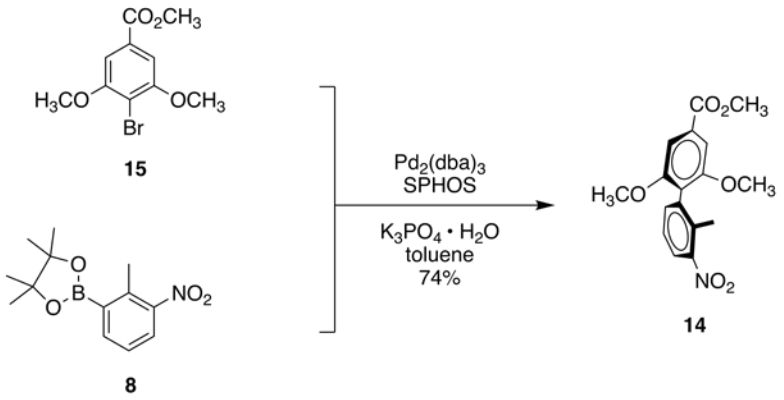

The synthesis of **5** was straightforward, using 3 equiv of dimethylsulfate (DMS) to methylate commercially available 4-bromo-3,5-dihydroxybenzoic acid **7** in quantitative yield following recrystallization (Scheme 9).[44a] An alternative procedure using methyl iodide also gave benzoate **5** from the Fischer esterification[33] product **13**, but with a slightly lower yield of 85%.[44b]

Scheme 9. Syntheses of coupling fragment bromide **15**.

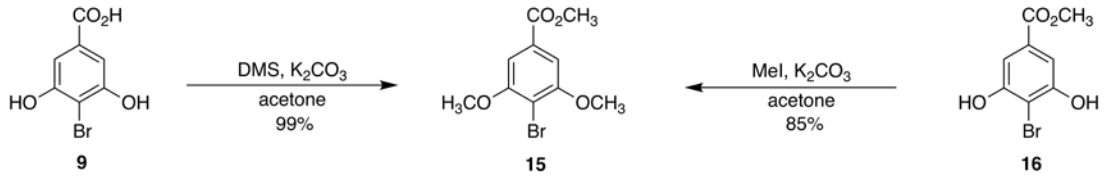

Attempted Suzuki-Miyaura cross-couplings of other top fragments (**16** and **23)** were first tried in efforts to form the biaryl core of the balance, using the same conditions as before (Scheme 10).[33] Failure to directly form biaryl from cross-coupling fragments **16** and **8** was most likely due to the phenols undergoing deprotonation in the presence of base. Next, cross-coupling of the silyl ether product **23** and **8** was attempted to give biaryl **25**. This too was unsuccessful. We believe the *t*-butyl silyl ethers sterically interfered with the C-C bond formation. Despite the methyl ester on coupling fragment **15**, the methyl ether was deduced to be the best protecting group for the diphenol due to its facile preparation and the exceptional yield of the cross-coupling reaction.

Scheme 10. Failed Suzuki-Miyaura cross-couplings.

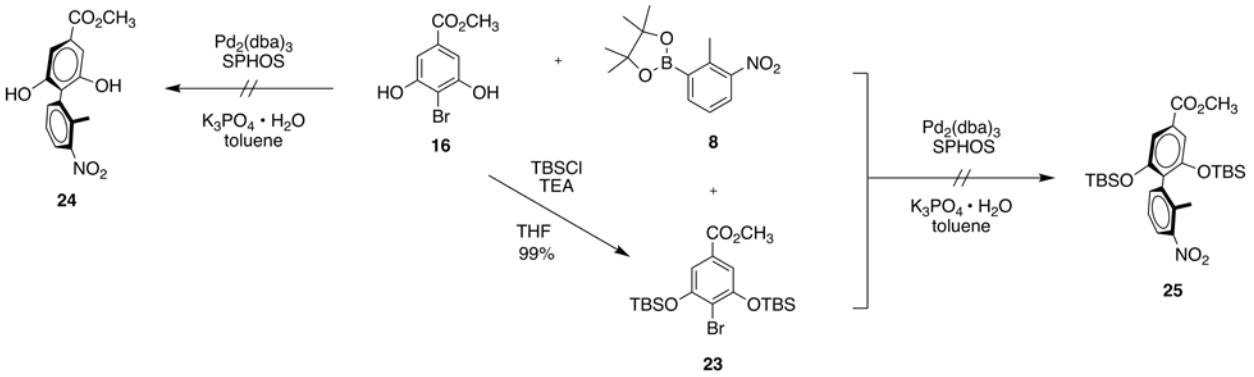

Now that the biaryl building block was in hand, ether cleavage was the next goal before functionalizing the top of the balance. We had hoped to execute a selective cleavage of the methyl ethers using magnesium iodide (MgI_2) in an ionic liquid to obtain the dihydroxy-biaryl **24**.[45] Treatment of biaryl **14** with 3 equiv of freshly prepared MgI[45c] in 1-butyl-3-methylimidazolium tetrafluoroborate ([bmim]BF_4) ionic liquid at 50 ˚C from 7 to 24 h resulted only in reisolation of starting material (Scheme 11).[45c]

Scheme 11. Attempted selective demethylation of aryl methyl ether.

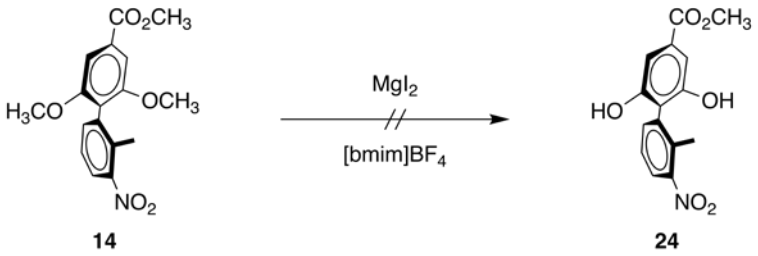

2.3.1 Model reactions for demethylation of biaryl ether 14.

Consideration of the drawbacks of aryl methyl ether cleavage procedures led us to conclude that ether cleavage without ester cleavage was unlikely.[46] We then envisioned a two-step reaction sequence of non-selective demethylation and successive Fischer esterification to afford dihydroxy-

biaryl **24**. Results of model experiments with coupling fragment **15** can be found in Table 2. Starting material was recovered in the majority of the reactions along with partially cleaved products **26** and **27** (entries 1-9). However, treatment with BBr_3[46] resulted in successful demethylation to yield benzoic acid **9** at 85% (entry 10). In the crucial experiment, subjecting biaryl **14** to 6 equiv of BBr_3 in DCM followed by immediate Fischer esterification of the acid readily produced dihydroxy-biaryl ester **24** in 78% yield.

Table 2. Conditions and yields for model demethylation reactions.

15

9: R^1, R^2, R^3 = H
26: R^1 = H, R^2, R^3 = CH_3
27: R^1, R^2 = H, R^3 = CH_3

Entry	Conditions[a]	Yield[b]
1	NaI, 15-crown-5, BBr_3, DCM, -40 ˚C, 5 hours	0%
2	ethanethiol, $AlCl_3$, rt, 1.5 hours	0%
3	NaCN (6 eq), DMF, 90 ˚C, 20 hours	74%[c]
4	NaCN (15 eq), DMF, 90 ˚C, 24 hours	67%[c]
5	NaI, $(CH_3)_3SiCl$, ACN, 50 ˚C, 20 hours	48%[c]
6	NaI, $(CH_3)_3SiCl$, ACN, 50 ˚C, 40 hours	34%[c]
7	methanesulfonic acid, 90 ˚C, 20 hours	0%
8	NaI, methanesulfonic acid, 90 ˚C, 20 hours	33%[c]
9	NaI, 15-crown-5, BBr_3, DCM, -40 ˚C, 9 hours	0%

10	BBr_3, DCM, 0 ˚C to rt, 7 hours	85%[d]

[a]Reaction scale based on 0.04-0.08 mmol of **15**. [b]Yield of major product determined by ^1H NMR; recovered material also included SM. [c]Yield of **9**. [d]Yield of **26**. [e]Yield of **27**.

Scheme 12. One-pot synthesis of demethylated biaryl analog **24**.°

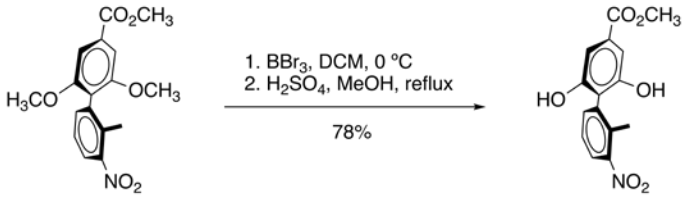

14 **24**

We next endeavored to carry out the bromination of the dihydroxy-biaryl ester **24**. This intermediate was an improved substrate for dibromination due to the presence of more strongly electron-donating hydroxyl groups, rather than the inductively less activating β-benzyloxycarbonyl ether groups. Steric effects are minimized in comparison to substrate **6** as well.

2.3.2 Model reactions for dibromination of the diphenol biaryl 24.

Our efforts to determine the best methodology to afford dibromo analog **13** are summarized in Table 3. We first subjected model substrate **7** to 2.5 equiv of Br_2 in AcOH/NaOAc buffer, as previously used on biaryl **12** (entry 1).[43] After 24 hours, **26** was afforded in 83% yield. We had earlier observed cleavage of *t*-butyl esters under these conditions, when ethers, rather than hydroxyls were present. To support future studies, we looked for a faster bromination process that might be more compatible with *t*-butyl esters.

Solvent substitution effects were investigated for the treatment of **14** with Br_2. A 6:1 solution of CH_3Cl:CH_3CN afforded **26** in 70% yield after only 6 hours (entry 2) and extending the reaction time to 24 hours only increased the yield by 5% (entry 3).[47] Substitution of CCl_4 as the

reaction solvent produced **26** in 82% yield after only 2 hours (entry 10).[48] An increased reaction time of 18 hours, slightly lowered the yield to 76% (entry 9). Other reported conditions were not further investigated because of the significantly lower yields.

Table 3. Conditions and yields for model dibromination reactions.

16

28: R^1, R^2 = Br
29: R^1 = Br, R^2 = H

Entry	Conditions[a]	Yield[b]
1	Br_2, AcOH/NaOAc, 24 h	83%
2	Br_2, 6:1 CH_3Cl:ACN, 6 h	70%
3	Br_2, 6:1 CH_3Cl:ACN, 24 h	75%
4	NBS, ACN, 24 h	0%
5	NBS, ACN, 48 h	8%
6	Br_2, $FeCl_3$, DCM, 12 h	43%
7	Br_2, $FeCl_3$, DCM, 20 h	55%
8	NH_4Br, H_2O_2, AcOH, 16 h	0%

9	Br_2, CCl_4, 18 h	76%
10	Br_2, CCl_4, 2 h	82%

[a]Reaction scale based on 0.1 mmol of **16**; all reactions were performed at room temperature.
[b]Yield of **28** as determined by ^{1}H NMR; recovered material also included **29** and SM.

2.4 SYNTHESIS OF THE SYMMETRICAL TORSION BALANCE

Based on the model bromination experiments, we chose to try Br_2 in CCl_4 for the bromination of the phenol. Treatment of **24** with 2.5 equiv of Br_2 in CCl_4 afforded dibromination product **13** in 76% yield (Scheme 13).[47] With the preparation of the core almost complete, etherification was the only remaining step before functionalizing the bottom portion of the balance (Scheme 13). Treatment of **13** with 2 equiv of commercially available benzyl bromoacetate by the Williamson aryl ether protocol afforded the symmetrical intermediate **30** in 80% yield. Several methods were then considered for the reduction of the nitro group to its amine derivative **31**.

Scheme 13. Steps towards constructing the symmetrical torsion balance core.

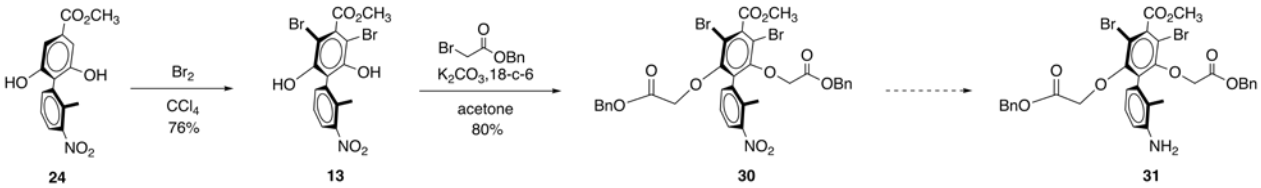

2.4.1 Model nitro group reductions.

We employed **32** as a model for biaryl **30** while evaluating reduction methods. Etherification conditions as used before were employed to generate **32** from commercially available nitrotoluene **33** in 89% yield. The reduction of **32** by H_2/PtO_2 produced **34** in 42% yield

at 1.5 hours (entry 1, Table 4) and 55% yield at 3 hours (entry 2).[48a] Employment of $SnCl_2$ with MeOH in DCM afforded **34** in 24% at 16 hours, but decomposition was also observed (entry 3).[48b] Reaction of **32** with Fe in the presence of AcOH and MeOH provided **34** at 29% (entry 5),[48c] while reduction with Zn and HCl[48d] in ethyl acetate gave an excellent yield of 92% (entry 5). Only decomposition was observed for entries 6 and 7.[48e,f]

Table 4. Results of model nitro group reductions.

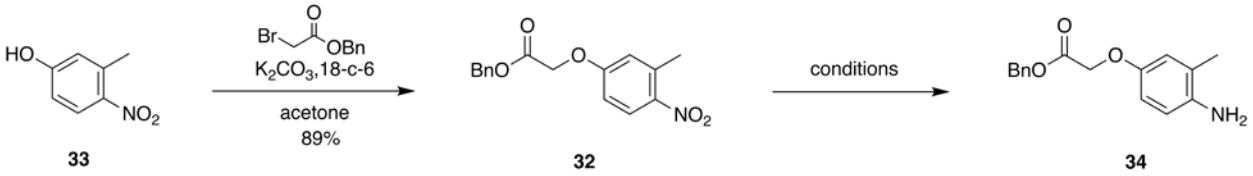

Entry	Conditions[a]	Yield[b]
1	H_2, PtO_2, ethyl acetate, rt, 1.5 h	42%
2	H_2, PtO_2, ethyl acetate, rt, 3 h	55%
3	$SnCl_2$, MeOH, DCM, 0 ˚C to rt, 16 h	24%[c]
4	Fe, AcOH, MeOH, DCM, 40 ˚C, 3 h	29%
5	Zn, HCl, ethyl acetate, 0 ˚C to rt, 16 h	92%
6	hydrazine hydrate, $FeSO_4 \cdot 7H_2O$, EtOH, H_2O, reflux, 15 h	0%[c]
7	Zn, formic acid, MeOH, rt, 3 h	0%[c]

[a]Reaction scale based on 0.17 mmol of **33**. [b]Isolated yield of **34**; recovered material also included SM except for entries 2, 3, and 5. [c]Decomposition observed.

With the results from the model reactions in hand, we returned to our biaryl substrate. Reduction of biaryl **30** by Zn/HCl gave an excellent yield of **30** at 80% (Scheme 14). Alternatively, treatment with H_2/PtO_2, gave only debenzylation product **35**, unlike the model, at 39% yield with the nitro group still intact. Despite the unsuccessful result, this reaction was able to serve as a model for the future debenzylation step.

Scheme 14. Nitro group reduction to obtain biaryl toluidine **31**.

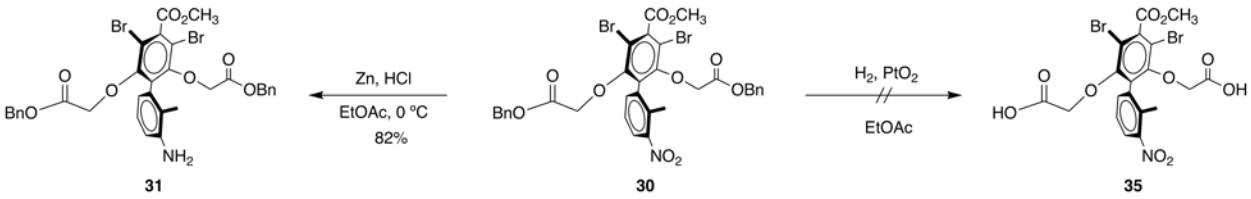

2.4.2 Final steps to the symmetrical torsion balance core.

2.4.2.1 Methods for mono N-methylation.

We then turned to the alkylation of toluidine **31**. Liberatore had previously designed an indirect N-methylation procedure based on partial protection of the aniline (Scheme 15).[9] Reaction of di-*tert*-butyl dicarbonate (Boc anhydride, or Boc_2O) with **31** gave protected derivative **36**. Alkylation by treatment with MeI and NaH in DMF resulted in a complex mixture of products as observed by TLC and ^{1}H NMR. Boc group cleavage with TFA afforded the methylation products **12**, **37**, and **38**.

Scheme 15. Boc protection, methylation, and deprotection of toluidine **31**.

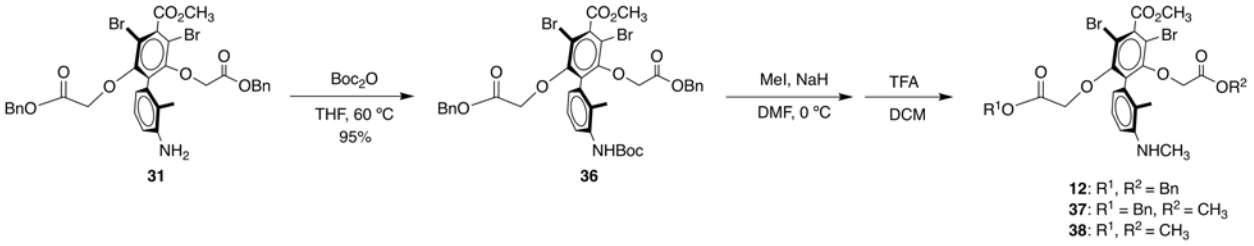

In efforts to elucidate the mechanism for the formation of **37** and **38**, we turned to model reactions of the Boc-protected derivative of aniline **34** to observe the effects between order of addition of MeI and NaH. The conversion of benzyl to methyl ester was only noted when NaH was added prior to MeI. Thus, we concluded that the side products were a result of benzyl ester hydrolysis. All precautions were then taken to eliminate the presence of water during the methylation of **31**, but only in one instance was desired methylated carbamate provided to give **12** in 20% yield, after Boc group cleavage. However, replication was unsuccessful. We suspected this was due to the initial presence of the hydroxide ion in the reaction. Potassium hydride was also substituted as base but did not have any effective increase in yield.

We examined another route to improve the yield and consistency of results (Scheme 16). Protection of **31** was achieved with commercially available 4-nitrobenzenesulfonyl chloride (NsCl) to generate its sulfonamide derivative **39**, which was subsequently treated with diazomethane.[49-51] The advantage of using the nosyl protecting group was to furnish a sulfonamide of exceptional acidity. This is known to increase the rate of formation of the methyl diazonium ion.[50,51] Commercially available *N*-methylurea **40** was used to generate the *N*-methyl-*N*-nitrosourea **41** and reacted with KOH directly before the alkylation step.[49a] Cleavage of the protecting group was attempted using mercaptoacetic acid and 1,8-diazabicyclo[5.4.0]undec-7-ene (DBU) in CH_3CN at 50 ˚C but was unsuccessful at 4 and 6 hours. After increasing reaction time

to 20 hours, evidence of dimerization of **12** was confirmed by HRMS. This was attributed to the instability of the alkylated intermediate under prolonged heat in the presence of DBU.

Scheme 16. Attempted N-methylation of **39** with diazomethane.

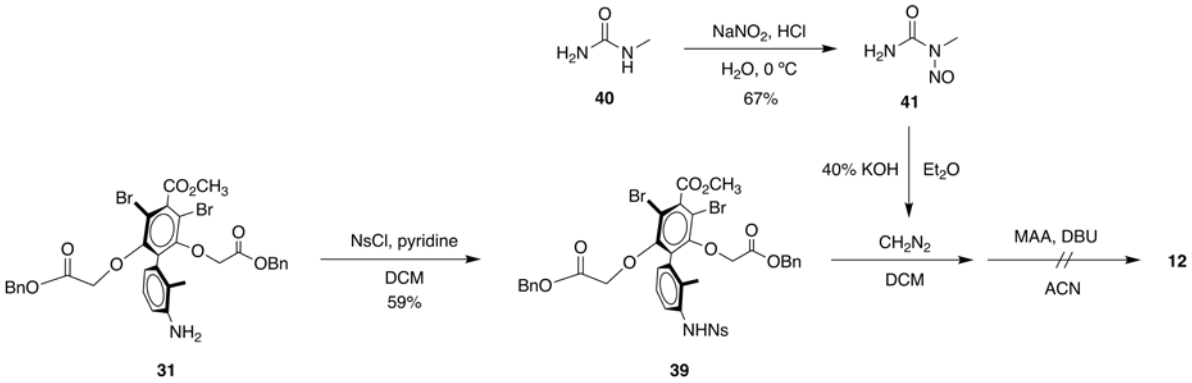

With the N-methylation proving more difficult than anticipated, we turned to an approach based on Katritzky's methods for the mono N-alkylation of anilines by Mannich reaction.[52] A two step reaction sequence was envisioned to achieve **12**. This involved aminomethylation of **31** with benzotriazole and formaldehyde, followed by subsequent reduction of the base with sodium borohydride. The described condensation procedure gave low and inconsistent yields, probably due to poor solubility of aniline **31** in EtOH, even after sonication. Formation of various byproducts was a direct result of the inability to control the imminium ion forming equilibrium at low reaction concentration. The substitution of THF for the reaction solvent led to prolonged reaction rates and an increase in byproducts. The dimethylaniline derivative (not shown) was observed by ^{1}H NMR and by HRMS on both biaryl substrate **31** and model substrate **34** after their reduction.

To improve the method described above, the reaction was modified by direct condensation of 1-hydroxymethylbenzotriazole **42** with aniline **31** (Scheme 17).[53] This removed one uncertainty

(the formalin reaction and related equilibria) in the process. Addition of benzotriazole **43** to formaldehyde in EtOH provided **42**, which was also converted to 1-chloromethylbenzotriazole by treatment with thionyl chloride.[52] In using model compound **34** as our substrate, treatment with **42** produced higher yields than the chloro-derivative, even in the presence of lithium iodide. Finally, condensation of **42** with biaryl **31** led to direct isolation of condensation product, which was readily reduced with $NaBH_4$ to afford the torsion balance core **12** in 53% yield. Effects of solvent substitution on the alkylation were also examined, as was catalysis by pyridinium *p*-toluenesulfonate, but no significant correlation with product yield was observed.

Scheme 17. Two-step sequence for mono N-methylation of biaryl toluidine **31**.

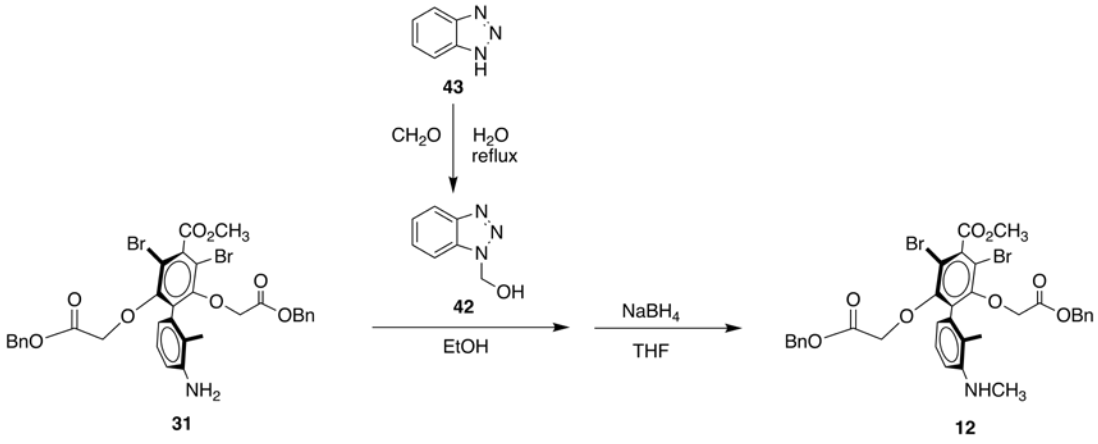

2.4.2.2 Amino acid coupling, deprotection, and acylation.

Our focus now turned to the amidation step remaining en route to finalizing the torsion balance (Scheme 18). The approach was based on Carpino's conditions,[38] initially converting commercially available *N*-9-fluorenylmethyloxycarbonyl-glycine (*N*-Fmoc-gly) **44** to its corresponding acid chloride **45** with thionyl chloride, which was coupled with biaryl **12** immediately after its formation due to its susceptibility to hydrolysis. Amide **46** was isolated in 67% yield. The final step to synthesize torsion balance **11** involved treatment of **46** with piperidine in DMF to deprotect the amino acid, followed by immediate acylation with acetic anhydride and pyridine (70% yield).

Scheme 18. Final steps to synthesize torsion balance **11**.

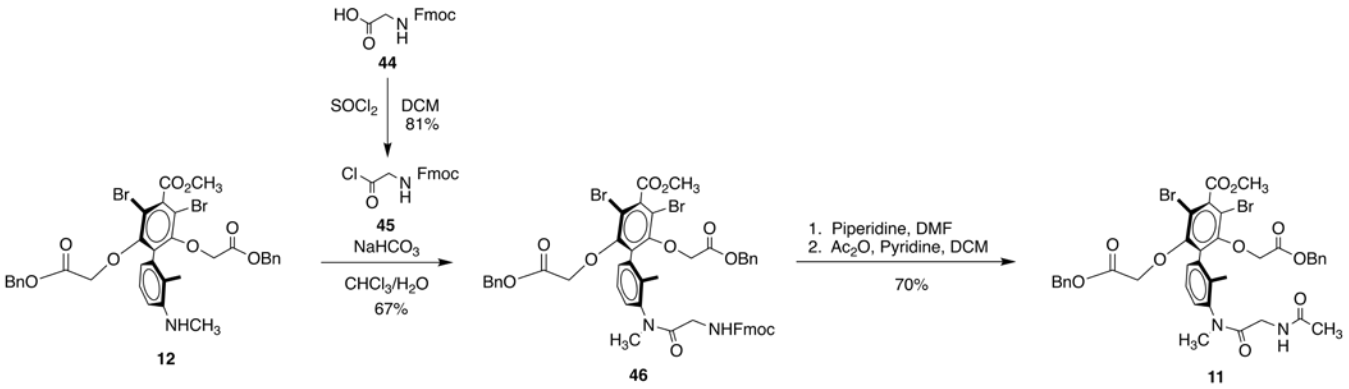

3.0 INITIAL NMR STUDIES OF THE TORSION BALANCE

3.1 ANALYSIS OF TORSION BALANCE FOLDING PREFERENCE

3.1.1 Folding preference of torsion balance 11.

After attaining torsion balance **11**, it was imperative to examine our conformationally controlled scaffold for improved antiparallel β-sheet configuration and hydrogen bonding distance. With this analog being symmetrical, we could only investigate the ability of the amino acid proton to hydrogen bond with the benzyl ester carbonyl. Previous line shape analysis and EXSY experiments on the asymmetrical first generation balance (Figure 1) had determined that the aryl-aryl bond rotational barrier was 35.7 kcal·mol^{-1} with a half-life of 2.2 days at 418 K and that of the N-aryl bond to be 20.9 kcal·mol^{-1} at 298 K.[9] Due to the presence of the *ortho* methyl substituent to the carbamate, the N-CO amide bond barrier to rotation (17 kcal·mol^{-1} at 298 K) was larger than expected based on results with Smith's carbamates.[54] Yet, with the second generation balance being symmetrical, the N-CO amide bond is the only site to invoke a conformational switch, as illustrated in Figure 5. The significance of the NMR analysis of the benzyl ester carbonyls can be realized when investigating folding preference and hydrogen bond selectivity in isomers of more advanced symmetrical torsion balances.

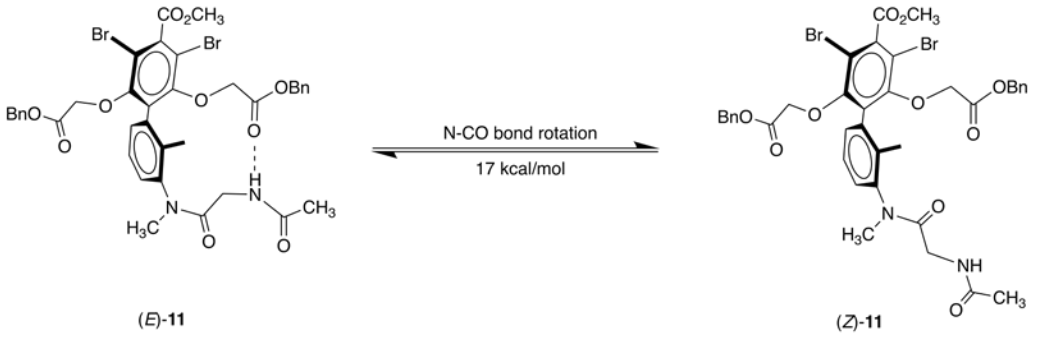

Figure 5. Two conformers of glycine target **11** by rotation around the N-CO amide bond.

The N-CO bond rotation affords the *E* and *Z* conformers of torsion balance **11** that are illustrated in Figure 5. The presence of the two conformations is evident from the two *N*-methyl group singlets in the ^{1}H NMR spectra of **11** at 298 K in both $CDCl_3$ and CD_2Cl_2 (Figure 6). A 15:1 ratio of the two *N*-methyl group singlets can be observed in both solvents; the chemical shift in $CDCl_3$ is slightly more downfield (δ = 3.25 ppm) than in CD_2Cl_2 (δ = 3.21 ppm). This result confirms that rotation around the N-CO amide bond is responsible for both conformers.

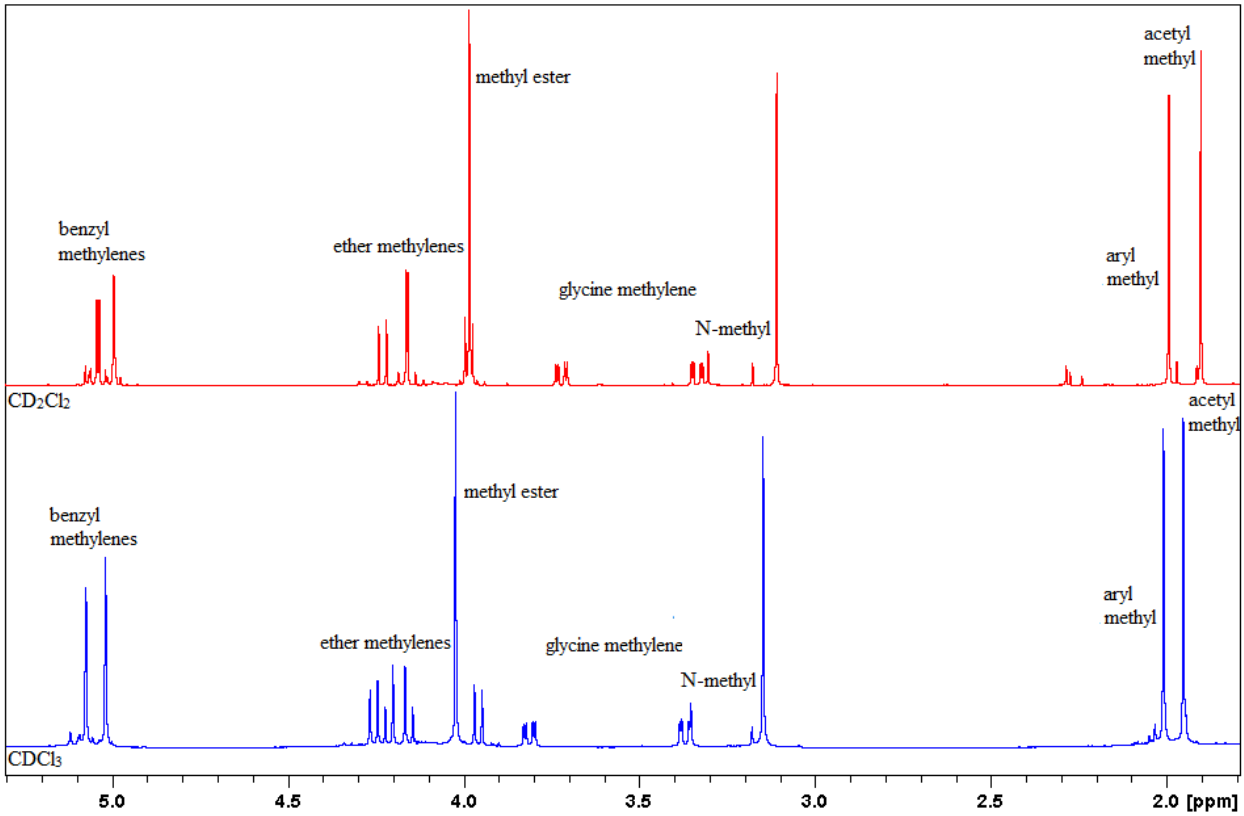

Figure 6. ^{1}H NMR spectra of glycine target **11** in $CDCl_3$ (bottom) and CD_2Cl_2 (top) at 298 K.

The ^{1}H NMR data reveal approximately the same ratio of *E* and *Z* rotamers about the N-CO amide bond as found for first generation balances (93% to 7%).[9] The 2D NMR ROESY data confirm that (*E*)-**11** is the major rotamer (94%) and (*Z*)-**11** is the minor rotamer (6%).

Based upon the configuration of the major component, the position of the amino acid amide proton appears to be within range to hydrogen bond to the carbonyl of the upper side chain for more advanced torsion balances. Thus, suggesting the conformationally controlled torsion balance scaffold may be an improved design for antiparallel β-sheet folding.

4.0 CONCLUSION

We report herein the synthesis of the core scaffold of a new conformationally controlled torsion balance that can be applied toward quantitative comparison of side chain interactions in the antiparallel β-sheet motif. The design has previously shown a restricted N-aryl bond rotation to impose a two-state folding manifold to mimic the potential folding dynamics of a β-turn. However, the dibromo design features an additional degree of conformational control by the incorporation of the bromo substituents *ortho* to the upper side chains. With the synthesis and analysis of ^{1}H and 2D ROESY NMR results of **11**, we conclude the torsion balance core scaffold has improved chain alignment between the top and bottom side chains to ultimately promote hydrogen bond formation in the final targets.

5.0 EXPERIMENTAL

Thin layer chromatography (TLC) was performed on E. Merck 60F 254 (0.25 mm) analytical glass plates. A Thomas Hoover capillary melting point apparatus was used to obtain melting points and are uncorrected. A Nicolet Avatar 360 FT-IR was utilized to determine infrared (IR) spectra. Bruker Avance 300, 400, and 500 MHz spectrometers were used to find proton and carbon nuclear magnetic resonance spectra (^{1}H and ^{13}C NMR). TMS (^{1}H) or residual solvent (^{13}C) peak were set as the reference value to report chemical shifts in parts per million (δ). ^{1}H NMR data was taken at room temperature (21 – 27 ˚C) and is reported using the following list of abbreviations: s = singlet; d = doublet; t = triplet; q = quartet; dd = doublet of doublets; m = multiplet; ABq = AB quartet; quartet of doublets = qd. High resolution mass spectra were recorded on a VG 7070 spectrometer. Percent yields are for material of >95% purity as indicated by ^{1}H NMR spectra.

Dry solvents were obtained prior to use by distilling the solvents from the appropriate drying agent under nitrogen atmosphere. DCM was distilled from CaH_2, toluene was distilled from $CaCl_2$, DMF was vacuum distilled from 4 Å molecular sieves, and diethyl ether and THF were distilled from sodium metal and benzophenone. Dry CCl_4 and DMSO were purchased from Aldrich and used as supplied. “Removal of volatile components under reduced pressure” refers to rotary evaporation of the sample at 21-65 °C at a pressure of 18-25 mm Hg followed by treatment under high vacuum (0.1 mm Hg) at room temperature.

5.1 EXPERIMENTAL PROCEDURES

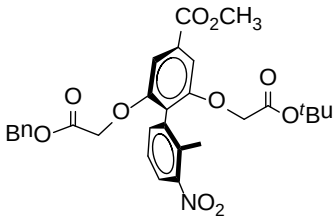

Methyl 2,6-dimethoxy-2'-methyl-3'-nitro-[1,1'-biphenyl]-4-carboxylate (6). In a round-bottom flask, 0.17 g (0.34 mmol) of benzoate **7**, 0.14 g (0.55 mmol) of boronic ester **8**, 0.013 g (0.014 mmol) of $Pd_2(dba)_3$, 0.022 g (0.055 mmol) of 2-dicyclohexylphosphino-2',6'-dimethoxybiphenyl (SPhos), and 0.24 g (1.03 mmol) of (ground) $PO_4 \bullet H_2O$ were added and dried under reduced pressure for 5 minutes and backfilled with nitrogen two times. Toluene (3 ml) was added, and the solution was degassed using the freeze-pump-thaw method three times under a nitrogen atmosphere. The flask was sealed; the reaction mixture was stirred at 90 °C for 18 h, and cooled to room temperature. The mixture was diluted with DCM (30 mL) and H_2O (30 mL); the organic layer was extracted, and the aqueous layer was washed with additional DCM (3 x 30 mL). The combined organic layers were dried over $MgSO_4$ and filtered, and volatile components were removed from the filtrate under reduced pressure to give a brown crude oil. The oil was purified by flash chromatography (SiO_2, hexanes/ethyl acetate, 5:1) to afford 0.13 g (67.6%) of **6** as a white foam: R_f 0.36 (hexanes/ethyl acetate, 4:1); IR (thin film, cm^{-1}) 3442, 2979, 1751, 1725, 1581, 1528, 1437, 1422, 1354, 1330, 1236, 1194, 1136; 1082, 1029, 999, 867, 844, 810, 771, 741, 698; ^1H NMR (400 MHz, $CDCl_3$) δ 7.83 (d, *J* = 8 Hz, 1H), 7.42 (d, *J* = 7 Hz, 1H), 7.33 (broad s, 4H), 7.27 (broad s, 2H), 7.19 (s, 2H), 5.16 (s, 2H), 4.67 (s, 2H), 4.49 (s, 2H), 3.91 (s, 3H), 2.27 (s, 3H), 1.44 (s, 9H); ^{13}C NMR (400 MHz, $CDCl_3$) δ 168.2, 167.4, 166.2, 156.2, 155.9, 150.8, 136.2, 135.3,

135.1, 132.8, 131.5, 128.8,128.6, 126.0, 123.9, 122.5, 106.5, 106.0, 82.9, 67.3, 66.0, 65.4, 52.6, 28.2, 16.5; HRMS (ESI-TOF) *m/z*: $[M+Na]^+$ calcd for $C_{30}H_{31}NO_{10}Na$ 588.1840, found 588.1854.

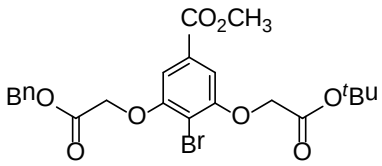

Methyl 3-(2-(benzyloxy)-2-oxoethoxy)-4-bromo-5-(2-tert-butoxy-2-oxoethoxy) benzoate (7). In a round bottom flask, 0.49 g (1.36 mmol) of benzoate **18**, 0.26 mL (1.63 mmol) of benzyl bromoacetate, 0.22 g (1.63 mmol) of K_2CO_3, and 0.08 g (0.33 mmol) of 18-crown-6 were dissolved in acetone (35.4 mL), and the reaction mixture was refluxed for 24 h. The volatile components were removed under reduced pressure, and the residue was diluted with DCM (25 mL) and water (25 mL); the organic layer was extracted, and the aqueous layer was washed with additional DCM (3 x 25 mL). The combined organic layers were dried over $MgSO_4$ and filtered, and the volatile components were removed from the filtrate under reduced pressure to give a crude yellow oil. The oil was purified by flash chromatography (SiO_2, hexanes/ethyl acetate, elution gradient 7:1/6:1/3:1) to yield 0.55 g (80.2%) of **7** as a white solid: R_f 0.48 (hexanes/ethyl acetate 3:2); mp 68-70 °C; IR (thin film, cm^{-1}) 2978, 1753, 1724, 1587, 1423, 1369, 1337, 1241, 1194, 1133, 1029, 1000, 844, 763; ^{1}H NMR (400 MHz, $CDCl_3$) δ 7.24 (s, 5H), 7.04 (d, J = 4 Hz, 2H), 5.14 (s, 2H), 4.70 (s, 2H), 4.56 (s, 2H), 3.77 (s, 3H), 1.40 (s, 9H); ^{13}C NMR (500 MHz, $CDCl_3$) δ 167.8, 166.9, 165.9, 155.8, 155.7, 149.9, 149.1, 143.4, 141.7, 140.0, 135.0, 130.5, 130.0, 128.7, 128.6, 128.6, 128.5, 128.5, 108.2, 107.4, 107.2, 82.9, 67.3, 67.2, 66.6, 66.3, 60.7, 52.5, 28.0; HRMS (ESI-TOF) *m/z*: $[M+Na]^+$ calcd for $C_{23}H_{25}O_8NaBr$ 531.0630, found 531.0663.

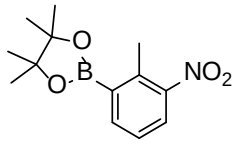

4, 4, 5, 5-tetramethyl-2-(2-methyl-3-nitrophenyl)-1,3,2-dioxaborolane (8). To a third flame-dried 200 ml round-bottom flask, 3.00 g (13.9 mmol) of **10**, 5.29 g (20.8 mmol) of $(Bpin)_2$, 4.09 g (41.7 mmol) of KOAc, and 0.45 g of [1,1'-bis(diphenylphosphino)ferrocene]dichloropalladium(II), complex with DCM ($Pd(dppf)Cl_2$•DCM; 0.56 mmol) were added. The reaction flask was then placed on vacuum line for 5 minutes and backfilled with nitrogen and repeated. DMSO (83.2 mL) was then added and the solution degassed using the freeze-pump-thaw method three times under a nitrogen atmosphere. The flask was sealed; the reaction mixture was stirred at 90 °C for 20 hours and then cooled to room temperature. The reaction mixture was then diluted with DCM (100 mL) and H_2O (100 mL). The organic layer was extracted and washed with H_2O (3 x 100 mL). The aqueous layer was washed with additional DCM (2 x 100 mL). Organic extracts were combined, and the volatile components were removed from the filtrate under reduced pressure to give a brown crude oil. The oil was purified twice by flash column chromatography (SiO_2, hexanes/ethyl acetate, elution gradient (2 columns) 10:1/6:1; then 30:1) to give 2.7 g (76%) of **8** as a pale yellow solid: R_f 0.89 (hexanes/ethyl acetate, 4:1); mp 52-53 °C; IR (thin film, cm^{-1}) 3055, 2982, 2933, 1603, 1569, 1527, 1474, 1439, 1344, 1267, 1214, 1144, 1109, 1026,1078, 963, 786, 739, 669, 579. 463; ^1H NMR (300 MHz, $CDCl_3$) δ 7.94 (d, *J* = 7 Hz, 1H), 7.77 (d, *J* = 8 Hz, 1H), 7.27 (t, *J* = 8 Hz, 1H), 2.67 (s, 3H), 1.36 (s, 12H); ^{13}C NMR (300 MHz, $CDCl_3$) δ 151.3, 139.9, 138.2, 126.3, 126.0, 84.4, 25.0, 18.0; HRMS (ESI-TOF) *m/z*: $[M+H]^+$ calcd for $C_{13}H_{19}BNO_4$ 264.1407, found 264.1405.[37b]

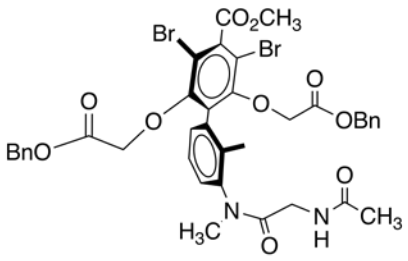

Dibenzyl 2, 2'-((3'-(2-acetamido-N-methylacetamido)-3,5-dibromo-4-(methoxycarbonyl)-2'-methyl-[1, 1'-biphenyl]-2,6-diyl)bis(oxy))diacetate (11). To 0.01 g (0.01 mmol) of **46** in a round-bottom flask was added 0.045 mL of a 20% piperidine/DMF solution, and the reaction mixture was stirred at room temperature for 20 min. Then 0.24 mL (mmol) of acetic anhydride and 0.71 mL (mmol) of pyridine were added, and the solution was stirred at room temperature for 30 min. The volatile components were removed from the filtrate under reduced pressure to give a yellow oil. The oil was purified by flash chromatography (SiO_2, hexanes/ethyl acetate/methanol elution gradient 1:1:0/2:3:0/0:1:0/0:9:1) to give 0.007 g (76%) of **11** as a white foam: R_f 0.34 (100% ethyl acetate); IR (thin film, cm^{-1}) 3338, 2932, 1751, 1723, 1655, 1580, 1423, 1393, 1369, 1329, 1235, 1193, 1135, 1029, 996, 844, 806, 733; ^1H NMR (700 MHz, $CDCl_3$) δ 7.34-7.27 (m, 8H), 7.22-7.19 (m, 4H), 7.14-7.13 (m, 1H), 6.26 (broad s, 1H), 5.07 (s, 2H), 5.02 (s, 2H), four protons of conformers: [4.25, 3.96 (qAB, *J* = 15 Hz), 4.20, 4.15 (qAB, *J* = 15 Hz)], 4.02 (s, 3H), two protons of conformers: [3.65 (qd, *J* = 4.9 Hz), 3.35 (s)], 3.15 (s, 3H), 2.01 (s, 3H), 1.95 (s, 3H); ^{13}C NMR (500 MHz, $CDCl_3$) δ 170.0, 169.0, 167.2, 167.1, 166.1, 153.5, 141.6, 139.6, 136.4, 135.6, 135.3, 133.9, 131.4, 131.3, 127.8, 111.7, 111.3, 69.5, 67.4, 67.1, 53.7, 42.2, 36.3, 23.4, 15.3; HRMS (ESI-TOF) *m/z*: $[M+CHO_2]^-$ calcd for $C_{39}H_{37}O_{12}N_2Br_2$ 885.0700, found 885.0709.

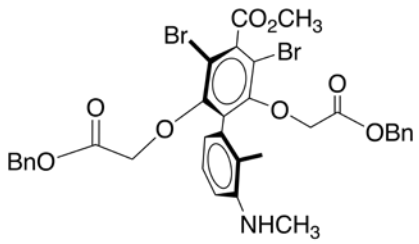

Dibenzyl 2,2'-((3,5-dibromo-4-(methoxycarbonyl)-2'-methyl-3'-(methylamino)-[1,1'-biphenyl]-2,6-diyl)bis(oxy))diacetate (12). 0.1 g (0.14 mmol) of **31** and 0.025 g (0.17 mmol) of **42** in THF (0.1 mL) were sonicated for 5 minutes to give a homogenous solution. The mixture was then diluted with EtOH (0.16 mL) and stirred at room temperature for 12 h. Volatile components were removed under reduced pressure, and reaction vial was cooled to 0 °C for 10 minutes. The residue was rinsed with chilled, dry DCM followed by hexanes to produce an off-white solid. The precipitate was isolated and taken up into DCM, dried over K_2CO_3, filtered, and volatile components were removed under reduced pressure to give an off-white solid. The dry intermediate was dissolved in THF (0.3 mL), and 0.01 g (0.18 mmol) of $NaBH_4$ were added and stirred for 14 h. The reaction mixture was concentrated under reduced pressure and the residue was diluted with ice, cold H_2O, and DCM; the organic layer was extracted and aqueous layer washed with additional DCM (2 x 4 mL). The combined organic layers were washed with additional H_2O (5 mL) and then brine (5 mL); the organic layer was dried over $MgSO_4$, filtered, and volatile components were removed from the filtrate under reduced pressure to give a yellow foam. The foam was purified by flash chromatography (SiO_2, hexanes/ethyl acetate, elution gradient 7:1/6:1) to yield 0.040 g (41%) of **12** as a white foam: R_f 0.38 (hexanes/ethyl acetate 2:1; IR (thin film, cm^{-1}) 3432, 3059, 2978, 2303, 2053, 1648, 1420, 1375, 1241, 1122, 892, 743; ^1H NMR (400 MHz, $CDCl_3$) δ 7.33 (broad s, 5H), 7.26 (broad s, 5H), 7.12 (t, J = 8 Hz, 1H), 6.59 (d, J = 8 Hz, 1H), 6.53 (d, J = 8 Hz, 1H), 5.04 (s, 4H), 4.12, 4.00 (ABq, J = 15 Hz, 4H) 4.01 (s, 3H), 3.66 (broad s, 2H), 2.87 (s, 3H),

1.86 (s, 3H); ^{13}C NMR (500 MHz, $CDCl_3$) δ 167.7, 166.4, 153.7, 147.9, 138.7, 135.5, 132.3, 131.1, 128.9, 128.8, 128.6, 127.2, 121.4, 119.2, 111.0, 109.9, 69.4, 67.0, 53.6, 31.2, 30.1, 28.7, 14.6, 14.5; HRMS (ESI-TOF) *m/z*: $[M+H]^+$ calcd for $C_{34}H_{32}Br_2NO_8$ 742.0495, found 742.0496.

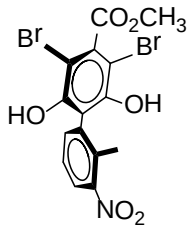

Methyl 3,5-dibromo-2,6-dihydroxy-2'-methyl-3'-nitro-[1,1'-biphenyl]-4-carboxylate (13). In an oven-dried round-bottom flask, 0.26 ml (4.12 mmol) of Br_2 in CCl_4 (2.9 mL) was added dropwise over 30 min to a stirred solution of 0.52 g (1.72 mmol) of **14** in CCl_4 (7 mL) in the dark. The reaction mixture was stirred for 1 h. Saturated $NaHSO_3$ was then added until red color dissipated. Mixture was diluted with ether (30 mL) and organic layer was extracted. The aqueous layer was washed with additional ether (2 x 30 mL). The combined organic layers were washed with brine (75 mL), dried over $MgSO_4$ and filtered, and the volatile components were removed from the filtrate under reduced pressure to yield a brown oil. The oil was purified by flash column chromatography to give 0.60 g (76%) of **13** as an off-white foam: R_f 0.36 (hexanes/ethyl acetate, 4:1); mp 158-159 °C; IR (thin film, cm^{-1}) 3431, 2101, 1642, 1264, 790; ^{1}H NMR (400 MHz, $CDCl_3$) δ 7.90 (dd, *J* = 7, 2 Hz, 1H), 7.44-7.39 (m, 2H), 5.91 (broad s, 2H), 4.02 (s, 3H), 2.28 (s, 3H); ^{13}C NMR (600 MHz, $CDCl_3$) δ 166.0, 151.1, 150.5, 137.0, 135.0, 134.6, 132.9, 126.8, 124.9, 115.7, 99.3, 53.7, 16.4; HRMS (ESI-TOF) *m/z*: calcd for $C_{15}H_{11}NO_6Br_2$ 461.8900, found 461.8882.

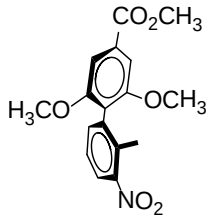

Methyl 2,6-dimethoxy-2'-methyl-3'-nitro-[1,1'-biphenyl]-4-carboxylate (14). In a round-bottom flask, 1.45 g (5.29 mmol) of benzoate **15**, 2.08 g (7.94 mmol) of boronic ester **8**, 0.19 g (0.21 mmol) of $Pd_2(dba)_3$, 0.35 g (0.85 mmol) of SPhos, and 3.66 g (15.87 mmol) of $K_3PO_4 \bullet H_2O$ (ground) were added and dried under reduced pressure for 5 minutes and backfilled with nitrogen two times. Toluene (30 ml) was added, and the solution was degassed using the freeze-pump-thaw method three times under a nitrogen atmosphere. The flask was sealed; the reaction mixture was stirred at 90 °C for 18 h and cooled to room temperature. The mixture was diluted with DCM (150 mL) and H_2O (150 mL); the organic layer was extracted, and the aqueous layer was washed with additional DCM (3 x 150 mL). The combined organic layers were washed with brine (200 mL), dried over $MgSO_4$ and filtered. Volatile components were removed from the filtrate under reduced pressure to give a reddish brown crude oil. The oil was purified by flash chromatography (SiO_2, hexanes/ethyl acetate, elution gradient, 8:1/6:1) to give 1.19 g (74%) of **14** as a pale yellow solid: R_f 0.28 (hexanes/ethyl acetate, 4:1); mp 119-120 °C; IR (thin film, cm^{-1}) 3436, 2919, 2881, 1721, 1580, 1527, 1456, 1434, 1409, 1351, 1326, 1242, 1126, 997, 770; ^{1}H NMR (400 MHz, $CDCl_3$) δ 7.84 (dd, *J* = 6, 3 Hz, 1H), 7.36-7.34 (m; 4H), 3.97 (s ,3H), 3.78 (s, 6H), 2.20 (s, 3H); ^{13}C NMR (400 MHz, $CDCl_3$) δ 167.0, 157.7, 150.9, 137.0, 135.4, 132.6, 131.8, 126.1, 123.8, 121.8, 105.4, 56.3, 52.7, 16.4; HRMS (ESI-TOF) *m/z*: $[M+H]^+$ calcd for $C_{17}H_{18}NO_6$ 332.1134, found 332.1124.

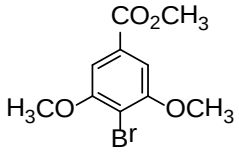

Methyl 4-bromo-3,5-dimethoxybenzoate (15). To a stirred solution of 2.50 g (10.7 mmol) of carboxylic acid **9** and 6.2 g (45.1 mmol) of K_2CO_3 in acetone (67.0 mL), 3.46 mL (36.5 mmol) of dimethyl sulfate was added. The mixture was stirred at reflux for 4.5 h, and cooled to room temperature. Volatile components were removed under reduced pressure. The residue was then diluted with ethyl acetate (75 mL) and H_2O (75 mL); the organic layer was extracted, and the aqueous layer was washed with additional ethyl acetate (2 x 75 mL). The combined organic layers were washed with brine (200 mL), dried over $MgSO_4$ and filtered, and the volatile components were removed under reduced pressure to yield a white solid. The solid was purified by recrystallization to give 2.9 g (100%) of benzoate **15** as white crystals: R_f 0.45 (hexanes/ethyl acetate, 4:1); mp 121-122˚C ; IR (thin film, cm^{-1}) ; ^1H NMR (300 MHz, $CDCl_3$) δ 7.23 (s, 2H), 3.95 (s, 6H), 3.93 (s, 3H); ^{13}C NMR (300 MHz, $CDCl_3$) 166.7, 157.3, 130.4, 106.9, 105.8, 56.9, 52.7; HRMS (ESI-TOF) *m/z* calc for $C_{10}H_{11}BrO_4$ 273.98, found 273.9829.

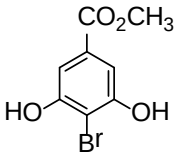

Methyl 4-bromo-3,5-dihydroxybenzoate (16). To 1.0 g (4.4 mmol) of carboxylic acid **9** in 6.8 mL of methanol was added .41 mL (7.6 mmol) of H_2SO_4 dropwise, and the reaction mixture was refluxed for 16 h. The reaction was quenched by addition of $NaHCO_3$ (1.2 g, 14.8 mmol) and the volatile components were removed under reduced pressure. The residue was diluted with ethyl acetate (25 mL) and water (25 mL); the organic layer was extracted, and the aqueous layer was washed with additional ethyl acetate (3 x 25 mL). The organic layers were dried over $MgSO_4$ and

filtered, and the volatile components were removed from the filtrate under reduced pressure to give 1.05 g (99%) of **16** as a white solid: R_f 0.34 (hexanes/ethyl acetate 3:2); mp 225-227 °C; IR (thin film, cm^{-1}) 3416, 3329, 1701, 1594, 1421, 1353, 1270, 1233, 1118, 1033, 990, 907, 857, 760, 705; ^1H NMR (300 MHz, MeOD) δ 7.03 (s, 2H), 4.85 (broad s, 2H), 3.85 (s, 3H); ^{13}C NMR (600 MHz, MeOD) δ 168.1, 156.7, 131.0, 108.6, 105.1, 52.7; HRMS (EI) *m/z* calcd for $C_8H_7O_4Br$ 245.9528, found 245.9519.

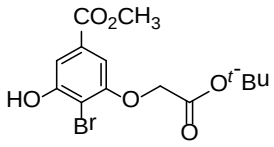

Methyl 4-bromo-3-(-2-tert-butoxy-2-oxoethoxy)-5-hydroxybenzoate (18). In a round-bottom flask, 1.0 g (4.2 mmol) of benzoate **16**, 0.62 mL (4.2 mmol) of *t*-butyl bromoacetate, 1.2 g (8.8 mmol) of K_2CO_3, and 0.05 g (0.2 mmol) of 18-crown-6 were dissolved in acetone (21.0 mL), and the reaction mixture was refluxed for 24 h. The volatile components were removed under reduced pressure, and the residue was diluted with ethyl acetate (50 mL) and water (50 mL); the organic layer was extracted, and the aqueous layer was washed with additional ethyl acetate (2 x 50 mL). The organic layers were dried over $MgSO_4$ and filtered, and the volatile components were removed from the filtrate under reduced pressure to give a crude yellow oil. The oil was purified by flash chromatography (SiO_2, hexanes/ethyl acetate, elution gradient 5:1/3:2/0:1) to give 0.49 g (32.4%) of **18** as a white solid: R_f 0.44 (hexanes/ethyl acetate 3:2); mp 117-118 °C; IR (thin film, cm^{-1}) 3393, 2923, 2852, 1724, 1590, 1497, 1438, 1354, 1247, 1158, 1117, 1011, 904, 870, 843, 767; ^1H NMR (400 MHz, $CDCl_3$) δ 7.24 (s, 1H), 6.92 (s, 1H), 6.41 (s, 1H), 4.57 (s, 2H), 3.81 (s, 3H), 1.18 (s, 9H); ^{13}C NMR (500 MHz, $CDCl_3$) δ 166.9, 166.0, 154.9, 153.7, 130.6, 110.4, 105.8, 105.2, 82.9, 66.4, 52.5, 28.0; HRMS (EI) *m/z* calculated for $C_{14}H_{17}BrO_6$ 360.0209, found 360.0205.

Benzoate **17** was generated as the major product (48%) en route to benzoate **18.** HRMS (EI) *m/z* calcd for $C_{14}H_{17}O_6Br$ 360.0209, found 360.0205.

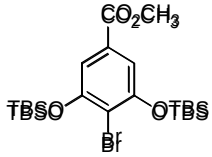

Methyl 4-bromo-3,5-bis((tert-butyldimethylsilyl)oxy)benzoate (23). To a stirred solution of 0.76 g (5.1 mmol) *tert*-butyldimethylsilyl chloride in 2.9 mL of THF, 0.5 g (2.0 mmol) **16** and 0.9 mL (6.5 mmol) TEA in THF (7.2 mL) was added and stirred for 15 h at room temperature. The mixture was diluted with Et_2O (30 mL) and H_2O (30 mL); the organic layer was extracted, and the aqueous layer was washed with additional Et_2O (3 x 30 mL). The combined organic layers were dried over $MgSO_4$ and filtered, and volatile components removed under reduced pressure to give a crude white powder. The powder was purified by flash chromatography (SiO_2, hexanes/ethyl acetate, 20:1) to afford 0.87 g (90.8%) of **23** as a white crystal: R_f 0.81 (hexanes/ethyl acetate, 4:1); mp ˚C ; IR (thin film, cm^{-1}); ^1H NMR (300 MHz, $CDCl_3$) δ 7.16 (s, 2H), 3.89 (s, 3H), 1.05 (s, 18H), 0.26 (s, 12H); ^{13}C NMR (400 MHz, $CDCl_3$) δ 166.7, 157.3, 130.4, 106.9, 105.8, 56.9, 53.2, 29.3, 17.1, 4.3; HRMS (ESI-TOF) *m/z* calcd for $C_{20}H_{35}BrO_4Si_2$ 476.12, found 476.1398.

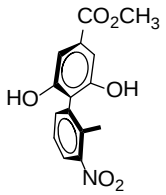

Methyl 2,6-dihydroxy-2'-methyl-3'-nitro-[1,1'-biphenyl]-4-carboxylate (24). In a third-flame dried round-bottom flask, 5.35 g (21.36 mmol) of a 1.0 M solution of BBr_3 in DCM was added dropwise over 30 minutes to a stirred solution of 1.18 g (3.56 mmol) of **14** in DCM (8 mL) at 0 °C. The reaction mixture was stirred at 0 °C for 3 hours and gradually warmed to room temperature

and stirred for an additional 21 h. The volatile components were removed under reduced pressure. The residue was charged with nitrogen and slowly diluted with MeOH (7 mL). 0.33 mL (6.14 mmol) of H_2SO_4 was added dropwise at 0 °C. The reaction mixture was then heated to reflux for 20 h. After cooling to room temperature, the reaction was quenched by addition of $NaHCO_3$ (1.03 g, 12.3 mmol) and the volatile components were removed under reduced pressure. The residue was diluted with ethyl acetate (75 mL) and H_2O (75 mL); the organic layer was extracted, and the aqueous layer was washed with additional ethyl acetate (2 x 75 mL). The combined organic layers were washed with brine (200 mL), dried over $MgSO_4$ and filtered. Volatile components were removed from the filtrate under reduced pressure to yield a brown oil. The oil was purified by flash column chromatography (SiO_2, hexanes/ethyl acetate, elution gradient, 2:1) to give 0.84 g (78%) of **24** as a white solid: R_f 0.22 (hexanes/ethyl acetate, 2:1); mp 160-161 °C; IR (thin film, cm^{-1}) 3310, 2524, 2219, 2043, 1653, 1451, 1113, 1034; ^1H NMR (300 MHz, $CDCl_3$) δ 7.92 (d, *J* = 6 Hz, 1H), 7.49-7.47 (m, 2H), 7.31 (s, 2H), 5.71 (broad s, 2H), 3.92 (s, 3H), 2.31 (s, 3H); ^{13}C NMR (400 MHz, $CDCl_3$) δ 154.4, 151.7, 135.53, 134.6, 133.7, 131.9, 127.5, 125.2, 118.6, 109.5, 53.0, 16.4; HRMS (ESI-TOF) *m/z*: $[M+H]^+$ calcd for $C_{15}H_{14}NO_6$ 304.0821, found 304.0837.

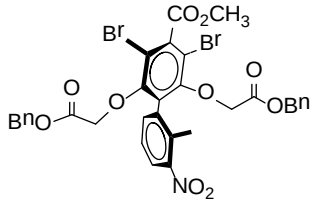

Dibenzyl 2,2'-((3,5-dibromo-4-(methoxycarbonyl)-2'-methyl-3'-nitro-[1,1'-biphenyl]-2,6-diyl)bis(oxy))diacetate (30). In an oven-dried round bottom flask, 0.46 g (1.0 mmol) of **13**, 0.38 mL (2.4 mmol) of benzyl bromoacetate, 0.42 g (3.0 mmol) of K_2CO_3, and 0.10 g (0.40 mmol) of 18-crown-6 were dissolved in acetone (11.1 mL), and the reaction mixture was refluxed for 24 h.

The volatile components were removed from the filtrate under reduced pressure, and the residue was diluted with DCM (30 mL) and water (30 mL); the organic layer was extracted, and the aqueous layer was washed with additional DCM (3 x 30 mL). The combined organic layers were washed with brine (90 mL), dried over $MgSO_4$ and filtered, and the volatile components were removed from the filtrate under reduced pressure to give a crude yellow oil. The oil was purified by flash chromatography (SiO_2, hexanes/ethyl acetate, elution gradient 6:1) to yield 0.60 g (80%) of **30** as a light yellow foam: R_f 0.48 (hexanes/ethyl acetate 2:1); ^{1}H NMR (400 MHz, CD_2Cl_2) δ 7.82 (d, *J* = 8 Hz, 1H), 7.43 (d, *J* = 8 Hz, 1H), 7.36-7.34 (m, 6H), 7.30 – 7.24 (m, 5H), 5.02 (q, *J* = 4 Hz, 4H), 4.22, 4.10 (ABq, J_{AB} = 15 Hz, 4H), 2.30 (s, 3H); ^{13}C NMR (400 MHz, CD_2Cl_2) δ 167.2, 166.1, 154.0, 151.3, 140.4, 135.8, 135.5, 134.5, 133.1, 131.0, 129.1, 129.0, 128.9, 127.1, 125.5, 111.7, 70.0, 67.4, 17.2; HRMS (ESI-TOF) *m/z*: $[M+H]^+$ calcd for $C_{33}H_{28}NO_{10}Br_2$ 758.01052, found 758.0080.

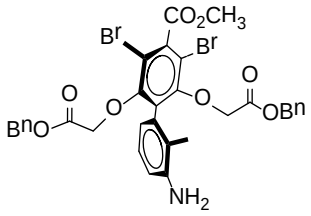

Dibenzyl 2,2'-((3'-amino-3,5-dibromo-4-(methoxycarbonyl)-2'-methyl-[1, 1'-biphenyl]-2,6-diyl)bis(oxy))diacetate (31). 0.5 g (0.67 mmol) of **30** were dissolved in ethyl acetate (11 ml) and concentrated HCl (0.33 ml). The solution was cooled to 0 °C and Zn powder (.21 g, 3.3 mmol) was added in portions over 20 min with stirring. The mixture was gradually warmed to room temperature and stirred for 15 h. The reaction mixture was passed through a Celite plug and washed with ethyl acetate (5 ml). The filtrate was washed with saturated $NaHCO_3$ solution (1 x 5 ml), water (1 x 5 ml), and brine (1 x 10 ml). The organic layer was dried over anhydrous $MgSO_4$,

filtered, and volatile components were removed from the filtrate under reduced pressure to give a crude yellow oil. The oil was purified by flash chromatography (SiO_2, hexanes/ethyl acetate, elution gradient 3:1/2:1) to yield 0.41 g (82%) of **31** as a light yellow foam: R_f 0.21 (hexanes/ethyl acetate 2:1); mp 58-59 °C; ^{1}H NMR (400 MHz, $CDCl_3$) δ 7.34-7.30 (m, 5H), 7.28-7.25 (m, 5H), 6.99 (t, *J* = 8 Hz, 1H), 6.64 (d, *J* = 8 Hz, 1H), 6.58 (d, *J* = 7 Hz, 1H), 5.05 (s, 4H), 4.17, 4.00 (ABq, J_{AB} = 15 Hz, 4H), 4.01 (s, 3H), 3.61 (broad s, 2H), 1.90 (s, 3H); ^{13}C NMR (400 MHz, $CDCl_3$) δ 167.6, 166.4, 153.6, 145.6, 138.7, 135.4, 132.1, 131.6, 128.9, 128.8, 128.7, 126.9, 121.9, 120.9, 115.9, 111.0, 69.4, 67.0, 53.6, 30.0, 14.8; HRMS (ESI-TOF) *m/z*: $[M+H]^+$ calcd for $C_{33}H_{30}NO_8Br_2$ 728.02395, found 728.02593.

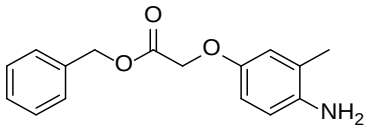

Benzyl 2-(4-amino-3-methylphenoxy)acetate (34). In a round bottom flask **32** (0.38 g, 0.50 mmol) was dissolved in ethyl acetate (10 ml) and concentrated HCl (0.25 ml). The solution was cooled to 0˚C and Zn powder (0.23 g, 3.51 mmol) was added in portions over 20 min with stirring. The mixture warmed to room temperature and stirred for 15 h. The reaction mixture was passed through a Celite plug and washed with ethyl acetate (5 ml). The filtrate was washed with satd. $NaHCO_3$ solution (1 x 5 ml), water (2 x 5 ml), and brine (1 x 10 ml). The organic layer was dried over anhydrous $MgSO_4$, filtered, and volatile components removed under reduced pressure to give a crude brown oil. The oil was purified by flash chromatography (SiO_2, hexanes/ethyl acetate, elution gradient 7:1/6:1/3:1) to yield 3.26 g (90.2%) of **34** as a white solid: R_f 0.48 (hexanes/ethyl acetate 3:2); mp 68-70 ˚C; IR (thin film, cm^{-1}) 3945, 3688, 3055, 2987, 2685, 2411, 2306, 1760, 1610, 1582, 1517, 1489, 1440, 1422, 1343, 1265, 1196. 1173, 1097, 958, 896, 839, 739; ^{1}H NMR

(300 MHz, $CDCl_3$) 2.11 δ (s, 3H), 3.37 (s, 2H), 4.57 (s, 2H), 5.22 (s, 2H), 7.30-7.40 (m, 5H); HRMS (ESI-TOF) *m/z* calcd for $[M+H]^+$ $C_{16}H_{17}NO_3$ 272.1200, found 272.1290.

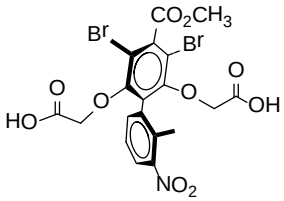

2,2'-((3,5-dibromo-4-(methoxycarbonyl)-2'-methyl-3'-nitro-[1,1'-biphenyl]-2,6-diyl)bis(oxy))diacetic acid (35). To a nitrogen charged flask, 0.03 g (.04 mmol) of **30** and 0.01 g (0.04mmol) of PtO_2 were added and dried under reduced pressure for 5 minutes and backfilled with nitrogen twice. Under hydrogen atmosphere, ethyl acetate (1 mL) was added and stirred for 2 hours. The reaction mixture was passed through a Celite plug and washed with ethyl acetate (3 ml). Volatile components removed under reduced pressure to obtain .01 g (39%) of **35** as a glass-like foam. R_f 0.1 (9:1 ethyl acetate:MeOH); IR (thin film, cm^{-1}); ^1H NMR (400 MHz, $CDCl_3$) δ 7.79 (d, *J* = 8 Hz, 1H) 7.46-3.39 (m, 2H), 7.16 (broad s, 2H), 4.24,4.15 (ABq, *J* = 16,15 Hz, 4H), 4.04, (s, 3H), 2.32 (s, 3H); ^{13}C NMR (400 MHz, $CDCl_3$) δ 198.3, 165.1, 151.2, 150.9, 138.7, 136.3, 133.8, 132.2, 127.9, 124.6, 100.5, 54.0, 29.6, 15.1; HRMS (ESI-TOF) *m/z* calcd for $[M-H]^-$ $C_{19}H_{15}Br_2NO_{10}$ 575.90, found 575.89710.

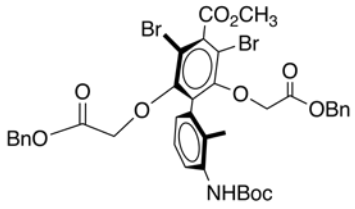

Dibenzyl 2,2'-((3,5-dibromo-3'-((tert-butoxycarbonyl)amino)-4-(methoxycarbonyl)-2'-methyl-[1,1'-biphenyl]-2,6-diyl)bis(oxy))diacetate (36). In a round-bottom flask, 0.20 g (.27 mmol) of **31** and 0.12 g (.54 mmol) of Boc anhydride were dissolved in THF (5 mL), and the reaction mixture

was heated to 60 ˚C for 32 h. The volatile components were removed under reduced pressure; the residue was diluted with DCM (15 mL), washed with 1.0 M HCl (2 x 15 mL) and water (15 mL), dried over MgSO4 and filtered, and the volatile components were removed under reduced pressure to give a crude light pink solid. The foam was purified by flash chromatography (SiO_2, hexanes/ethyl acetate, elution gradient 7:1/6:1/3:1) to yield .2 g (89%) of **36** as an off-white solid: R_f 0.49 (hexanes/ethyl acetate 2:1); IR (thin film, cm^{-1}) 3429, 3055, 2975, 2305, 2092, 1643, 1422, 1265, 896, 745; ^{1}H NMR (300 MHz, $CDCl_3$) δ 7.93 (d, *J* = 8, 1H), 7.37-7.31 (m, 5H), 7.25-7.14 (m, 5H), 7.17 (t, *J* = 8 Hz, 1H) 6.89 (d, *J* = 8 Hz, 1H), 6.31 (broad s, 1H), 5.03 (q, *J* = 2 Hz, 4H), 4.13,3.96 (ABq, *J* = 15 Hz, 4H) 4.01 (s, 3H), 1.98 (s, 3H), 1.54 (s, 9H); ^{13}C NMR (300 MHz, $CDCl_3$) δ 167.3, 166.1, 153.5, 153.1, 139.0, 137.5, 135.3, 131.7, 131.5, 128.7, 128.7, 126.8, 126.6, 125.6, 121.3, 111.2, 80.9, 69.3, 67.06, 53.5, 28.6, 28.6, 15.1; HRMS (ESI-TOF) *m/z* calcd for $[M+H]^+$ $C_{38}H_{37}Br_2NO_{10}$ 828.0800, found.828.08016.

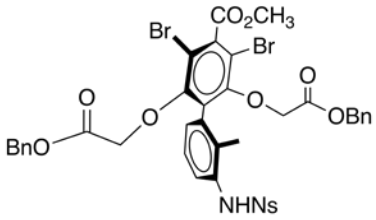

Dibenzyl 2,2'-((3,5-dibromo-4-methoxycarbonyl)-2'-methyl-3'-(4-nitrophenylsulfonamido)-(1,1'-biphenyl-2,6-diyl)bis(oxy))diacetate (39). A solution of 0.05 g (0.23 mmol) nosyl chloride in 2.3 mL of DCM was added dropwise over 15 min to a stirred solution of 0.18 g (0.25 mmol) of **31** and 0.02 mL of pyridine (0.25 mmol) in DCM (3 mL). The resulting mixture was stirred at room temperature for 12 h. A 1.0 M HCl solution (5 mL) was added and the acidified aqueous phase was separated and extracted with DCM (3 x 5 mL). The combined organic extracts were washed with brine (10 mL), dried over $MgSO_4$, and volatile components removed under reduced

pressure to give a yellow oil. The oil was purified by flash chromatography (SiO_2, hexanes/ethyl acetate, elution gradient 4:1/3:1) to yield 0.16 g (69%) of **39** as a white solid: R_f 0.43 (hexanes/ethyl acetate 2:1); IR (thin film, cm^{-1}); ^1H NMR (300 MHz, $CDCl_3$) δ 8.20 (d, *J* = 9, 2H), 7.83 (d, *J* = 9, 2H), 7.36-7.31 (m, 5H), 7.26-7.23 (m, 5H), 7.13 (t, *J* = 8 Hz, 1H) 7.06 (d, *J* = 7 Hz, 1H), 6.58 (broad s, 1H), 5.04 (s, 4H), 4.10,3.92 (ABq, *J* = 15 Hz, 4H) 3.99 (s, 3H), 1.69 (s, 3H);^{13}C NMR (300 MHz, $CDCl_3$) δ 167.2, 166.0, 153.4, 150.5, 145.7, 139.5, 135.2, 134.7, 133.0, 132.9, 131.1, 129.5, 129.0, 128.7, 128.6, 127.0, 124.7, 111.4, 69.4, 67.3, 15.5, 14.5; HRMS (ESI-TOF) *m/z* calcd for $[M-H]^-$ $C_{39}H_{32}Br_2N_2O_{12}S$ 911.0000, found 910.9822.

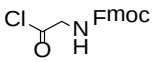

(9H-fluoren-9-yl)methyl (2-chloro-2-oxoethyl)carbamate (45). To a solution of 0.030 g (0.1 mmol) of commercially available Fmoc-gly (**44)** in DCM (0.5 mL) was added 0.07 ml (1.0 mmol) of thionyl chloride ($SOCl_2$) and the reaction mixture was refluxed for 30-45 min. The solution was cooled to room temperature and the volatile components were removed under reduced pressure. The residue was dissolved in minimal DCM followed by hexanes to produce an off-white precipitate. The solid was filtered and dried in vacuo to afford 0.025 g (81%) of **45** as an off-white solid. Only an IR spectra was obtained to confirm this highly reactive intermediate: (thin film, cm-1) 3315, 3066, 2967, 2947, 1811, 1702, 1540, 1477, 1448, 1395, 1349, 1271, 1182, 1104, 1087, 1051, 991, 955, 919, 780, 758, 742.'

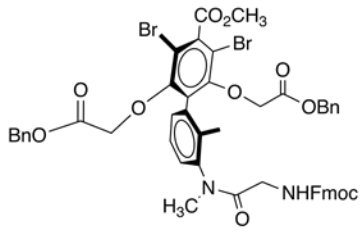

Dibenzyl 2, 2'-((3'-(2-((((9H-fluoren-9-yl)methoxy)carbonyl)amino)-N-methylacetamido)-3,5-dibromo-4-(methoxycarbonyl)-2;-methyl-[1,1'-biphenyl]-2,6-diyl)bis(oxy))diacetate (46). To 0.050 g (0.07 mmol) of **12** in 0.62 mL of $CHCl_3$ was added 0.03 g (0.09 mmol) of Fmoc-gly acid chloride **45** (generated according to above procedure and used immediately thereafter) in 0.37 mL of $CHCl_3$ followed by 0.62 mL of saturated $NaHCO_3$ solution, and the reaction mixture was stirred at room temperature for 20 min. The solution was diluted with DCM (10 mL) and saturated $NaHCO_3$ solution (10 mL), the organic layer was extracted, and the aqueous layer was washed with DCM (3 × 10 mL). The organics were dried over $MgSO_4$ and filtered, and the volatile components were removed from the filtrate under reduced pressure to give a light brown crude oil. The oil was purified by flash chromatography (SiO_2, hexanes/ethyl acetate, elution gradient 5:1/3:1/2:1) to give 0.046 g (67%) of **46** as a white foam: R_f 0.31 (hexanes/ethyl acetate, 1:1); IR (thin film, cm^{-1}) 3392, 2926, 2855, 1751, 1722, 1660, 1581, 1421, 1369, 1329, 1299, 1234, 1193, 1134, 1028, 998, 864, 845, 806, 735; ^1H NMR (400 MHz, $CDCl_3$) δ 7.66 (d, *J* = 7 Hz, 2H), 7.48 (d, *J* = 7 Hz, 2H), 7.32-7.25 (m, 5H), 7.22-7.18 (m, 5H), 7.14-7.06 (m, 7H), 5.49 (broad s, 1H), 4.94 (s, 4H), 4.23-4.14 (m, 4H), 4.10-4.01 (m, 4H), 3.94 (s, 3H), 3.88 (d, *J* = 15 Hz, 2H), 3.65, 3.32 (qd, *J* = 4, 17 Hz, 2H), 3.08 (s, 3H), 1.95 (s, 3H); ^{13}C NMR (400 MHz, $CDCl_3$) δ 168.6, 166.8, 165.8, 156.1, 153.1, 144.0, 143.9, 141.3, 141.3, 139.3, 136.2, 135.1, 135.0, 133.6, 131.0, 128.7, 128.6, 128.5, 128.4, 128.3, 127.7, 127.4, 127.1, 125.2, 120.0, 111.3, 111.0, 69.2, 69.1, 67.0, 66.8,

53.4, 47.1, 43.2, 36.3, 15.3; HRMS (ESI-TOF) *m/z*: $[M+H]^+$ calcd for $C_{51}H_{45}N_2O_{11}Br_2$ 1019.13846, found 1019.13665.

APPENDIX

^{1}H, ^{13}C NMR SPECTRA

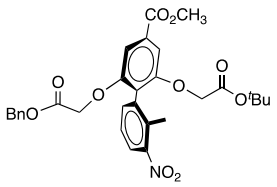
CO2CH3
O
O
BnO
O
O
O
tBu
NO2

6

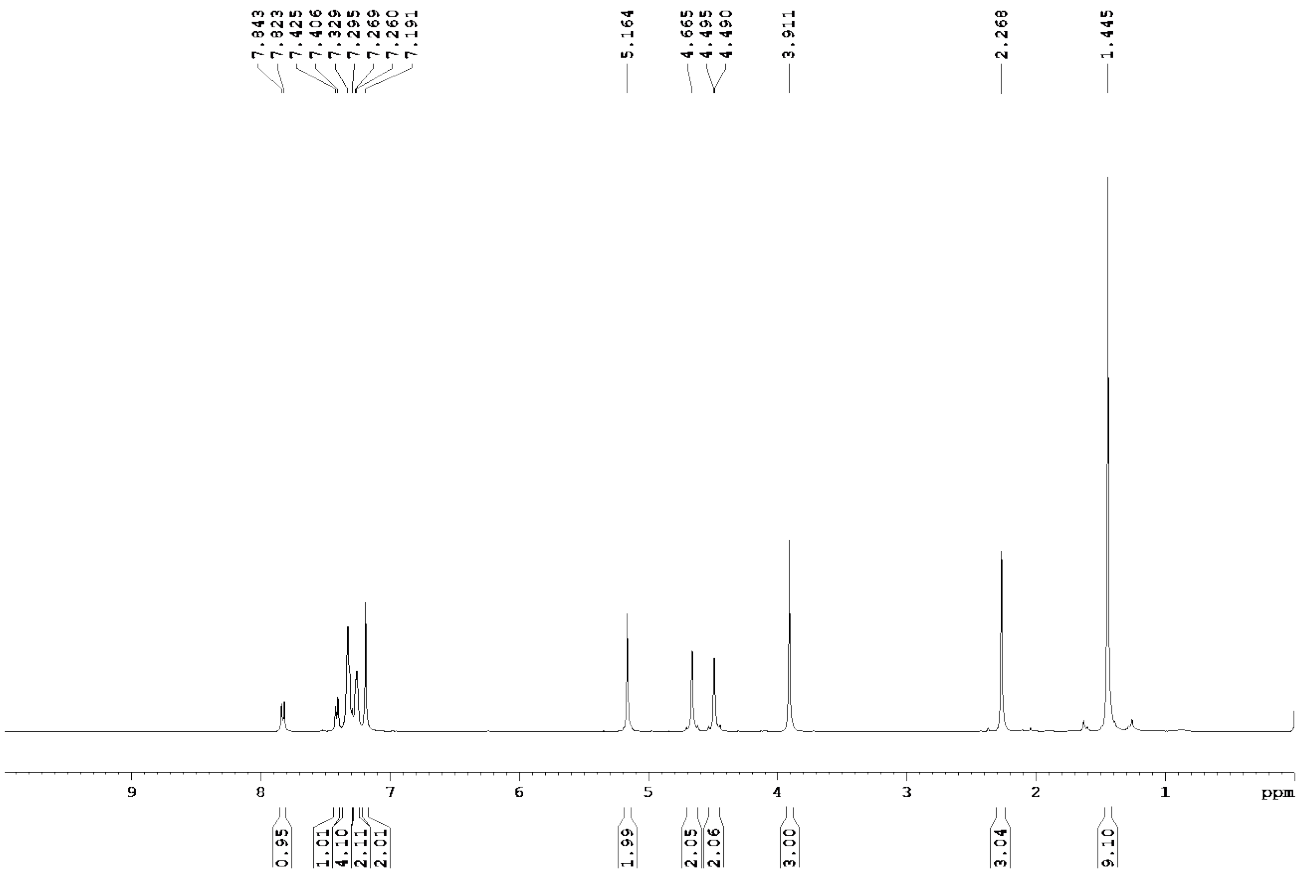
7.843
7.823
7.425
7.406
7.329
7.295
7.269
7.260
7.191
5.164
4.665
4.495
4.490
3.911
2.268
1.445
9
8
7
6
5
4
3
2
1
ppm
0.95
1.01
4.10
2.11
2.01
1.99
2.05
2.08
3.00
3.04
9.10

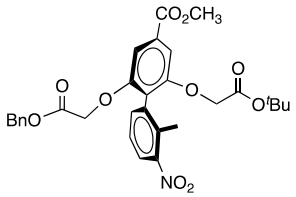
CO2CH3
O
O
BnO
O
O
O
tBu
NO2

6

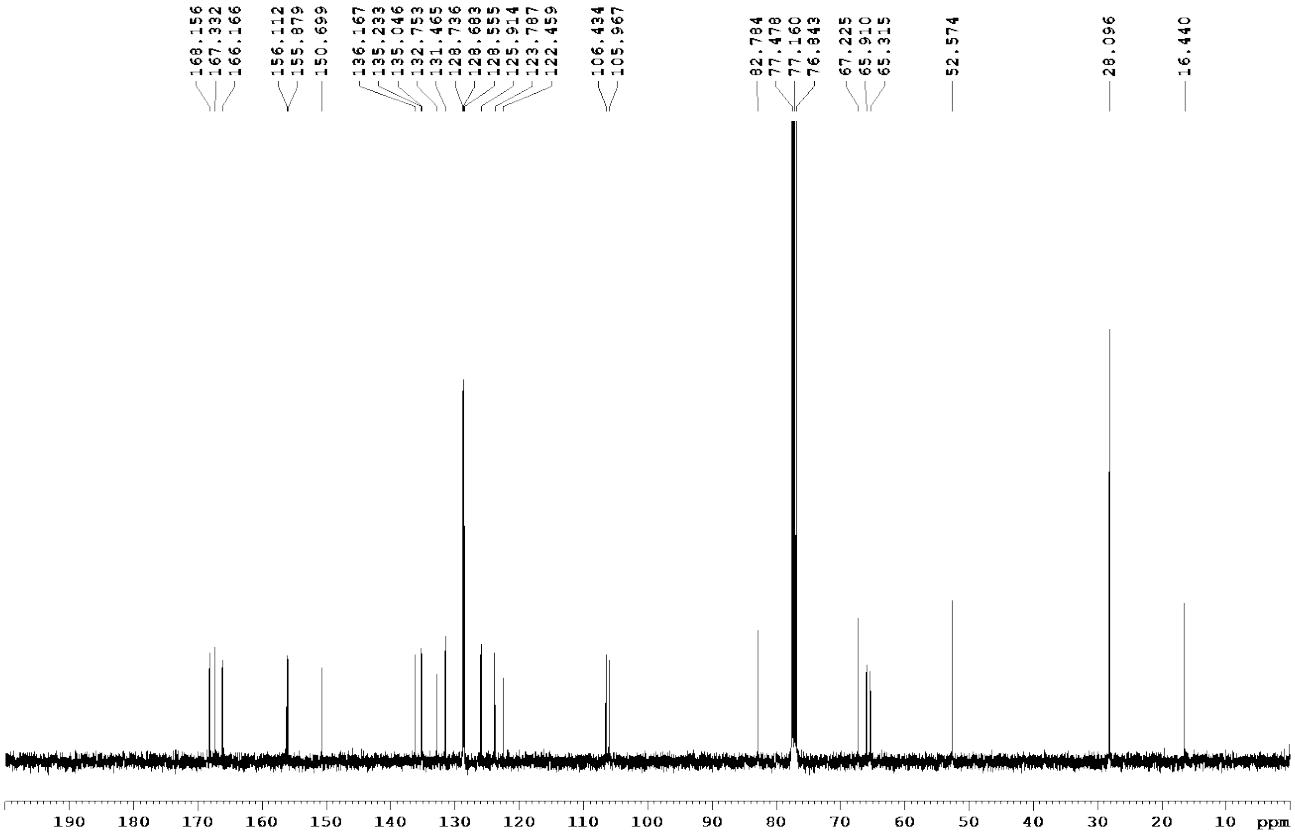
168.156
167.332
166.166
156.112
155.879
150.699
136.167
135.233
135.046
132.753
131.465
128.736
128.683
128.555
125.914
123.787
122.459
106.434
105.967
82.784
77.478
77.160
76.843
67.225
65.910
65.315
52.574
28.096
16.440
190
180
170
160
150
140
130
120
110
100
90
80
70
60
50
40
30
20
10
ppm

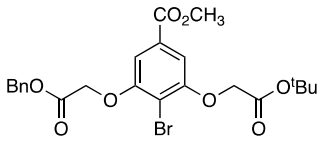
CO2CH3
BnO
O
O
Br
O
O
OtBu
O

7

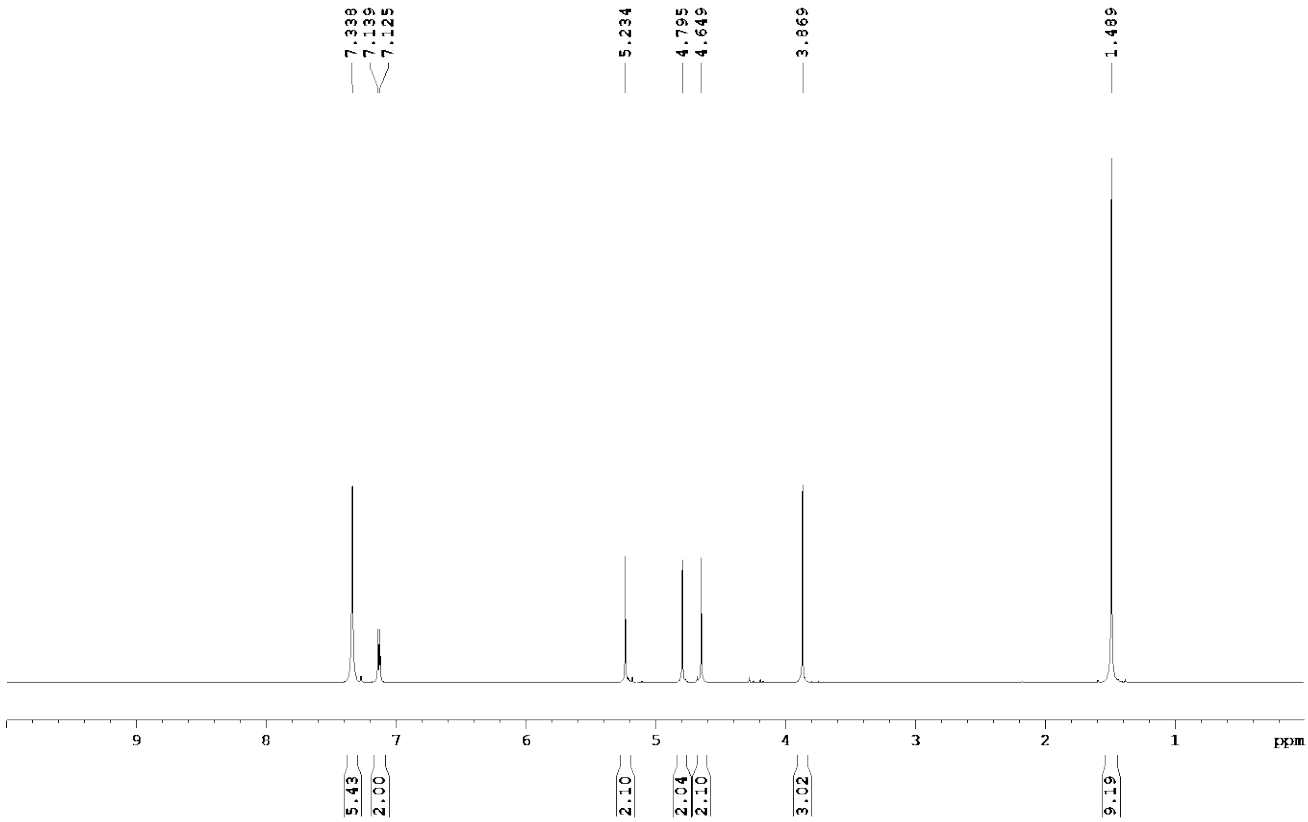
7.338
7.139
7.125
5.234
4.795
4.649
3.869
1.489
9
8
7
6
5
4
3
2
1
ppm
5.43
2.00
2.10
2.04
2.10
3.02
9.19

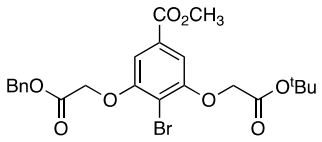
CO2CH3
BnO
O
O
Br
O
O
OtBu
O

7

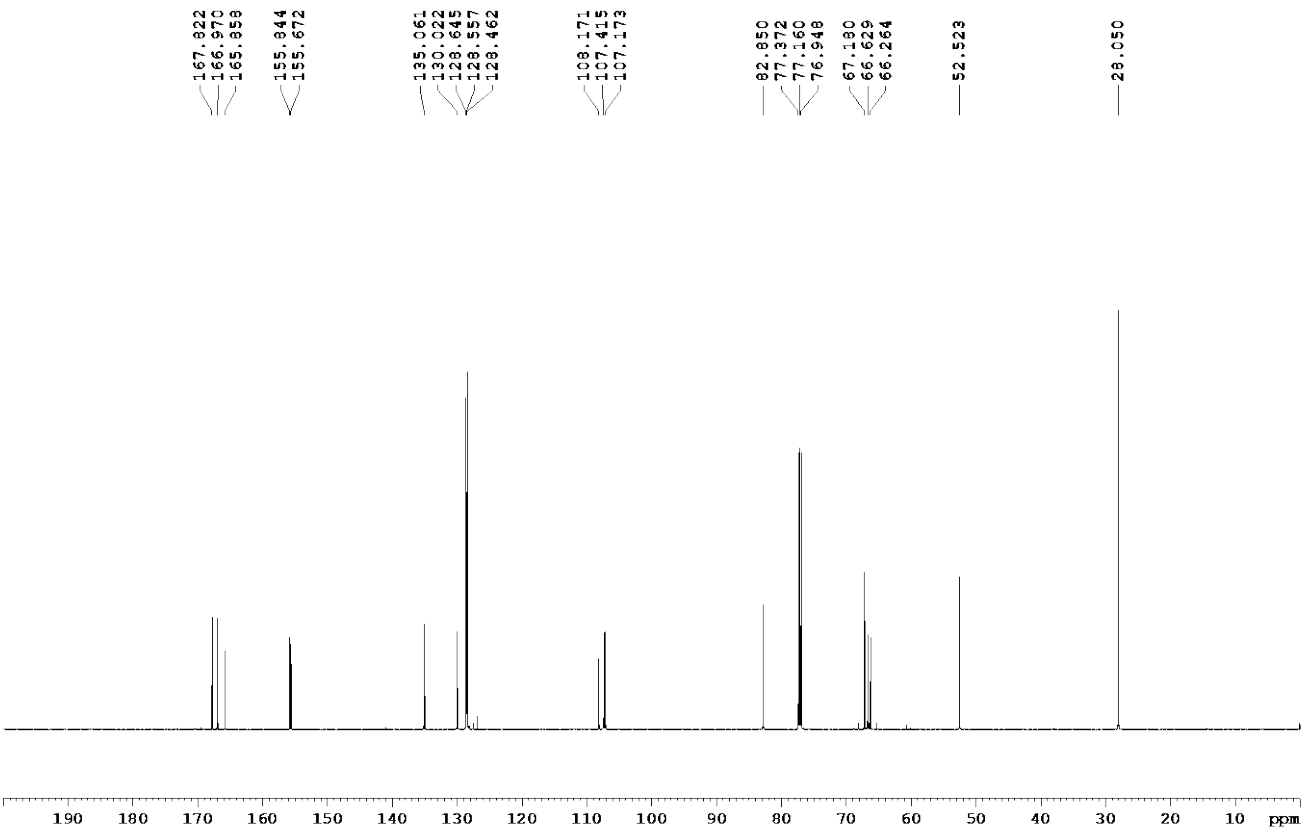
167.822
166.970
165.858
155.844
155.672
135.061
130.022
128.645
128.557
128.462
108.171
107.415
107.173
82.850
77.372
77.160
76.948
67.180
66.629
66.264
52.523
28.050
190
180
170
160
150
140
130
120
110
100
90
80
70
60
50
40
30
20
10
ppm

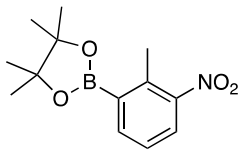
O
B
O
NO2

8

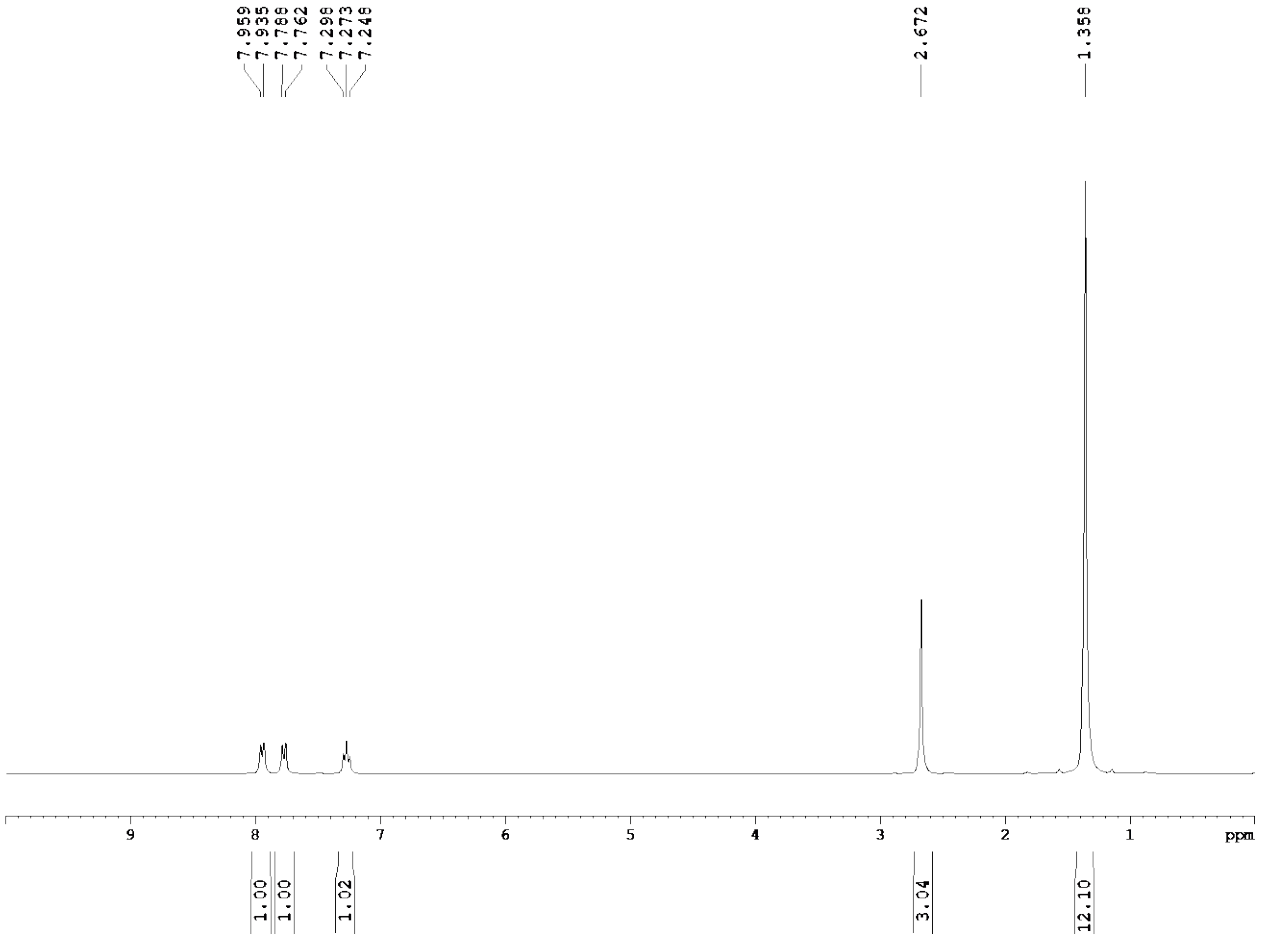
7.959
7.935
7.788
7.762
7.290
7.273
7.249
2.672
1.358
9
8
7
6
5
4
3
2
1
ppm
1.00
1.00
1.02
3.04
12.10

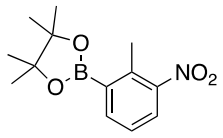

8

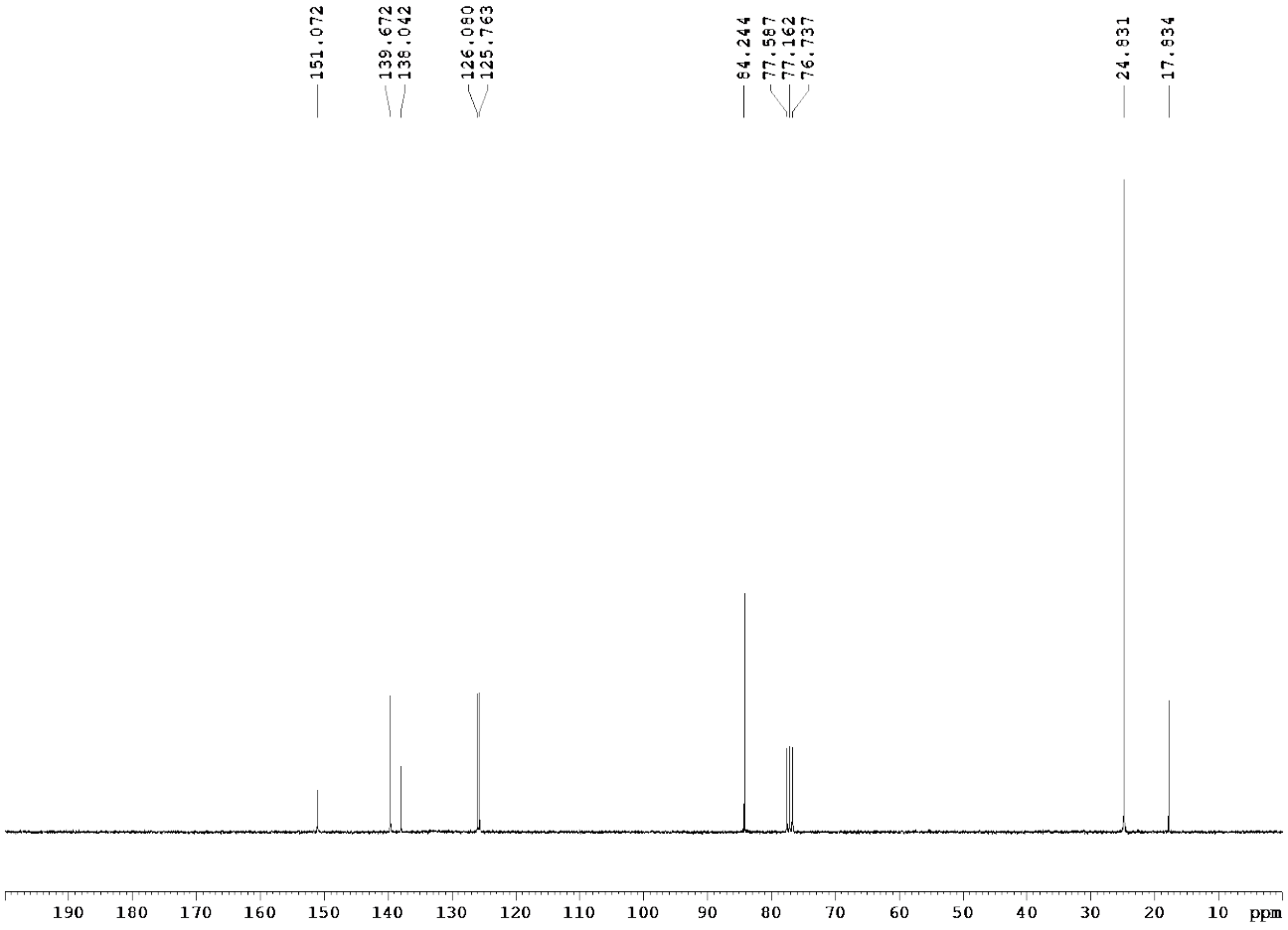
151.072
139.672
136.042
126.060
125.763
84.244
77.587
77.162
76.737
24.831
17.834
190 180 170 160 150 140 130 120 110 100 90 80 70 60 50 40 30 20 10 ppm

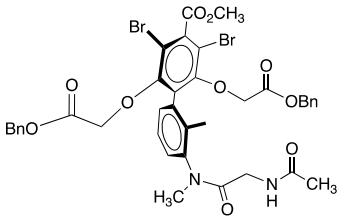
Br
CO2CH3
Br
O
O
O
OBn
BnO
O
O
N
H3C
O
N
H
CH3

11

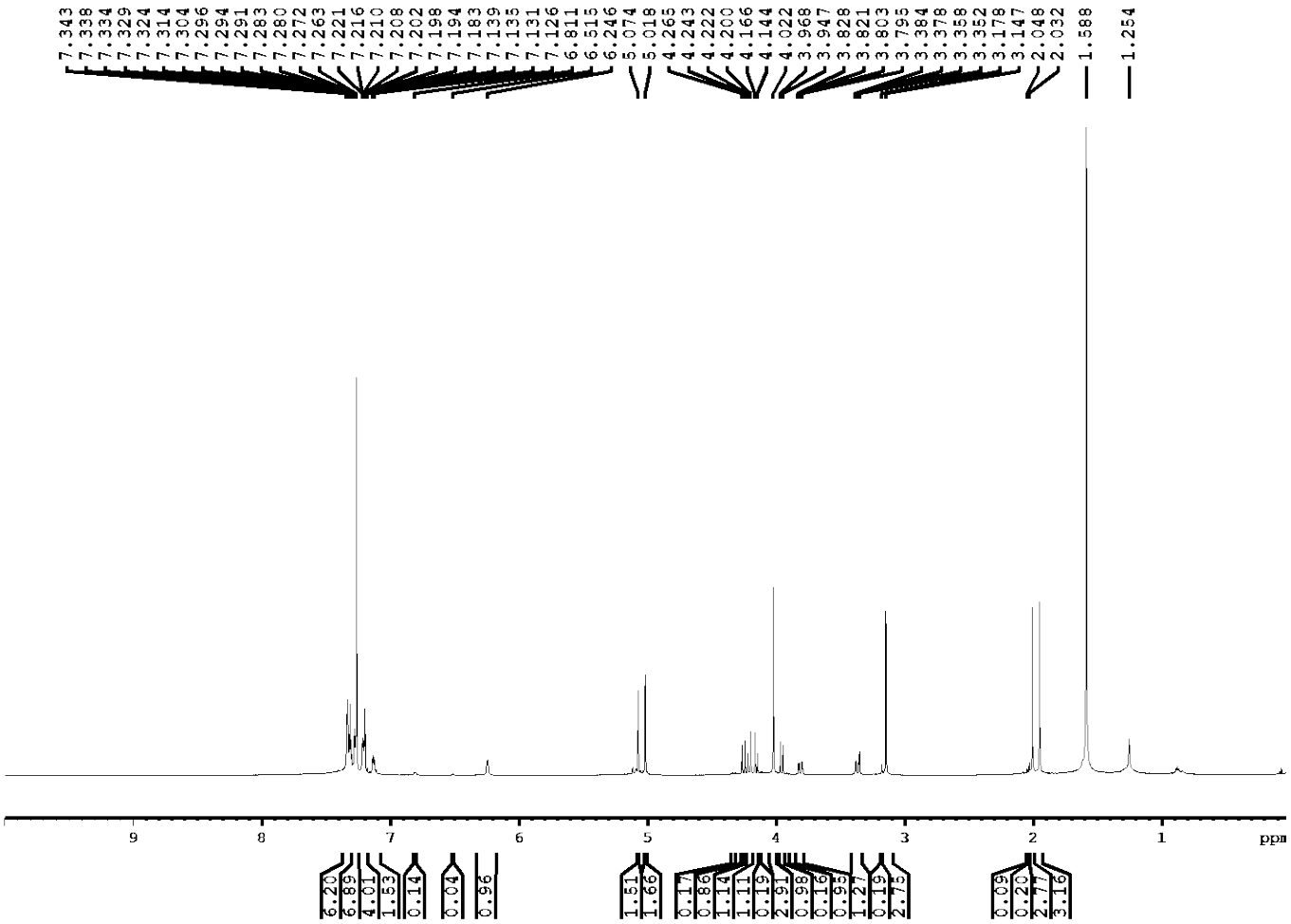
7.343
7.338
7.334
7.329
7.324
7.314
7.304
7.296
7.294
7.291
7.283
7.280
7.272
7.263
7.221
7.216
7.210
7.208
7.202
7.198
7.194
7.183
7.139
7.135
7.131
7.126
6.811
6.515
6.246
5.074
5.018
4.265
4.243
4.222
4.200
4.166
4.144
4.022
3.968
3.947
3.828
3.821
3.803
3.795
3.384
3.378
3.358
3.352
3.178
3.147
2.048
2.032
1.588
1.254
9
8
7
6
5
4
3
2
1
ppm
6.20
6.89
4.01
1.53
0.14
0.04
0.96
1.51
1.66
0.17
0.86
1.14
1.11
0.19
2.91
0.98
0.16
0.95
1.27
0.19
2.75
0.09
0.20
2.77
3.16

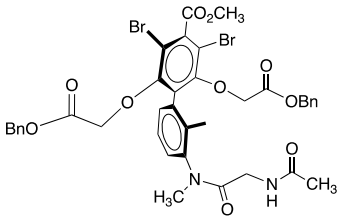
Br
CO2CH3
Br
O
O
OBn
BnO
O
O
N
H3C
O
N
H
O
CH3

11

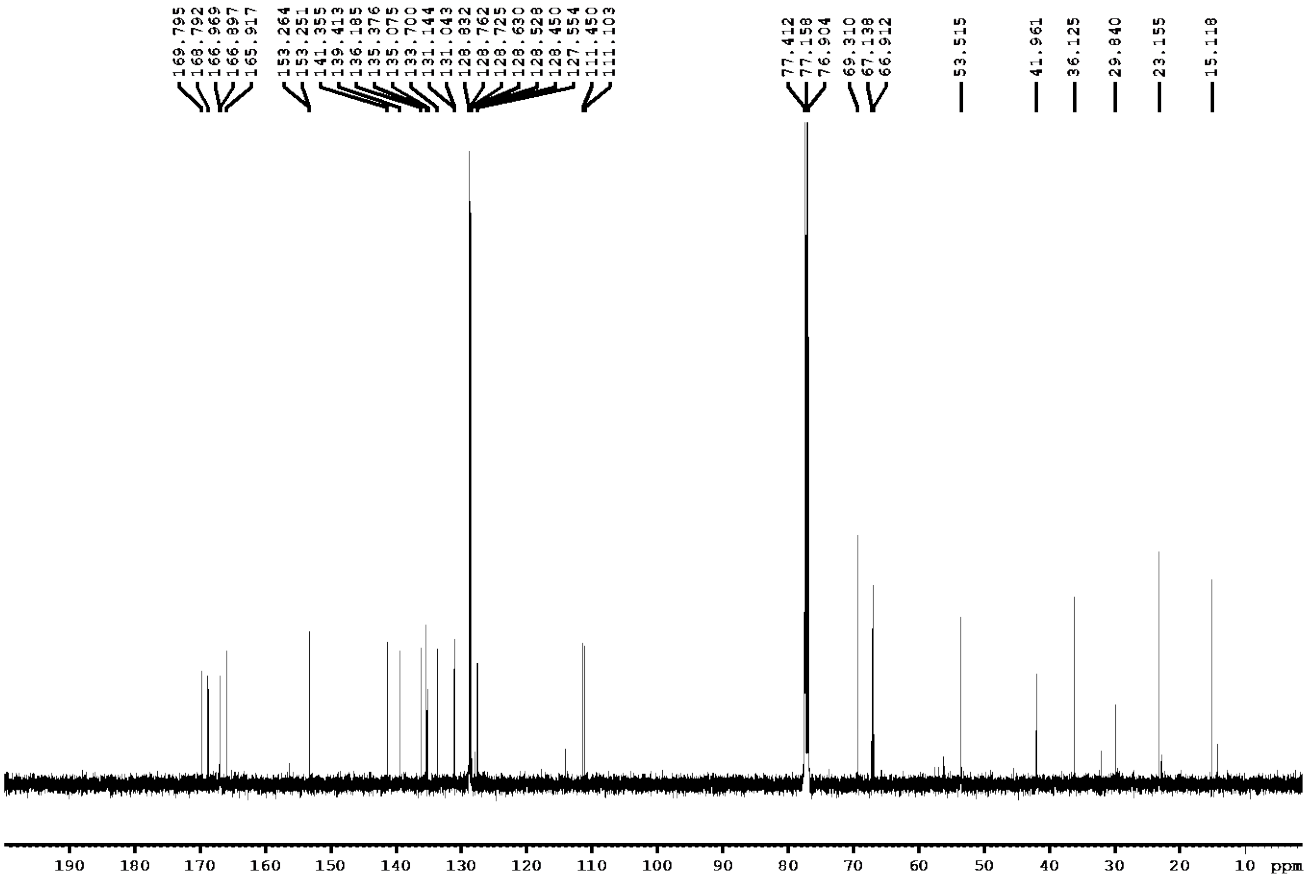
169.795
168.792
166.969
166.897
165.917
153.264
153.251
141.355
139.413
136.185
135.376
135.075
133.700
131.144
131.043
128.832
128.762
128.725
128.630
128.528
128.450
127.554
111.450
111.103
77.412
77.158
76.904
69.310
67.138
66.912
53.515
41.961
36.125
29.840
23.155
15.118
190
180
170
160
150
140
130
120
110
100
90
80
70
60
50
40
30
20
10
ppm

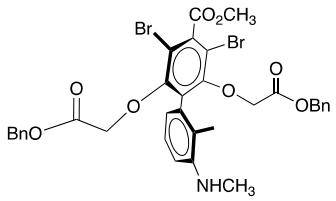
CO2CH3
Br
Br
O
O
O
O
OBn
BnO
NHCH3

12

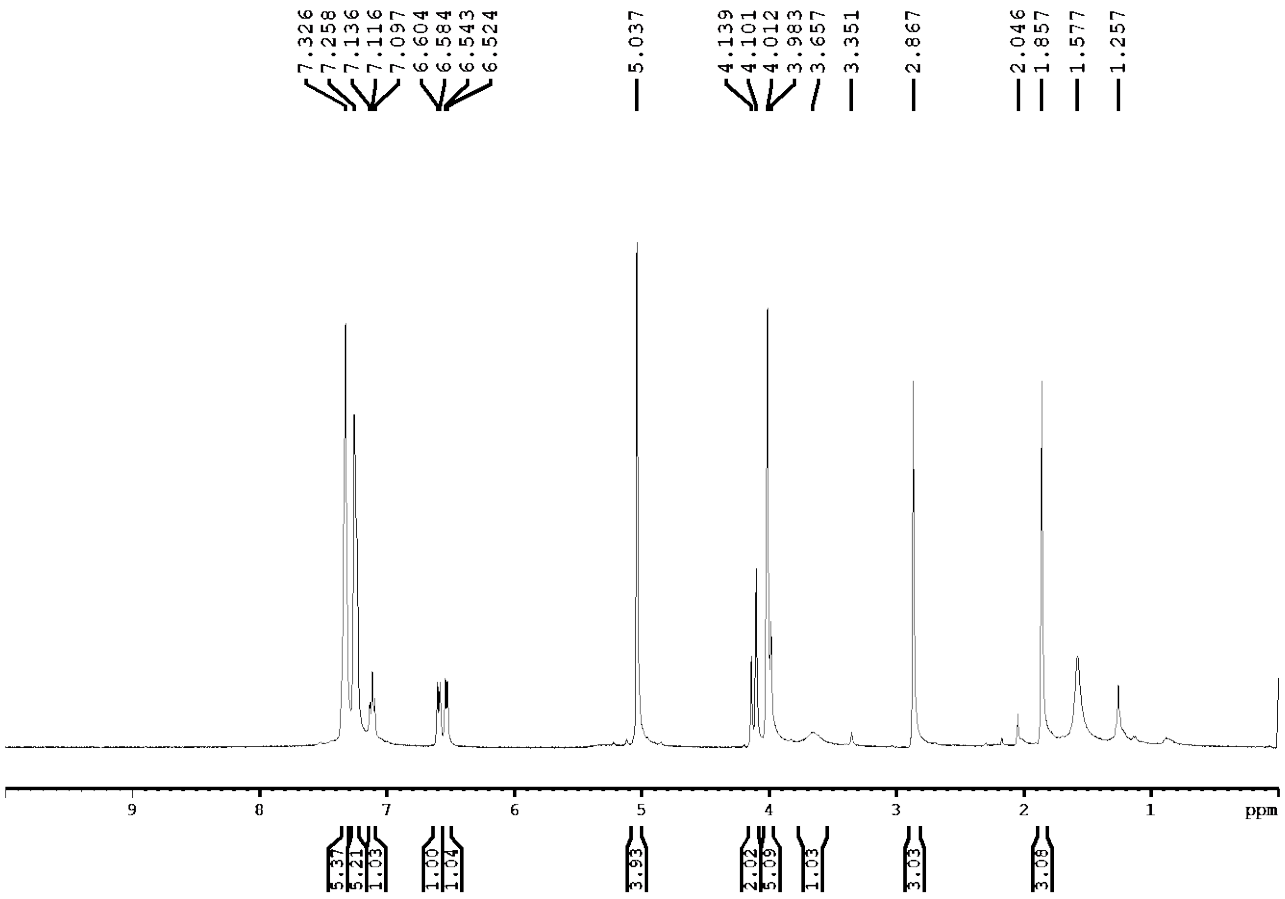
7.326
7.258
7.136
7.116
7.097
6.604
6.584
6.543
6.524
5.037
4.139
4.101
4.012
3.983
3.657
3.351
2.867
2.046
1.857
1.577
1.257
9
8
7
6
5
4
3
2
1
ppm
5.37
5.21
1.03
1.00
1.04
3.93
2.02
5.09
1.03
3.03
3.08

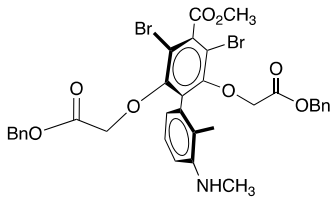
CO2CH3
Br
Br
O
O
O
O
OBn
BnO
NHCH3

12

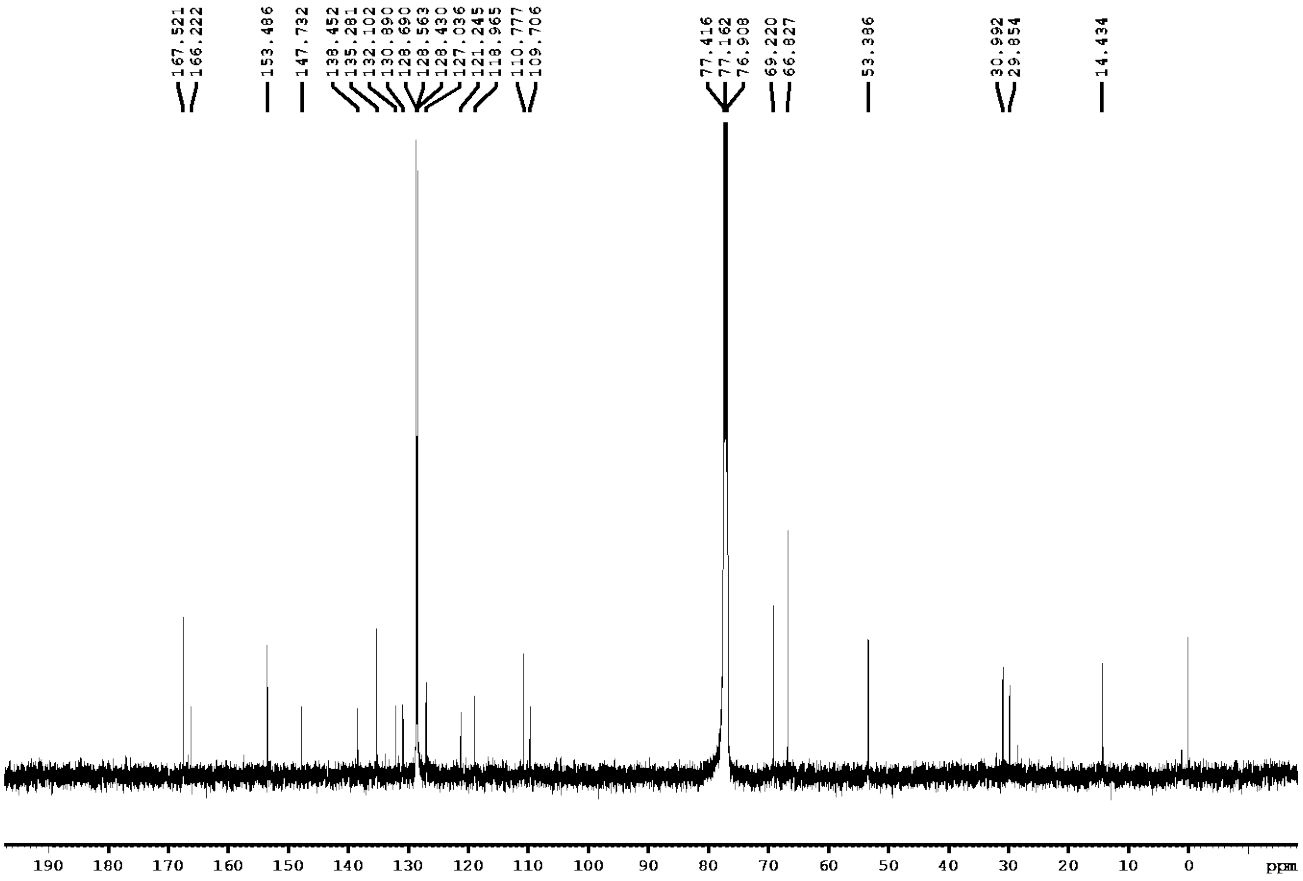
167.521
166.222
153.486
147.732
138.452
135.281
132.102
130.890
128.690
128.563
128.430
127.036
121.245
118.965
110.777
109.706
77.416
77.162
76.908
69.220
66.827
53.386
30.992
29.854
14.434
190
180
170
160
150
140
130
120
110
100
90
80
70
60
50
40
30
20
10
0
ppm

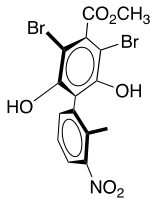
CO2CH3
Br
Br
OH
HO
NO2

13

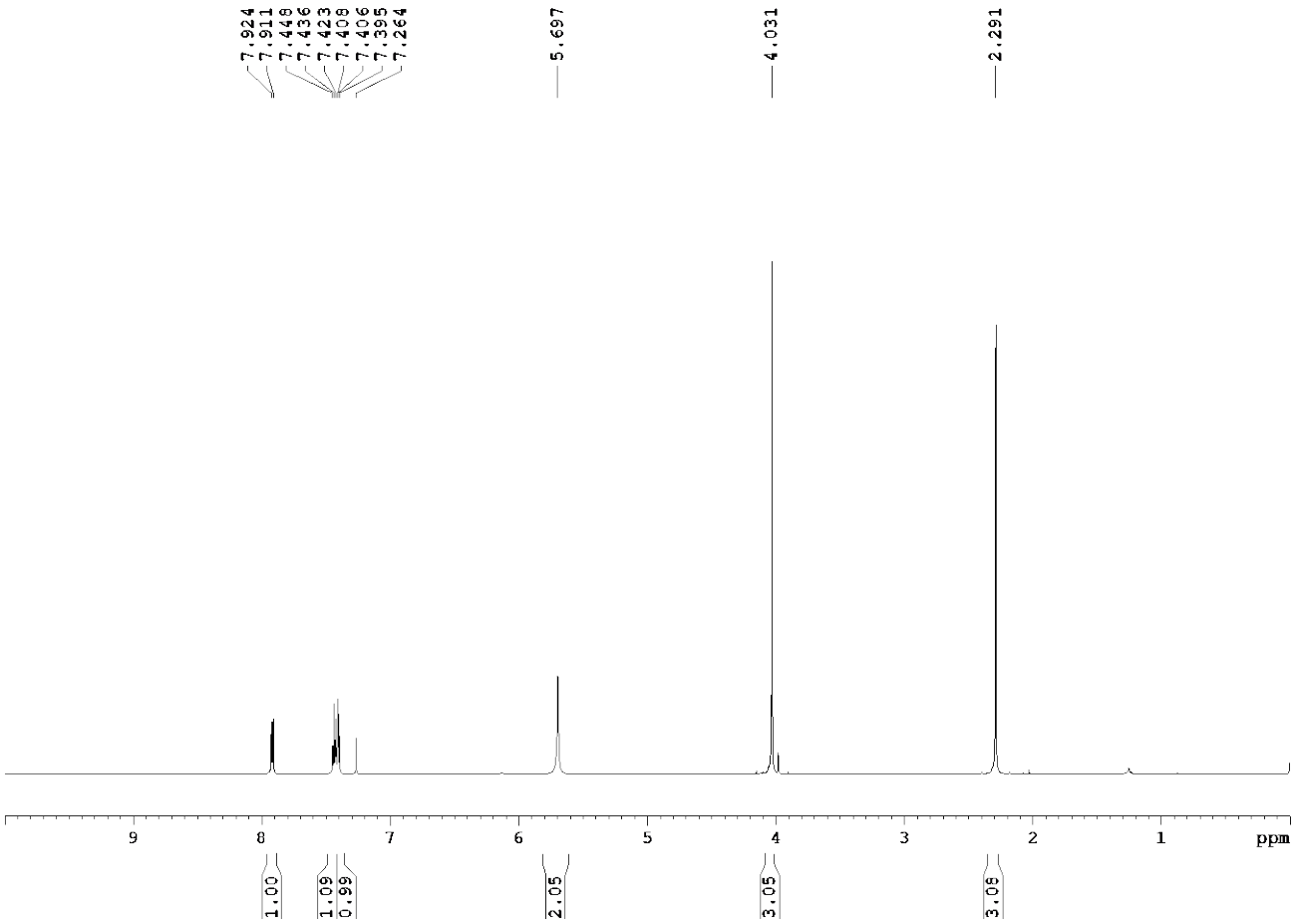
7.924
7.911
7.448
7.436
7.423
7.408
7.406
7.395
7.264
5.697
4.031
2.291
9
8
7
6
5
4
3
2
1
ppm
1.00
1.09
0.99
2.05
3.05
3.06

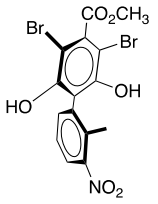
CO2CH3
Br
Br
OH
HO
NO2

13

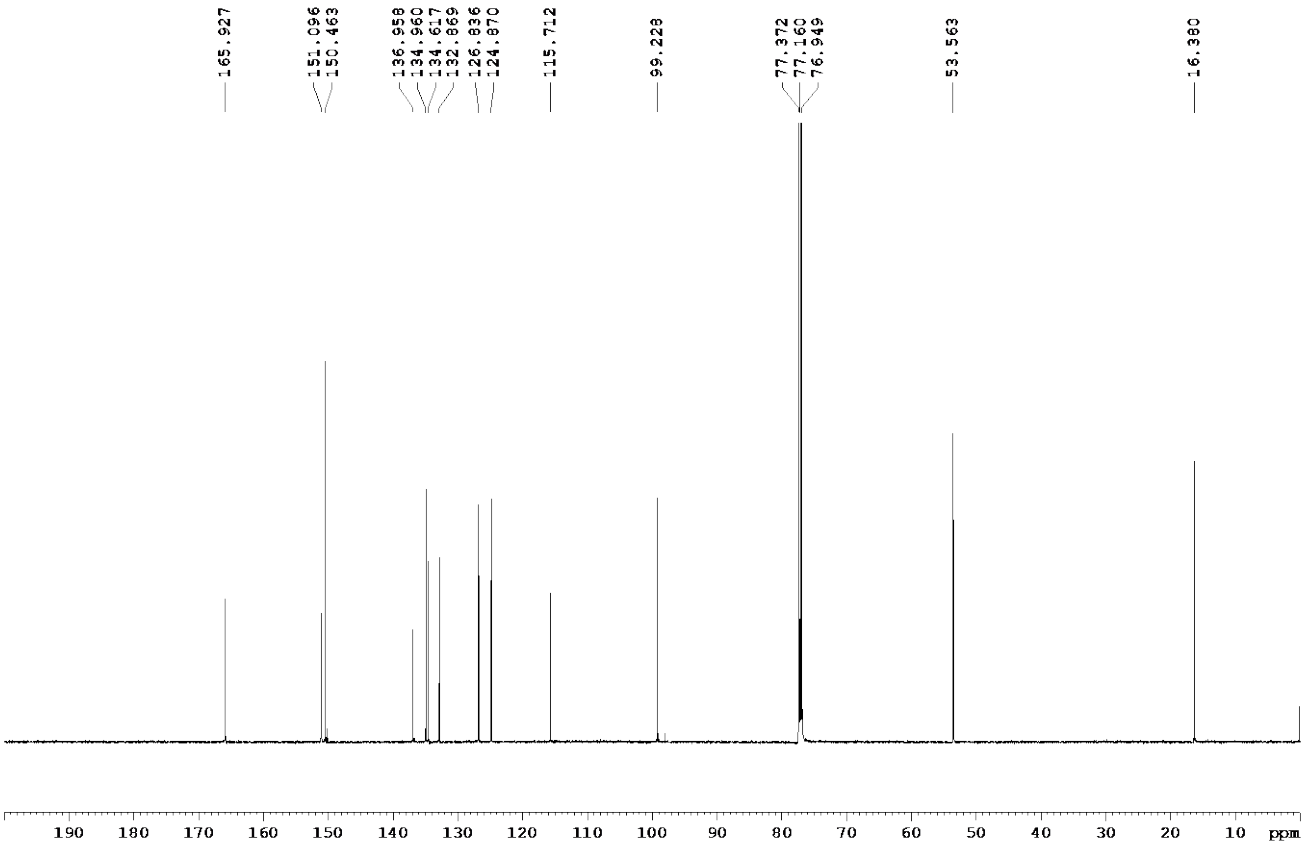
165.927
151.096
150.463
136.958
134.960
134.617
132.869
126.836
124.870
115.712
99.228
77.372
77.160
76.949
53.563
16.380
190
180
170
160
150
140
130
120
110
100
90
80
70
60
50
40
30
20
10
ppm

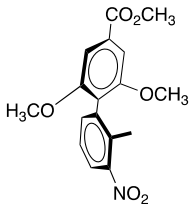
CO2CH3
H3CO
OCH3
NO2

14

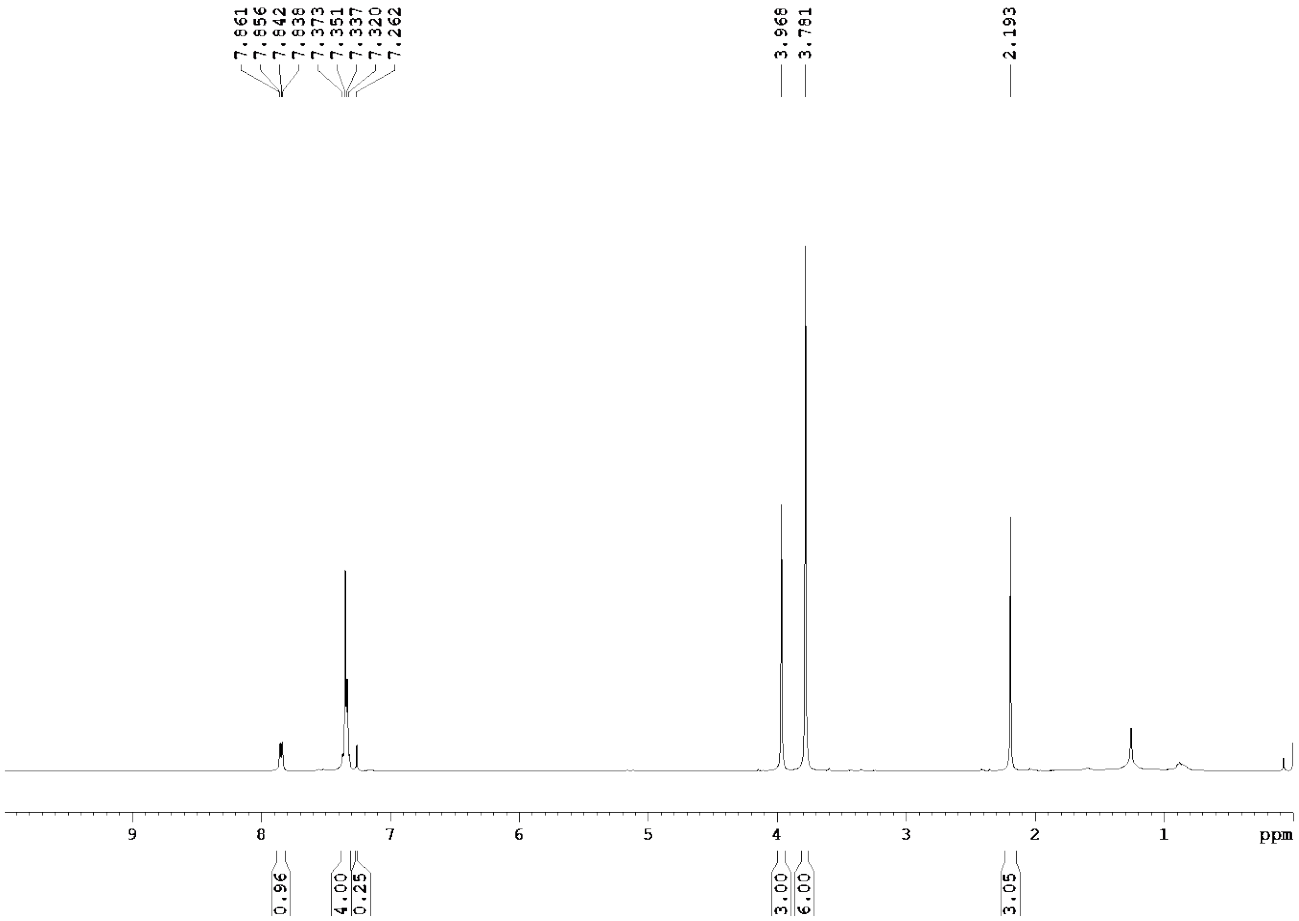
7.661
7.656
7.642
7.638
7.373
7.351
7.337
7.320
7.262
3.966
3.781
2.193
9
8
7
6
5
4
3
2
1
ppm
0.96
4.00
0.25
3.00
6.00
3.05

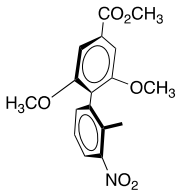
CO2CH3
H3CO
OCH3
NO2

14

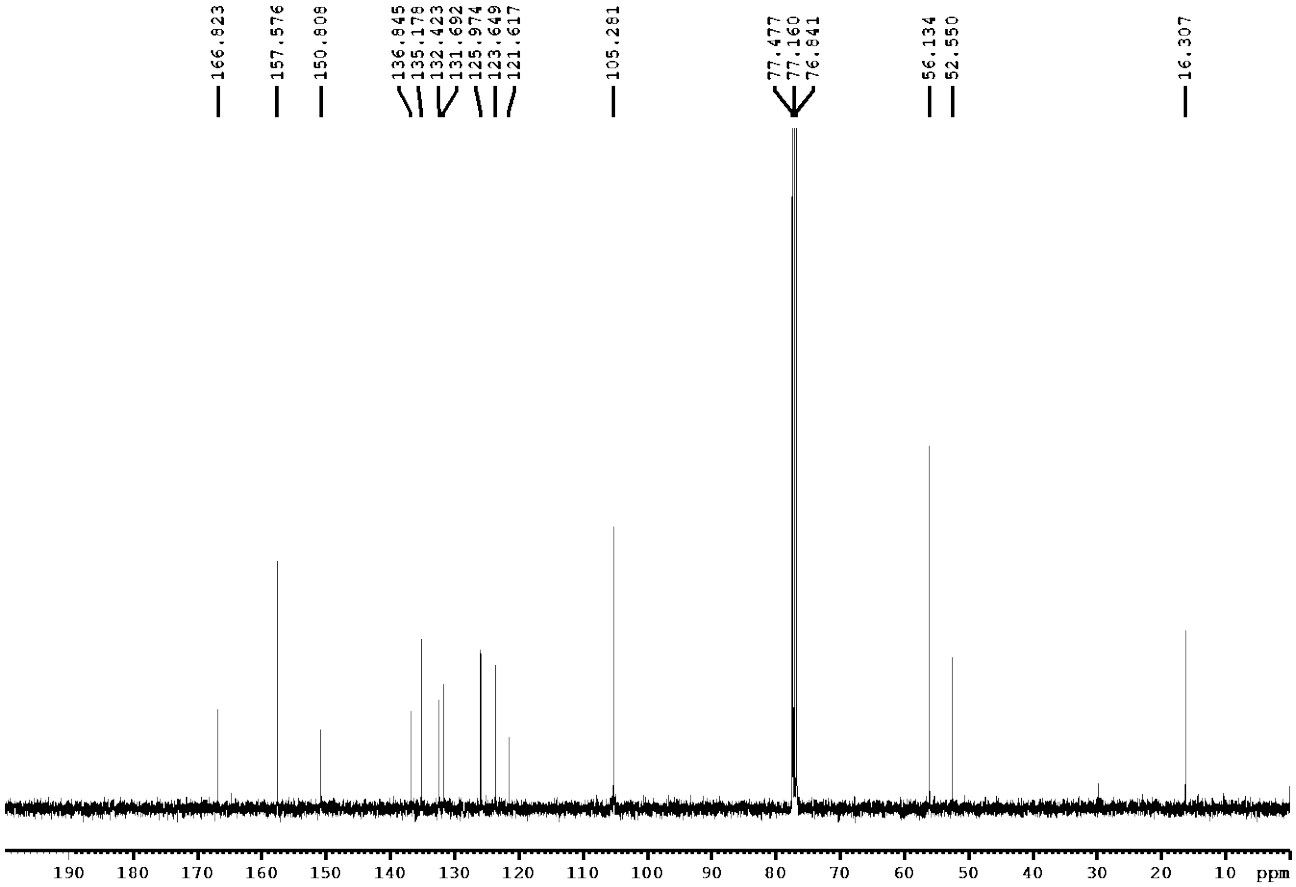
166.823
157.576
150.809
136.845
135.179
132.423
131.692
125.974
123.649
121.617
105.281
77.477
77.160
76.841
56.134
52.550
16.307
190 180 170 160 150 140 130 120 110 100 90 80 70 60 50 40 30 20 10 ppm

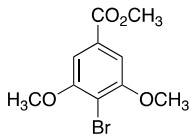

15

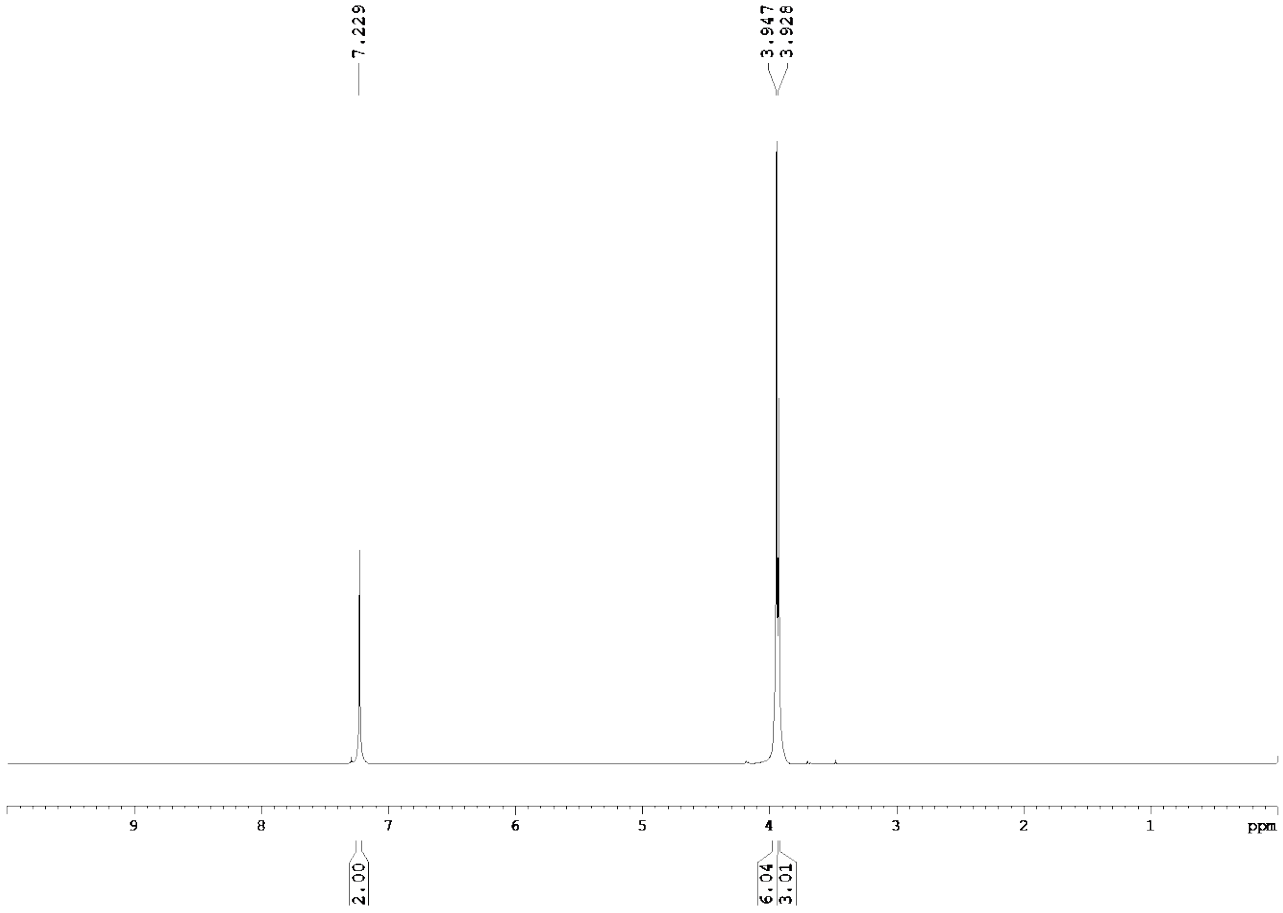

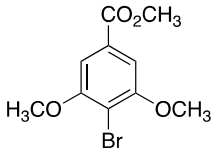
CO2CH3
H3CO
OCH3
Br

15

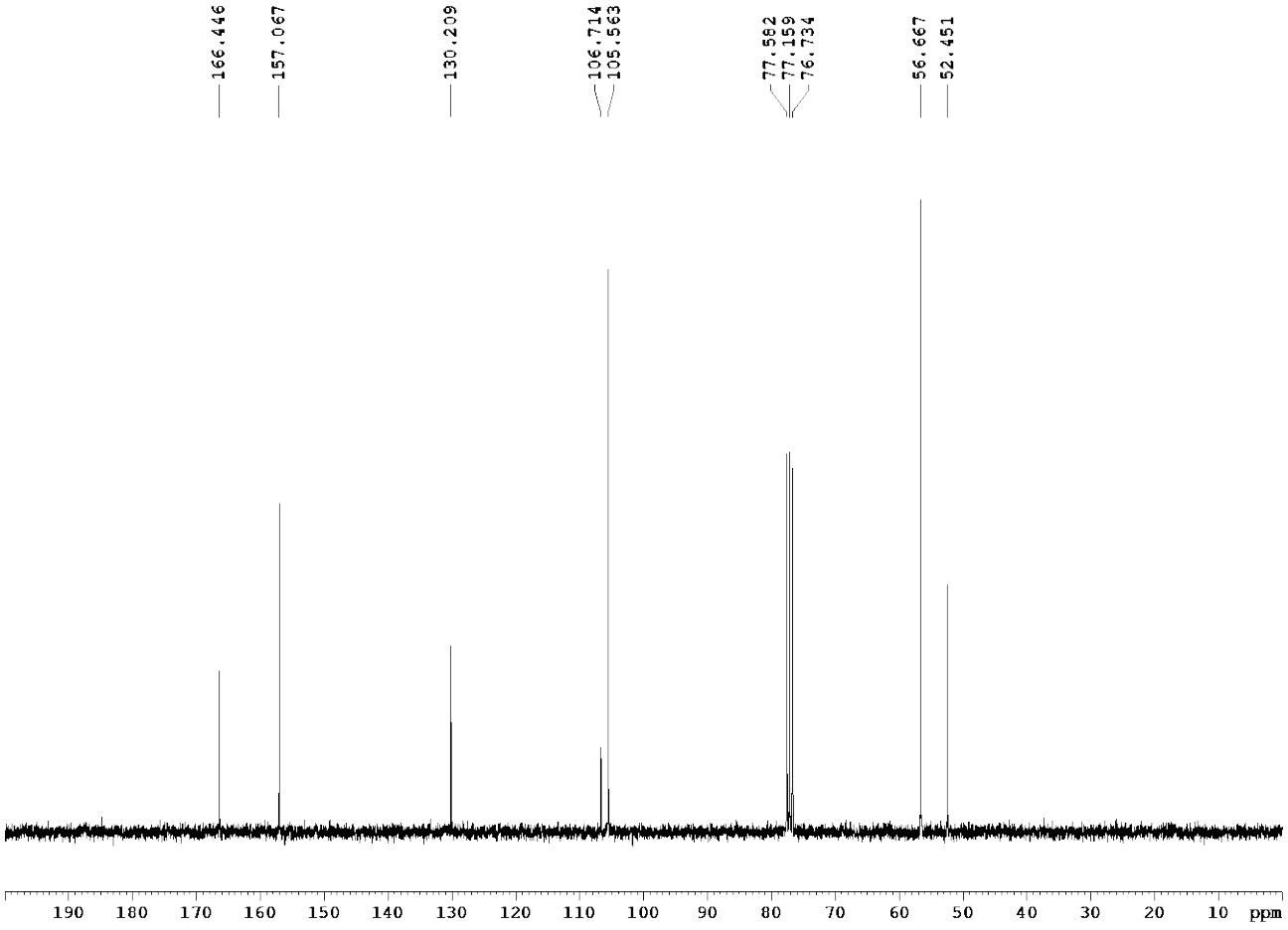
166.446
157.067
130.209
106.714
105.563
77.582
77.159
76.734
56.667
52.451
190 180 170 160 150 140 130 120 110 100 90 80 70 60 50 40 30 20 10 ppm

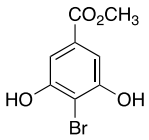
CO2CH3
HO
OH
Br

16

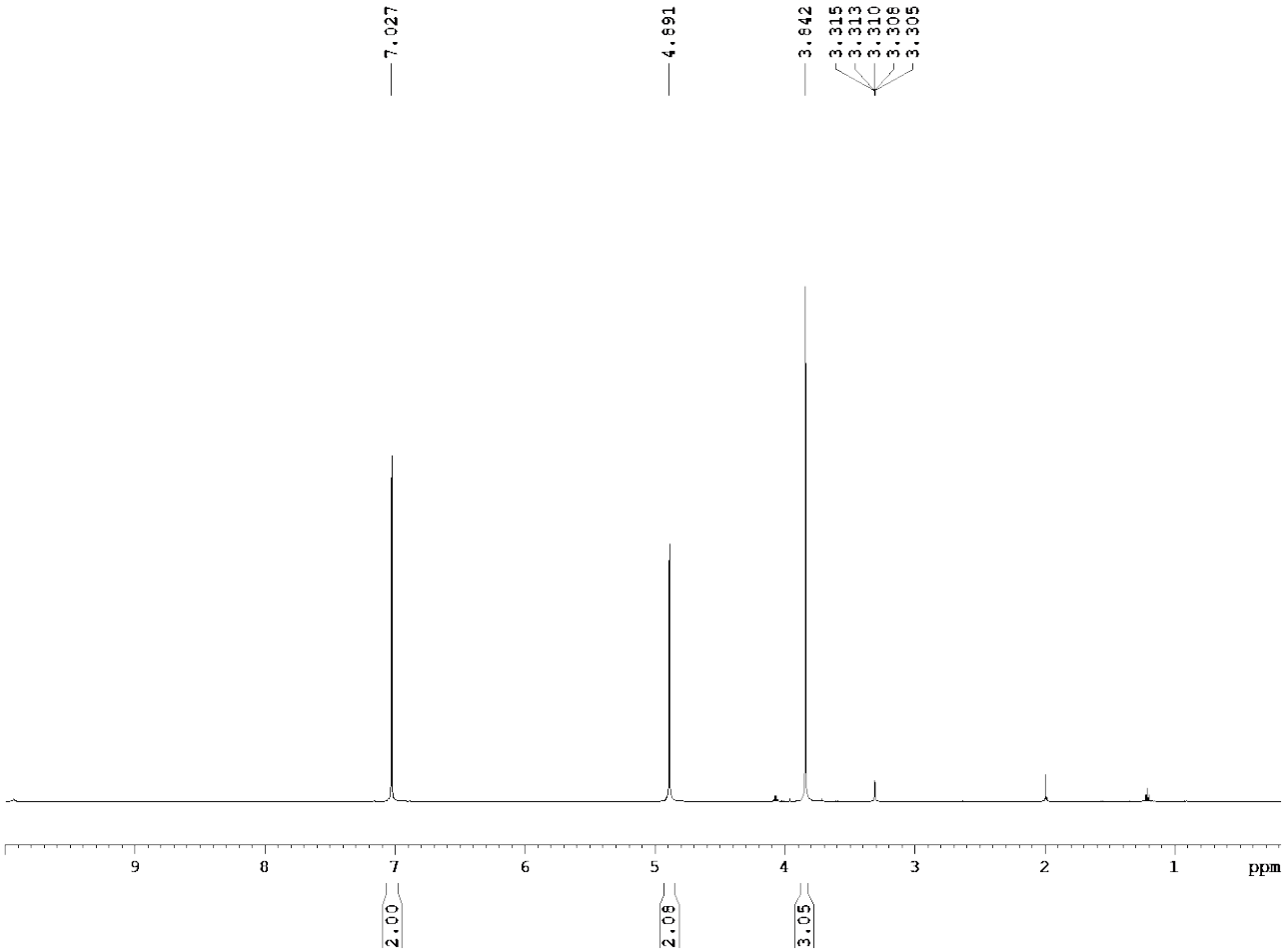
7.027
4.691
3.642
3.315
3.313
3.310
3.306
3.305
9
8
7
6
5
4
3
2
1
ppm
2.00
2.09
3.05

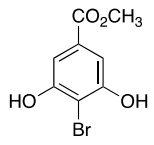
CO2CH3
HO
OH
Br

16

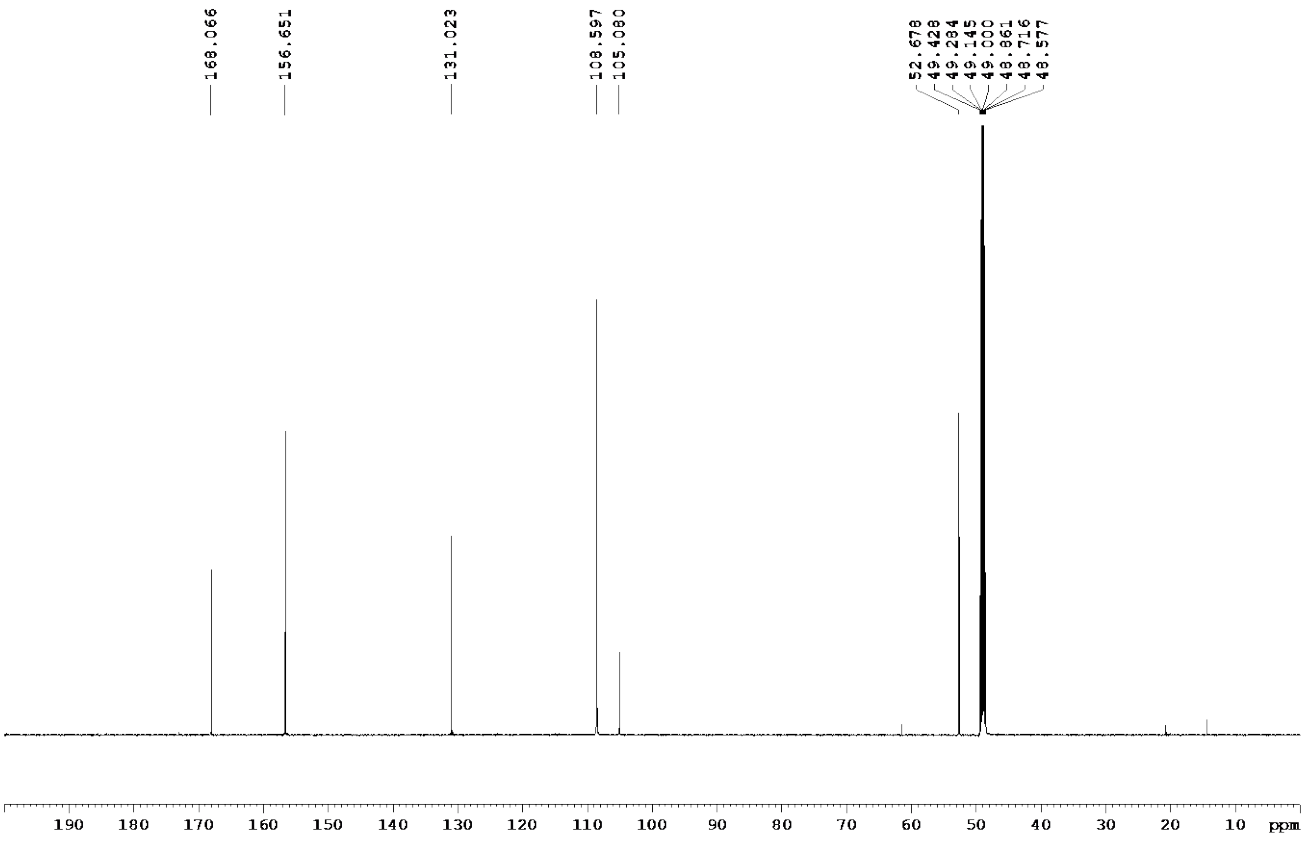
168.066
156.651
131.023
108.597
105.080
52.678
49.428
49.284
49.145
49.000
48.861
48.716
48.577
190
180
170
160
150
140
130
120
110
100
90
80
70
60
50
40
30
20
10
ppm

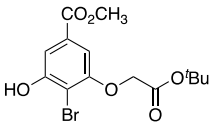
CO2CH3
HO
Br
O
O
OtBu

18

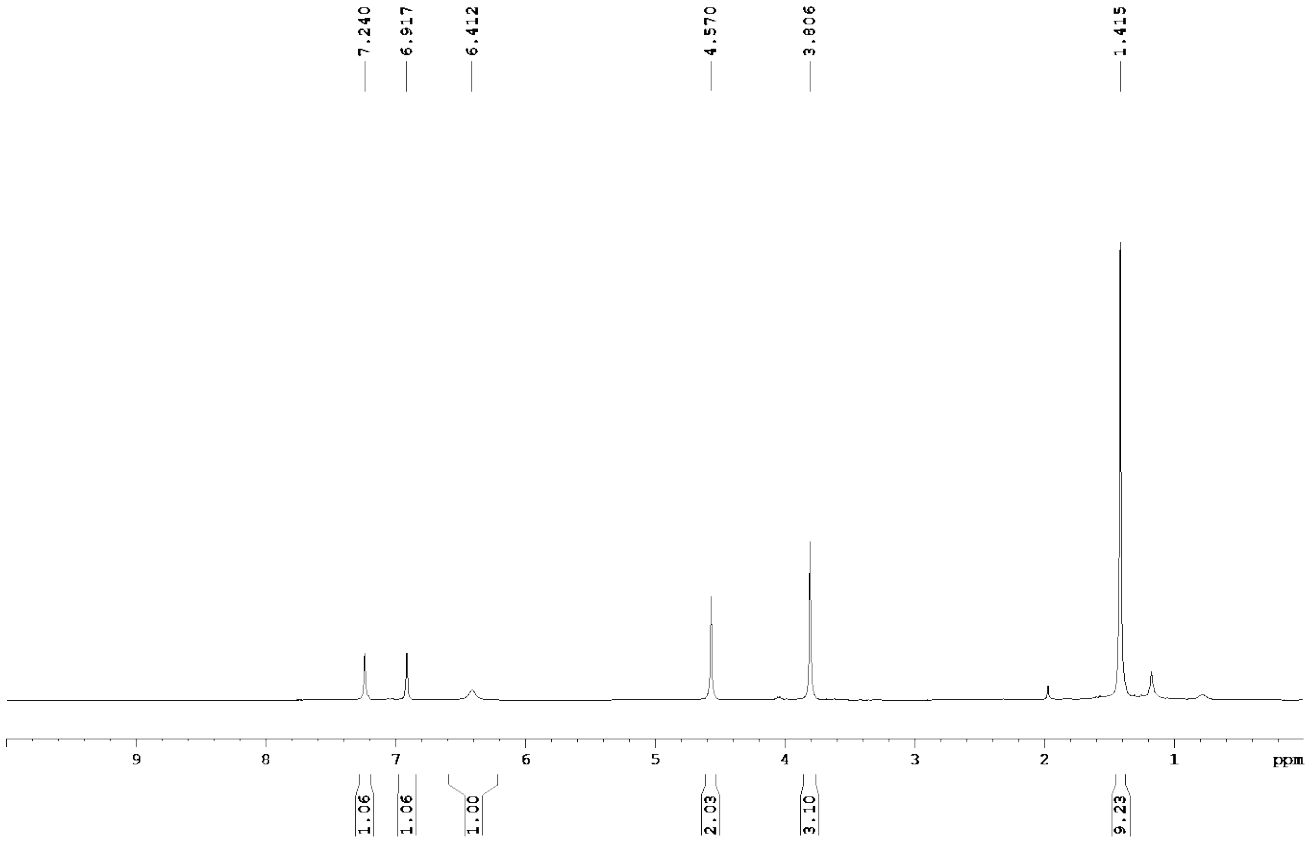
7.240
6.917
6.412
4.570
3.806
1.415
9
8
7
6
5
4
3
2
1
ppm
1.06
1.06
1.00
2.03
3.10
9.23

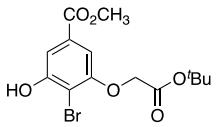
CO2CH3
HO
Br
O
O
OtBu

18

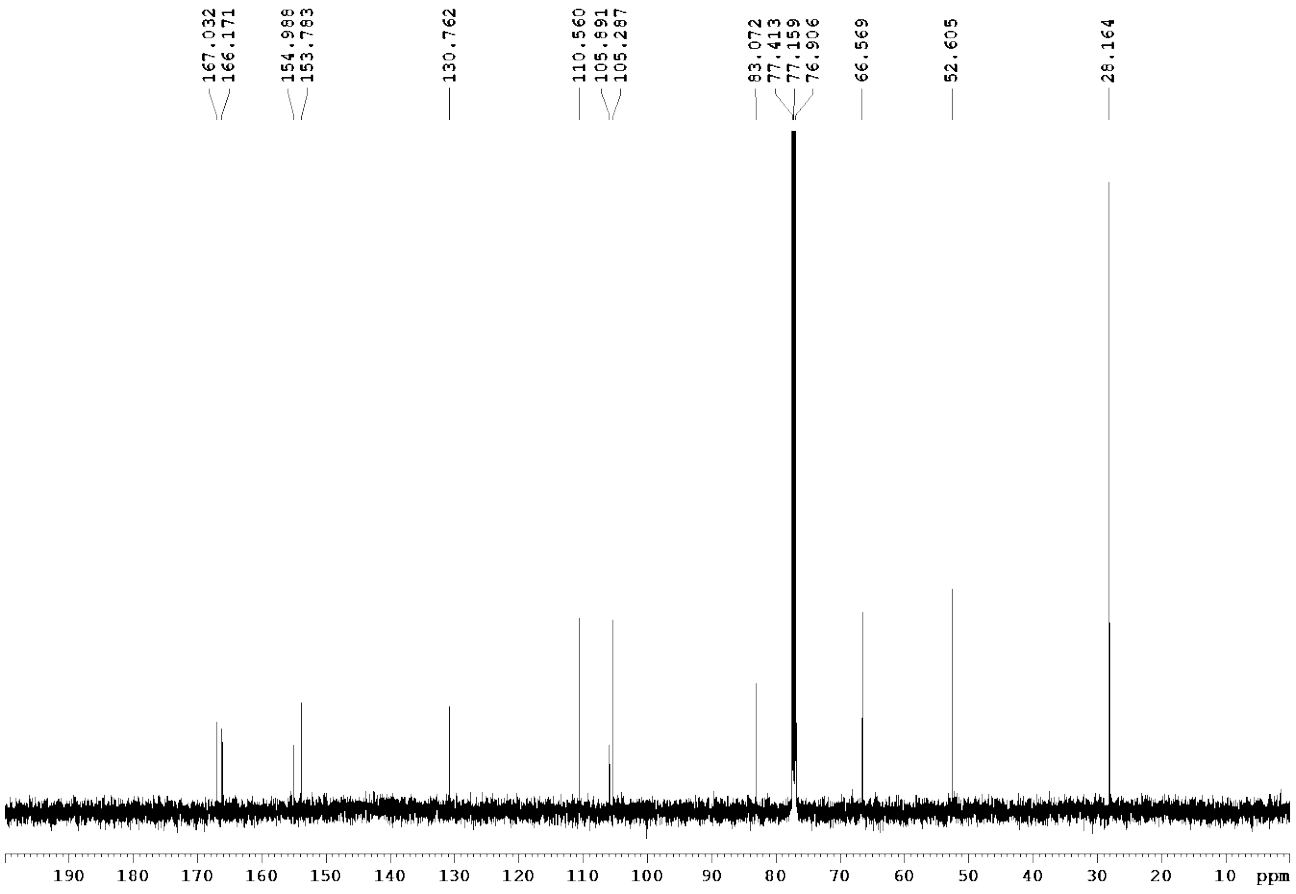
167.032
166.171
154.988
153.783
130.762
110.560
105.891
105.287
83.072
77.413
77.159
76.906
66.569
52.605
28.164
190
180
170
160
150
140
130
120
110
100
90
80
70
60
50
40
30
20
10
ppm

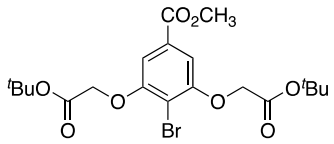
CO2CH3
tBuO
O
O
Br
O
O
OtBu
O

17

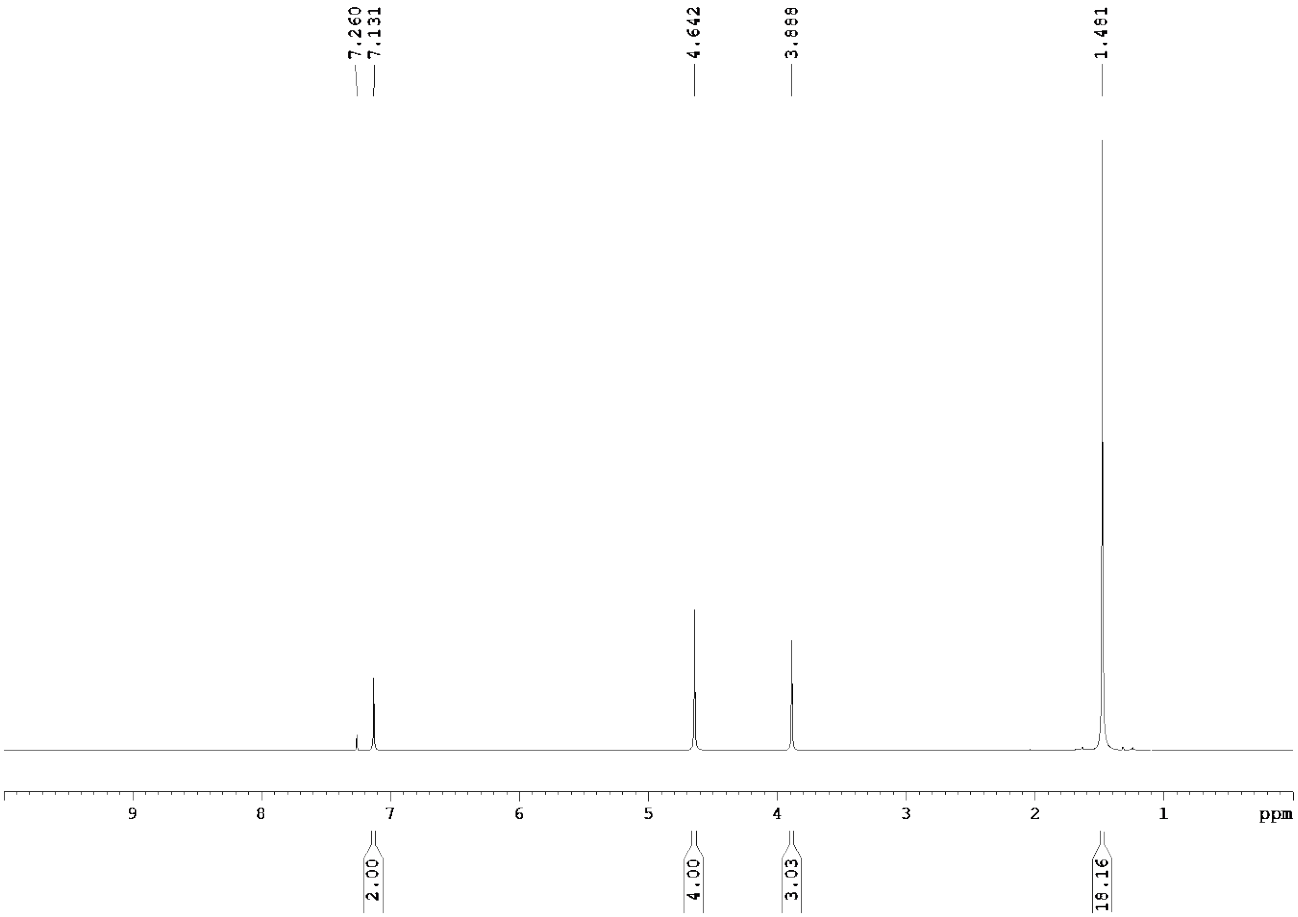
7.260
7.131
4.642
3.868
1.481
9
8
7
6
5
4
3
2
1
ppm
2.00
4.00
3.03
18.16

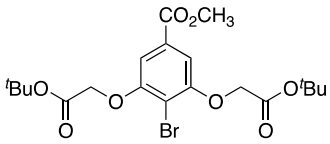
CO2CH3
tBuO
O
O
Br
O
OtBu
O

17

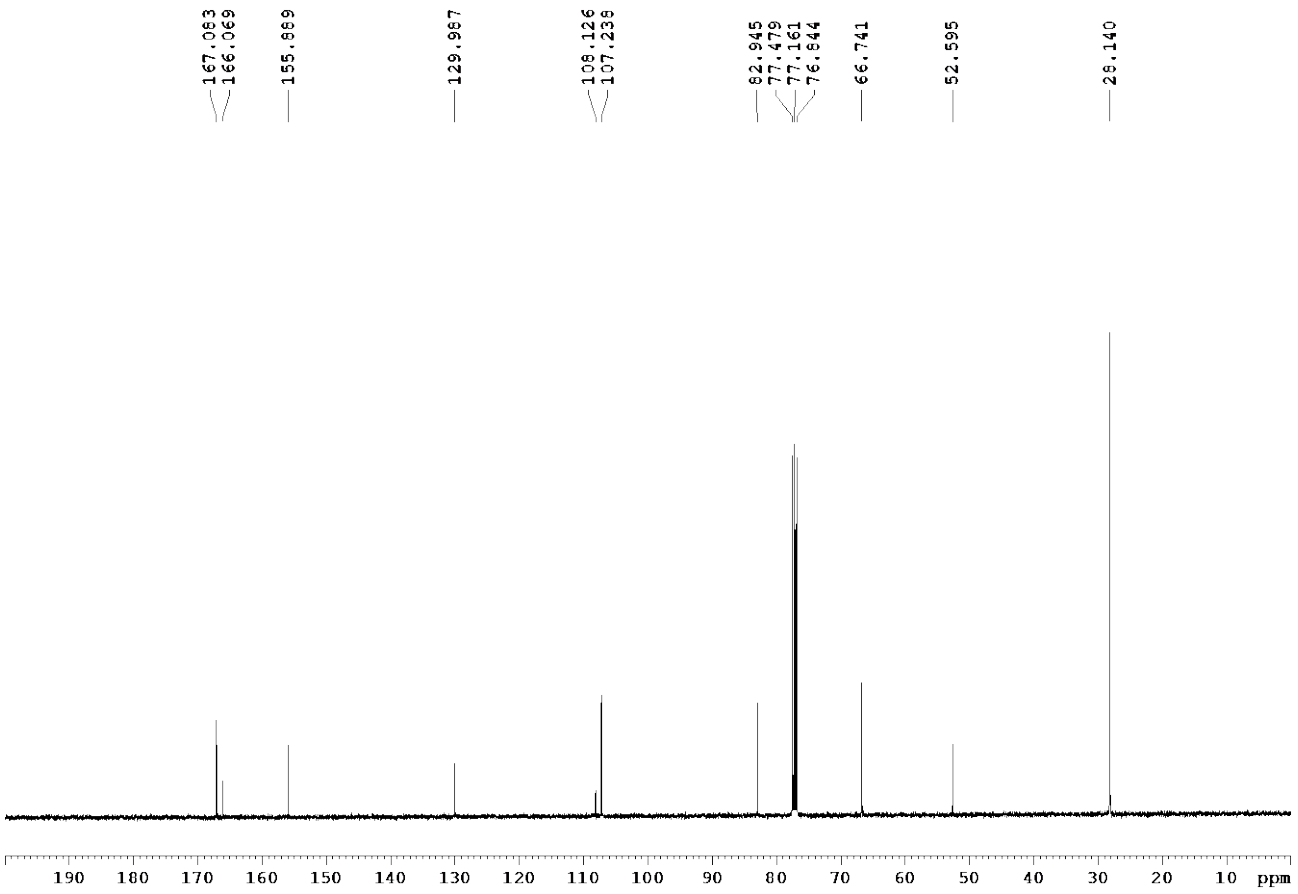
167.083
166.069
155.869
129.967
108.126
107.239
82.945
77.479
77.161
76.844
66.741
52.595
28.140
190 180 170 160 150 140 130 120 110 100 90 80 70 60 50 40 30 20 10 ppm

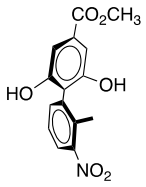
CO2CH3
HO
OH
NO2

24

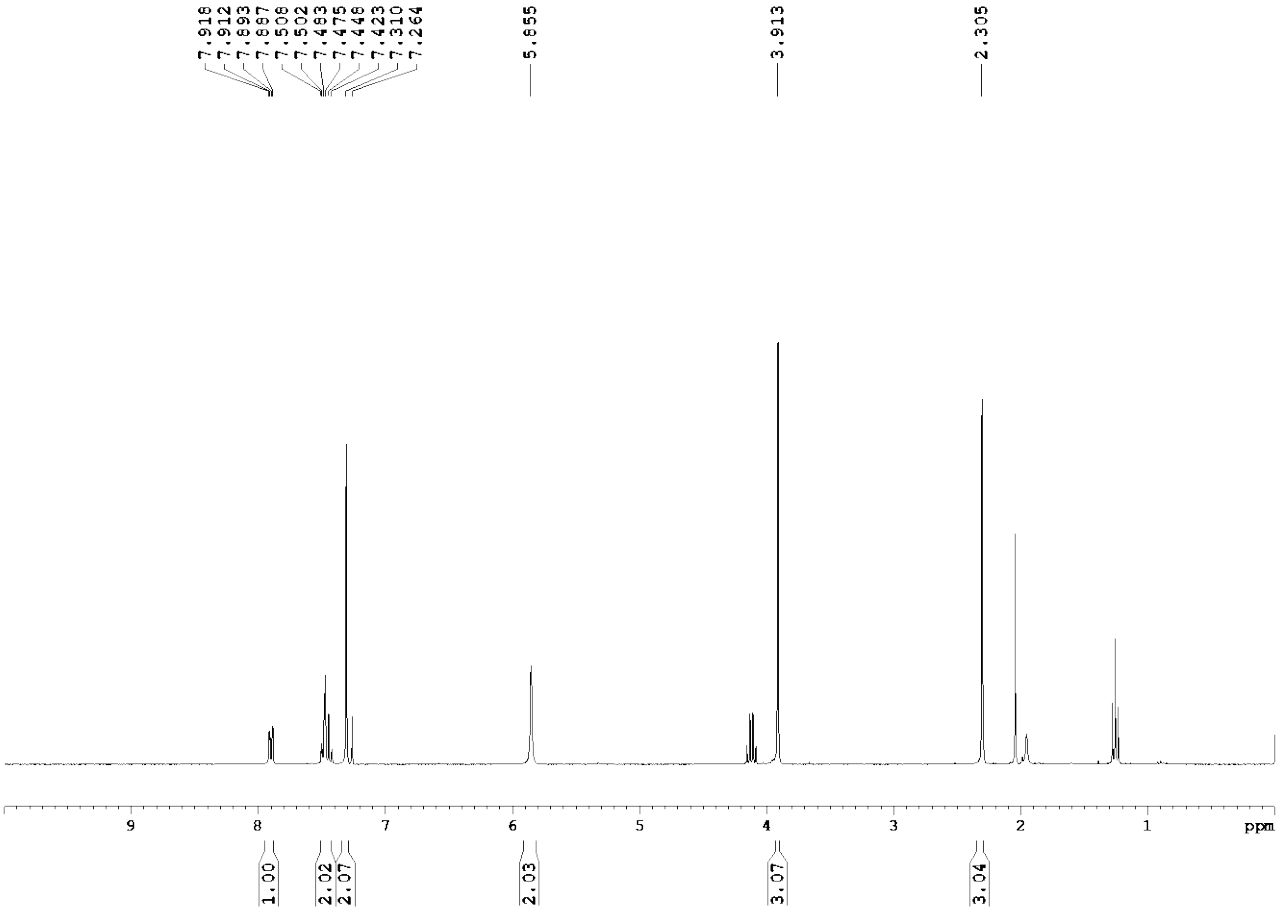
7.918
7.912
7.693
7.687
7.508
7.502
7.483
7.475
7.448
7.423
7.310
7.264
5.855
3.913
2.305
9
8
7
6
5
4
3
2
1
ppm
1.00
2.02
2.07
2.03
3.07
3.04

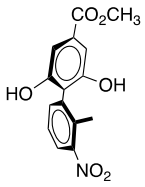
CO2CH3
HO
OH
NO2

24

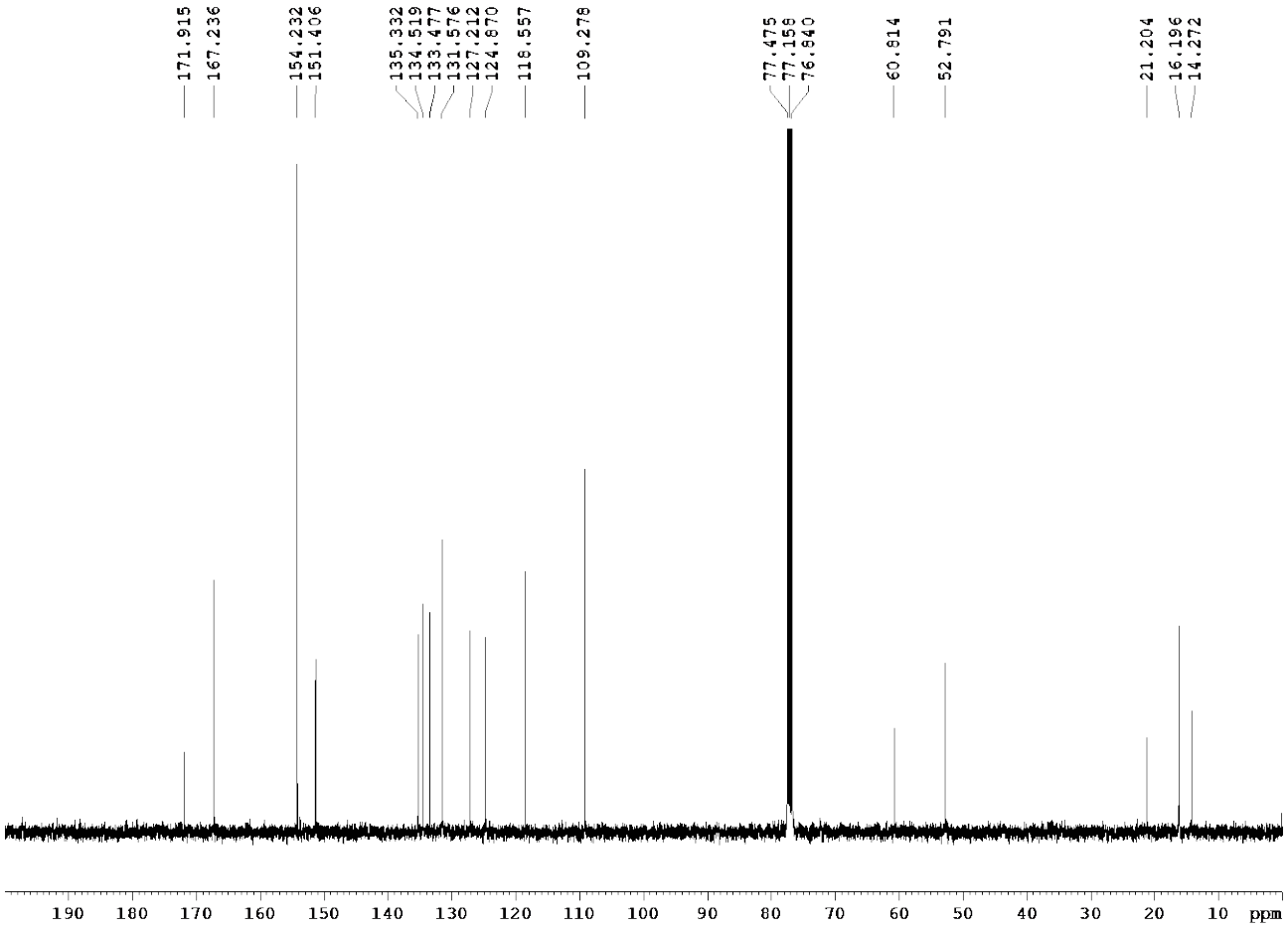
171.915
167.236
154.232
151.406
135.332
134.519
133.477
131.576
127.212
124.870
118.557
109.278
77.475
77.159
76.840
60.914
52.791
21.204
16.196
14.272
190 180 170 160 150 140 130 120 110 100 90 80 70 60 50 40 30 20 10 ppm

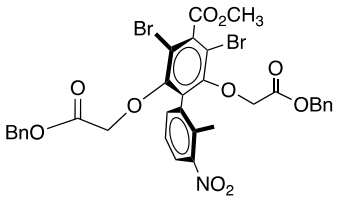
Br
CO2CH3
Br
O
O
O
O
OBn
BnO
NO2

30

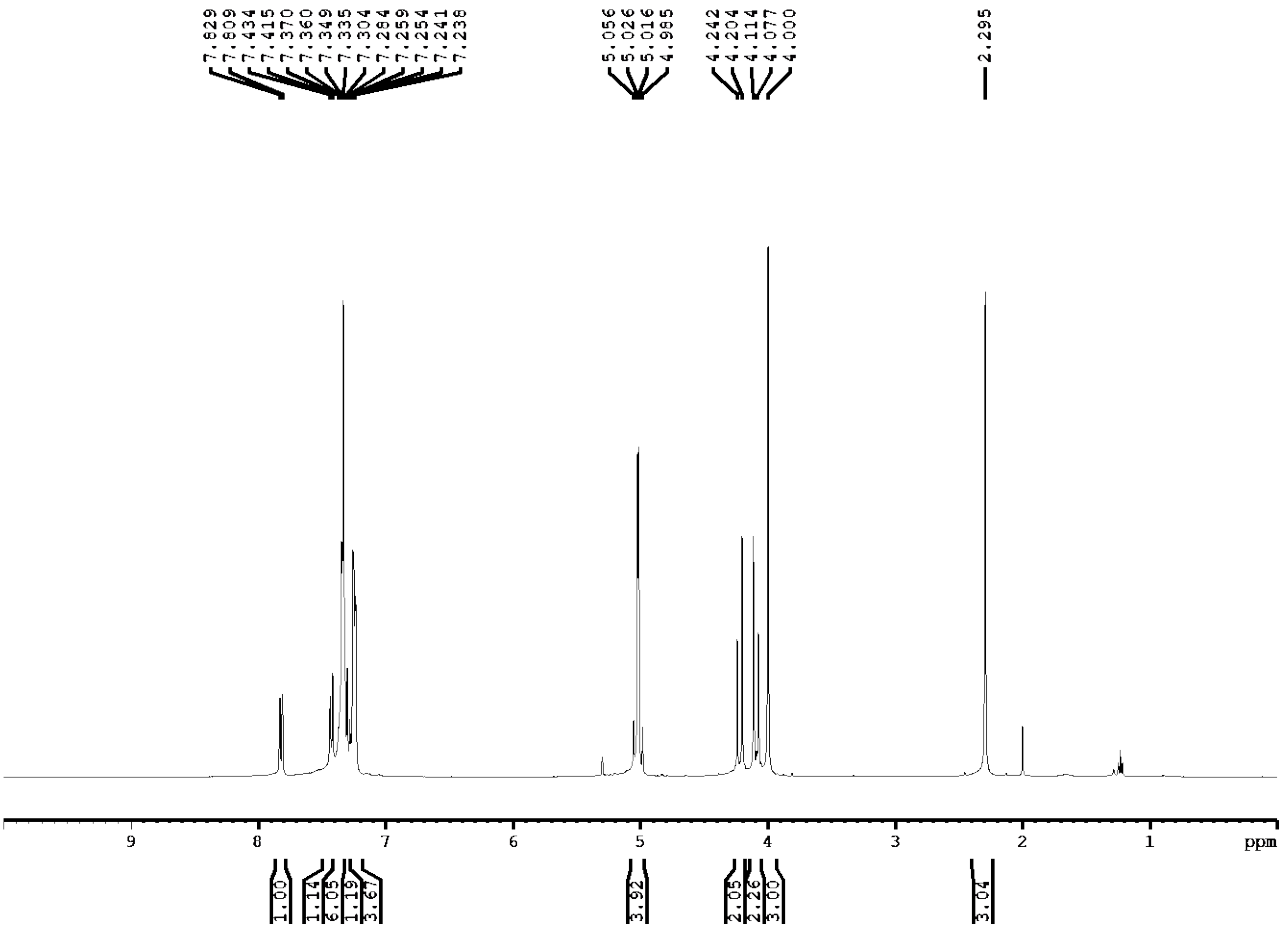
7.629
7.609
7.434
7.415
7.370
7.360
7.349
7.335
7.304
7.284
7.259
7.254
7.241
7.236
5.056
5.026
5.016
4.985
4.242
4.204
4.114
4.077
4.000
2.295
9
8
7
6
5
4
3
2
1
ppm
1.00
1.14
6.05
1.16
3.87
3.92
2.05
2.26
3.00
3.04

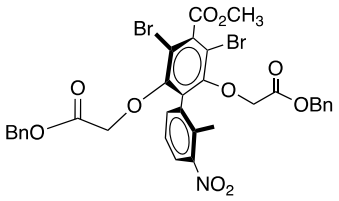
Br
CO2CH3
Br
O
O
O
O
OBn
BnO
NO2

30

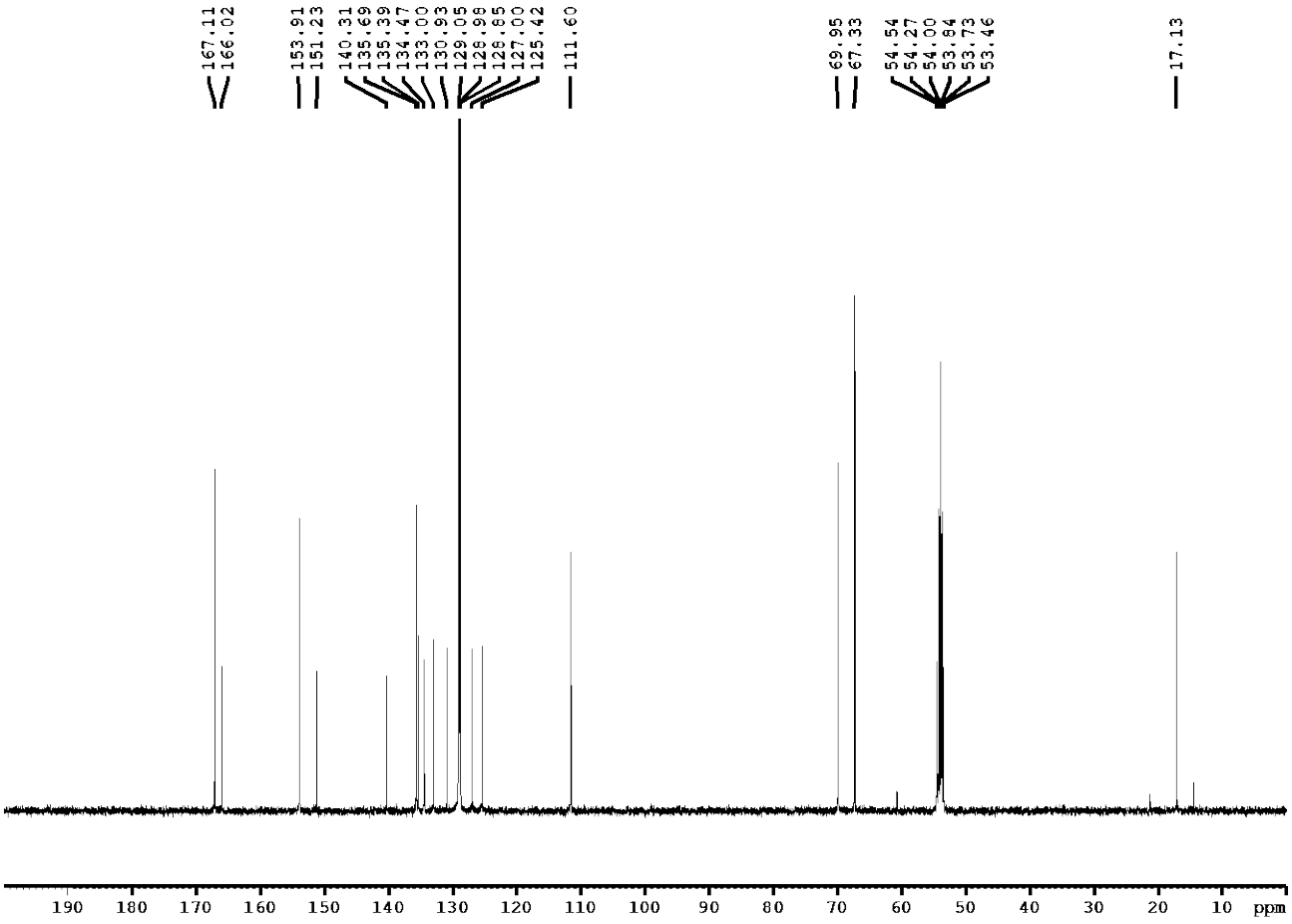
167.11
166.02
153.91
151.23
140.31
135.69
135.39
134.47
133.00
130.93
129.05
128.98
126.85
127.00
125.42
111.60
69.95
67.33
54.54
54.27
54.00
53.84
53.73
53.46
17.13
190 180 170 160 150 140 130 120 110 100 90 80 70 60 50 40 30 20 10 ppm

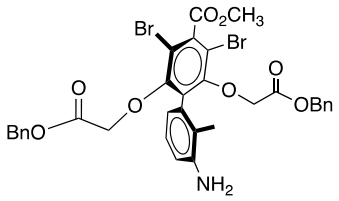
Br
CO2CH3
Br
O
O
O
O
OBn
BnO
NH2

31

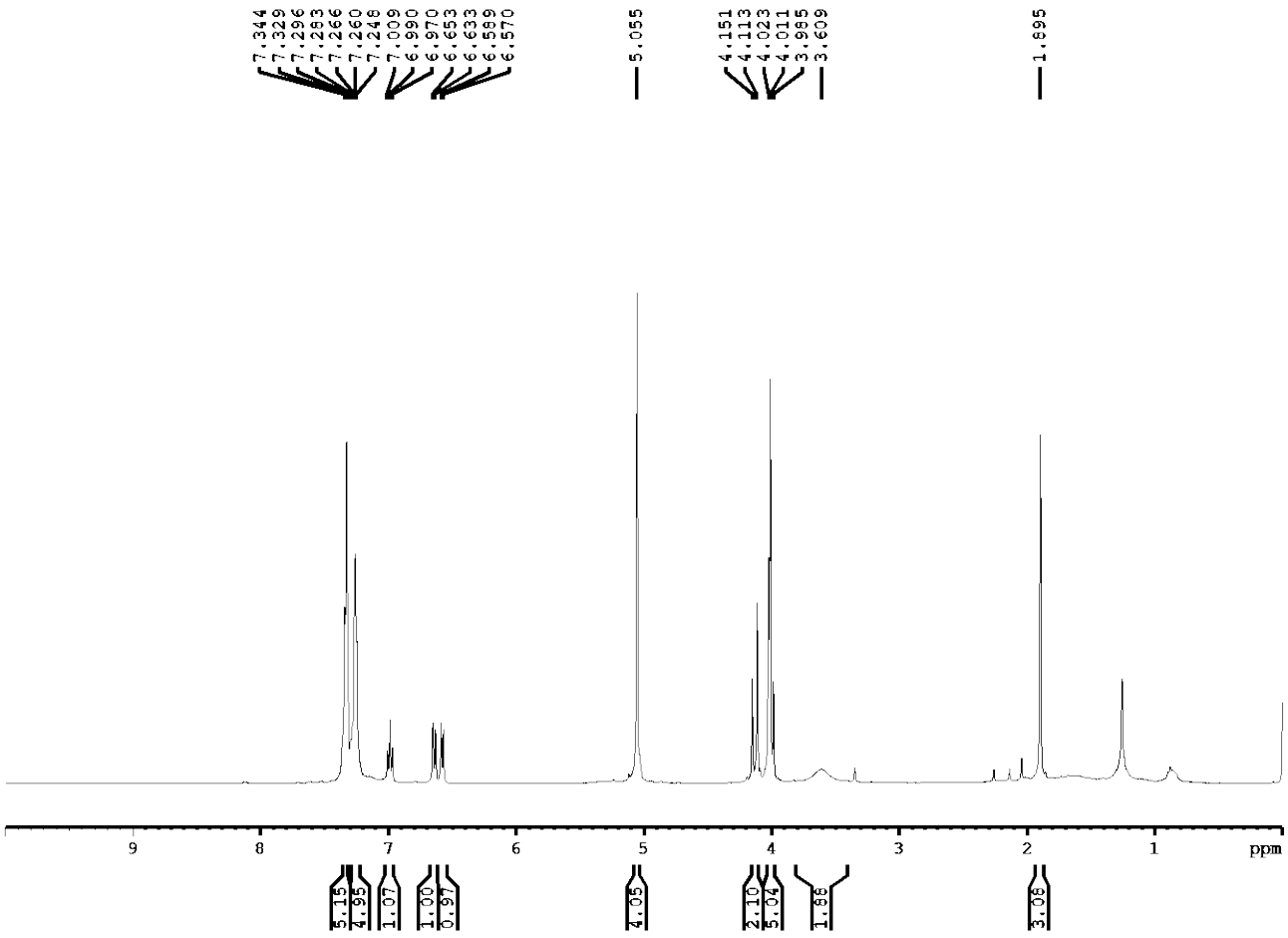
7.344
7.329
7.296
7.283
7.266
7.260
7.248
7.009
6.990
6.970
6.653
6.633
6.589
6.570
5.055
4.151
4.113
4.023
4.011
3.985
3.609
1.895
9
8
7
6
5
4
3
2
1
ppm
5.15
4.95
1.07
1.00
0.97
4.05
2.10
5.04
1.86
3.08

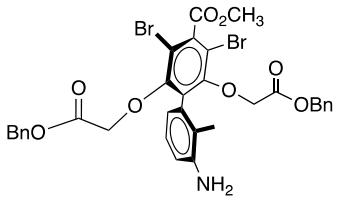
Br
CO2CH3
Br
O
O
O
O
OBn
BnO
NH2

31

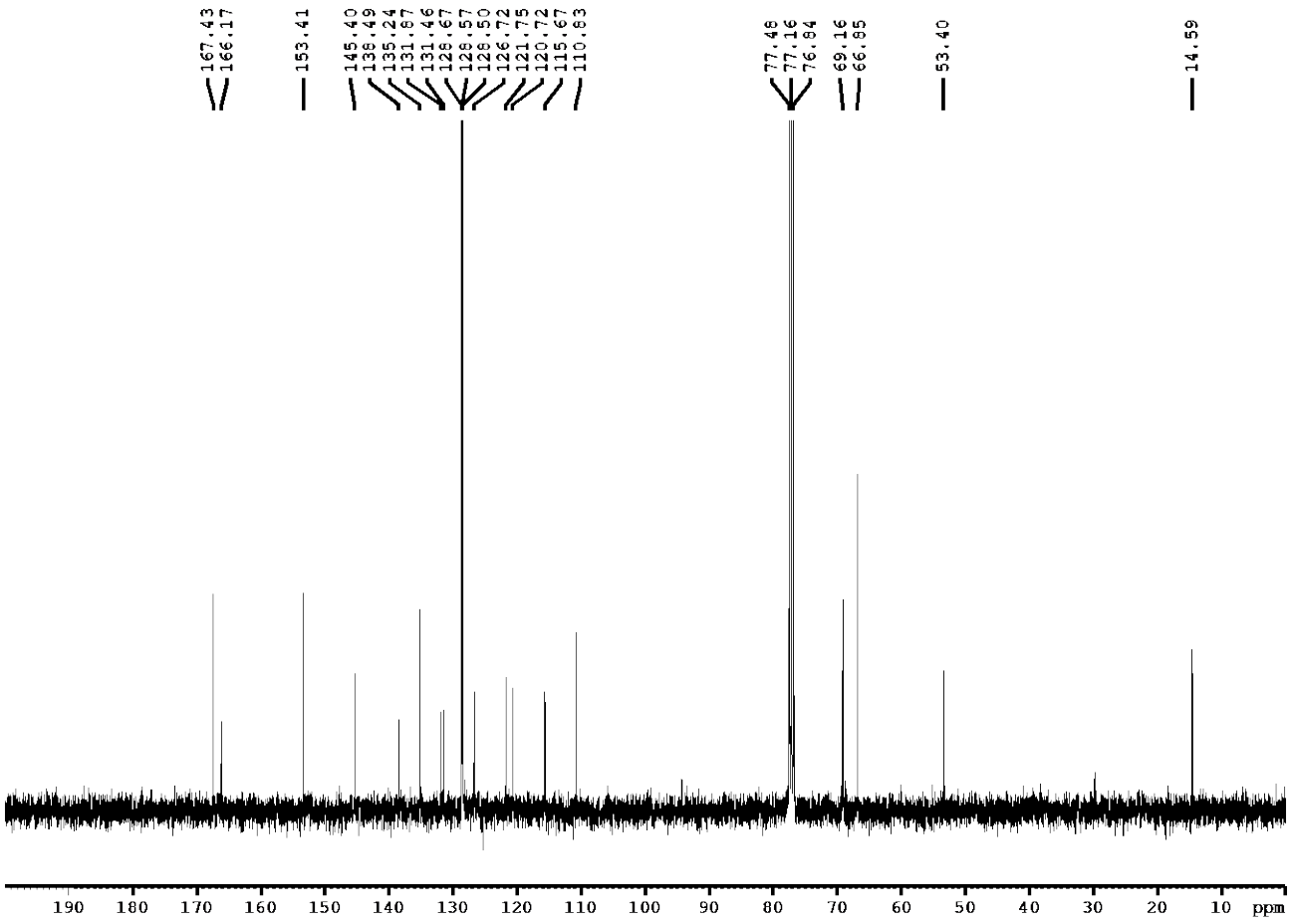
167.43
166.17
153.41
145.40
138.49
135.24
131.87
131.46
126.67
126.57
126.50
126.72
121.75
120.72
115.67
110.83
77.48
77.16
76.84
69.16
66.85
53.40
14.59
190
180
170
160
150
140
130
120
110
100
90
80
70
60
50
40
30
20
10
ppm

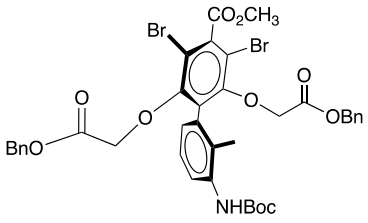
CO2CH3
Br
Br
O
O
O
O
OBn
BnO
NHBoc

35

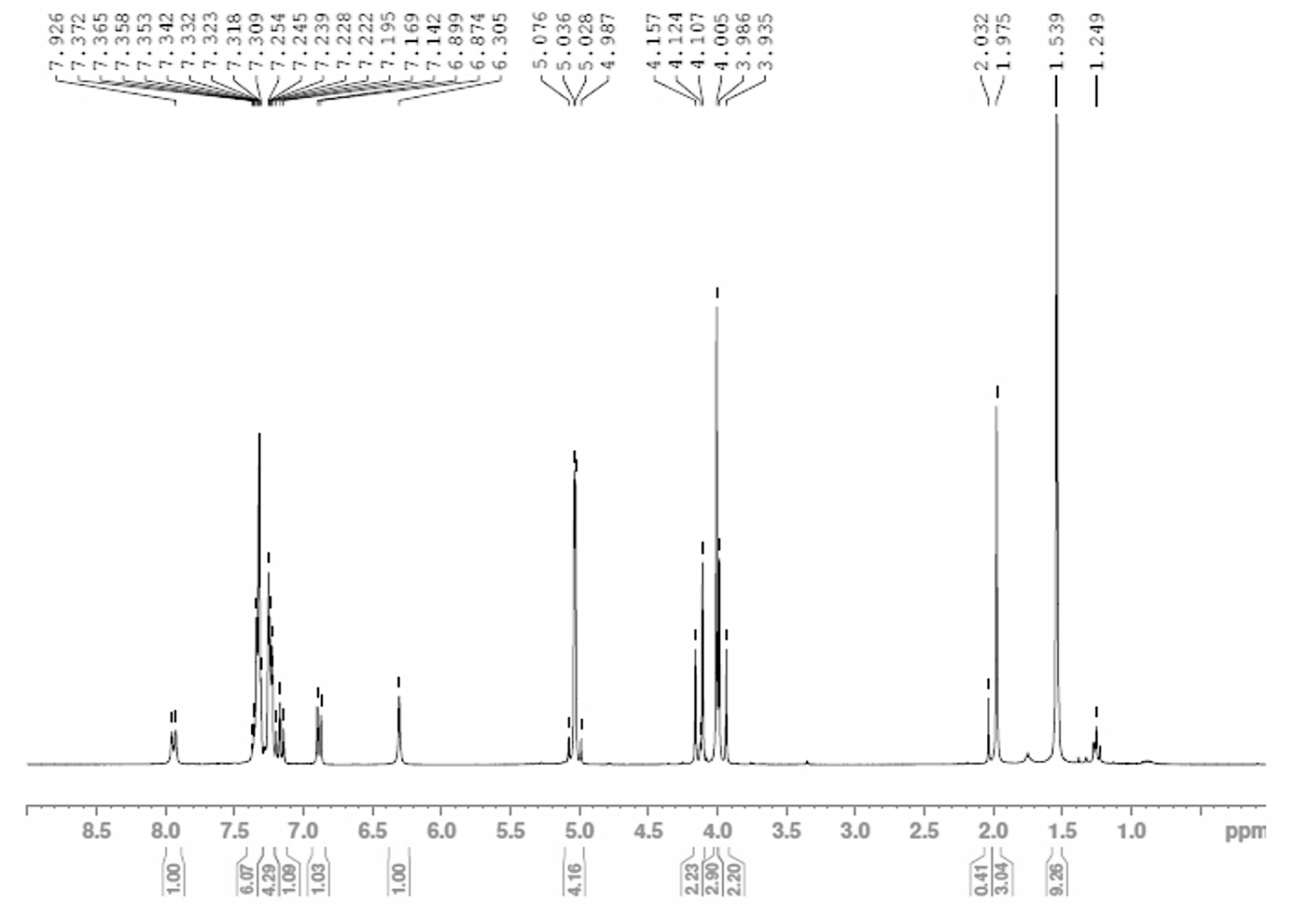
7.926
7.372
7.365
7.358
7.353
7.342
7.332
7.323
7.318
7.309
7.254
7.245
7.239
7.228
7.222
7.195
7.169
7.142
6.899
6.874
6.305
5.076
5.036
5.028
4.987
4.157
4.124
4.107
4.005
3.986
3.935
2.032
1.975
1.539
1.249
8.5
8.0
7.5
7.0
6.5
6.0
5.5
5.0
4.5
4.0
3.5
3.0
2.5
2.0
1.5
1.0
ppm
1.00
6.07
4.29
1.09
1.03
1.00
4.16
2.23
2.90
2.20
0.41
3.04
9.26

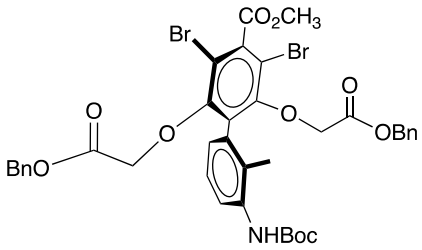
Br
CO_2CH_3
Br
O
O
O
O
OBn
BnO
NHBoc

35

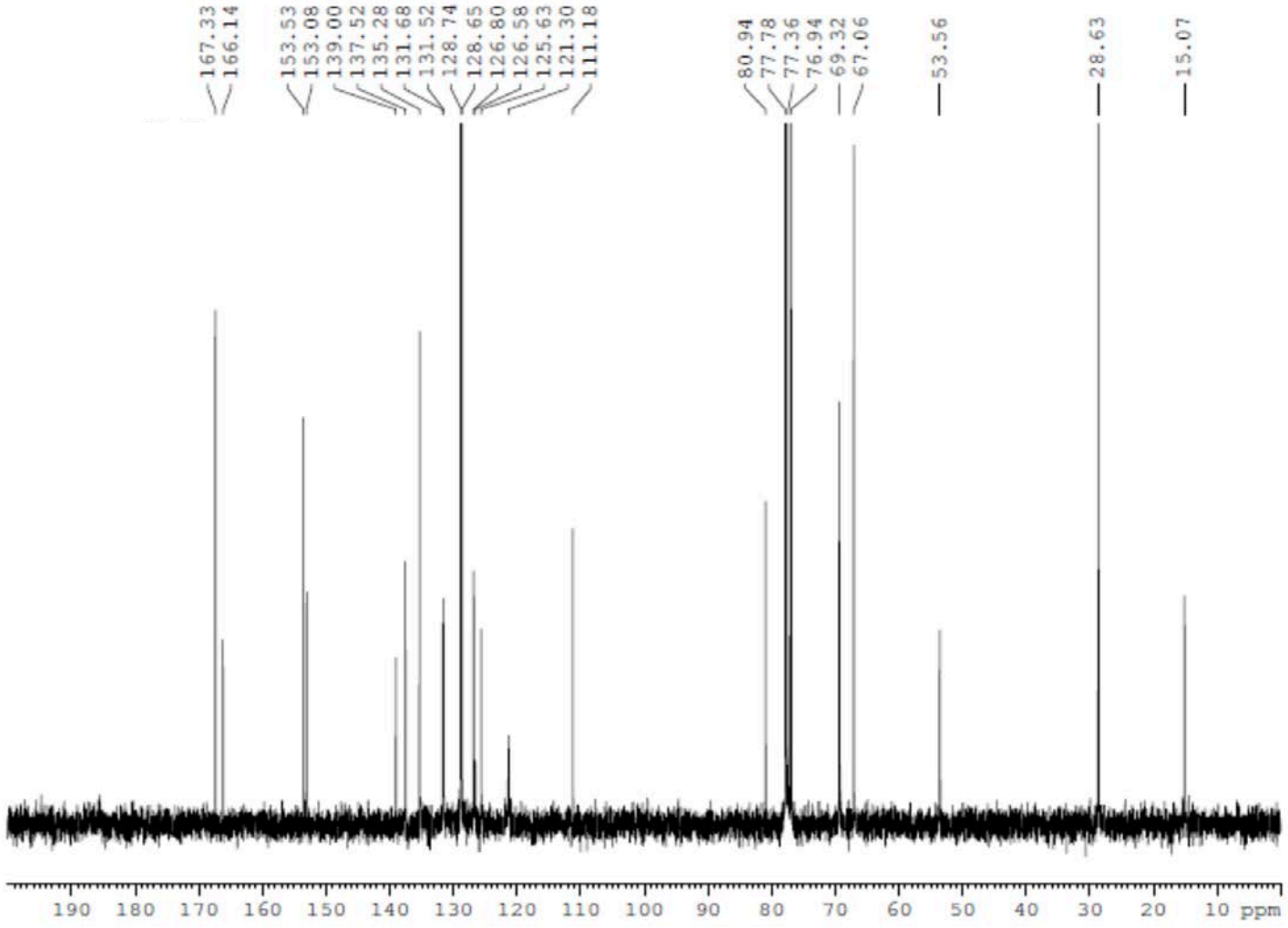
167.33
166.14
153.53
153.08
139.00
137.52
135.28
131.68
131.52
128.74
128.65
126.80
126.58
125.63
121.30
111.18
80.94
77.78
77.36
76.94
69.32
67.06
53.56
28.63
15.07
190 180 170 160 150 140 130 120 110 100 90 80 70 60 50 40 30 20 10 ppm

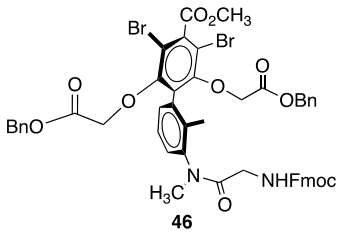
Br
CO2CH3
Br
O
O
OBn
BnO
O
O
N
H3C
O
NHFmoc

46

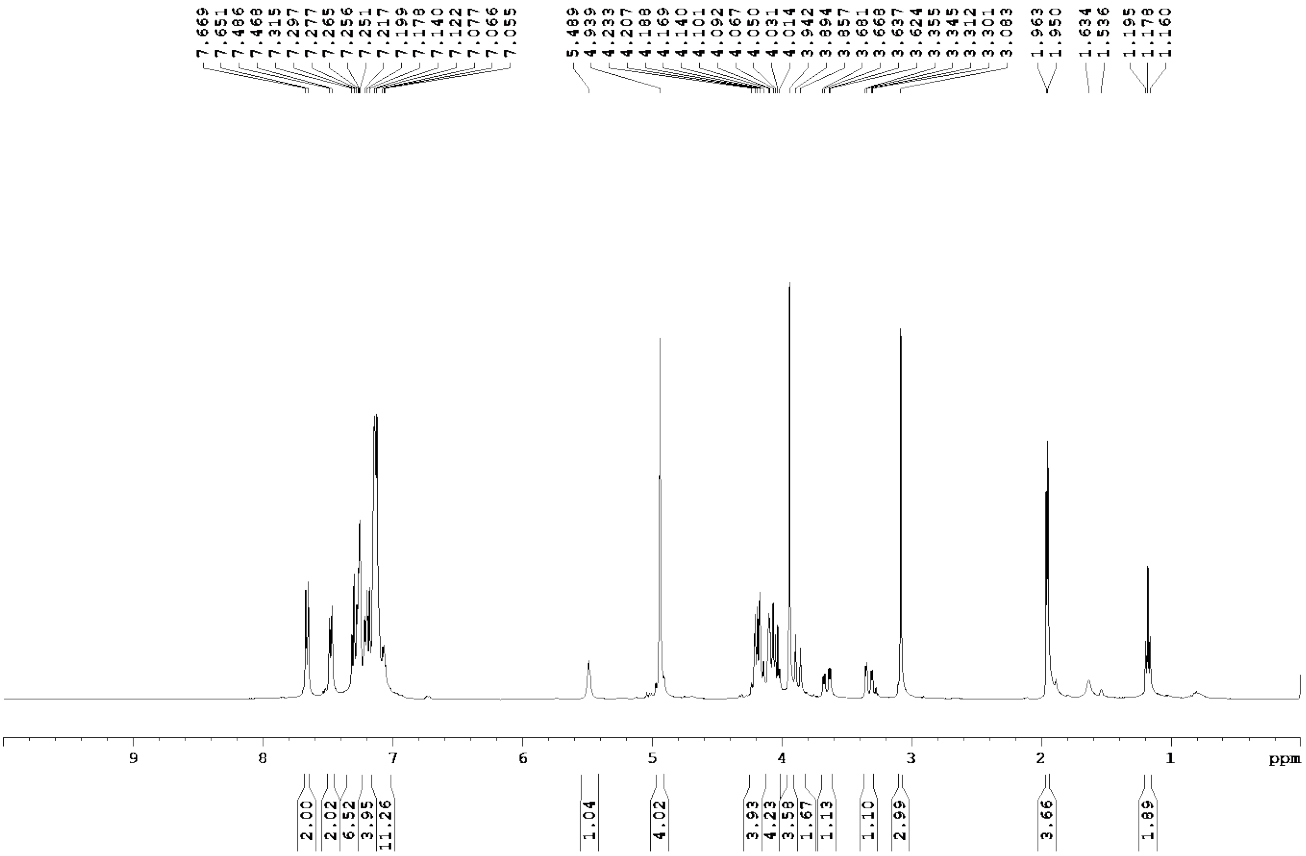
7.669
7.651
7.486
7.468
7.315
7.297
7.277
7.265
7.256
7.251
7.217
7.199
7.178
7.140
7.122
7.077
7.066
7.055
5.489
4.939
4.233
4.207
4.188
4.169
4.140
4.101
4.092
4.067
4.050
4.033
4.014
3.942
3.894
3.857
3.681
3.668
3.637
3.624
3.355
3.345
3.312
3.301
3.083
1.963
1.950
1.634
1.536
1.195
1.178
1.160
9
8
7
6
5
4
3
2
1
ppm
2.00
2.02
6.52
3.95
11.26
1.04
4.02
3.93
4.23
3.58
1.67
1.13
1.10
2.99
3.66
1.89

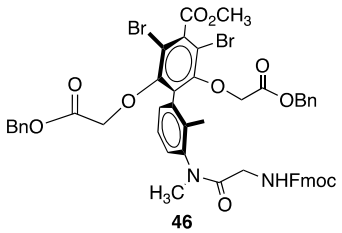
Br
CO2CH3
Br
O
O
OBn
BnO
O
O
N
H3C
O
NHFmoc

46

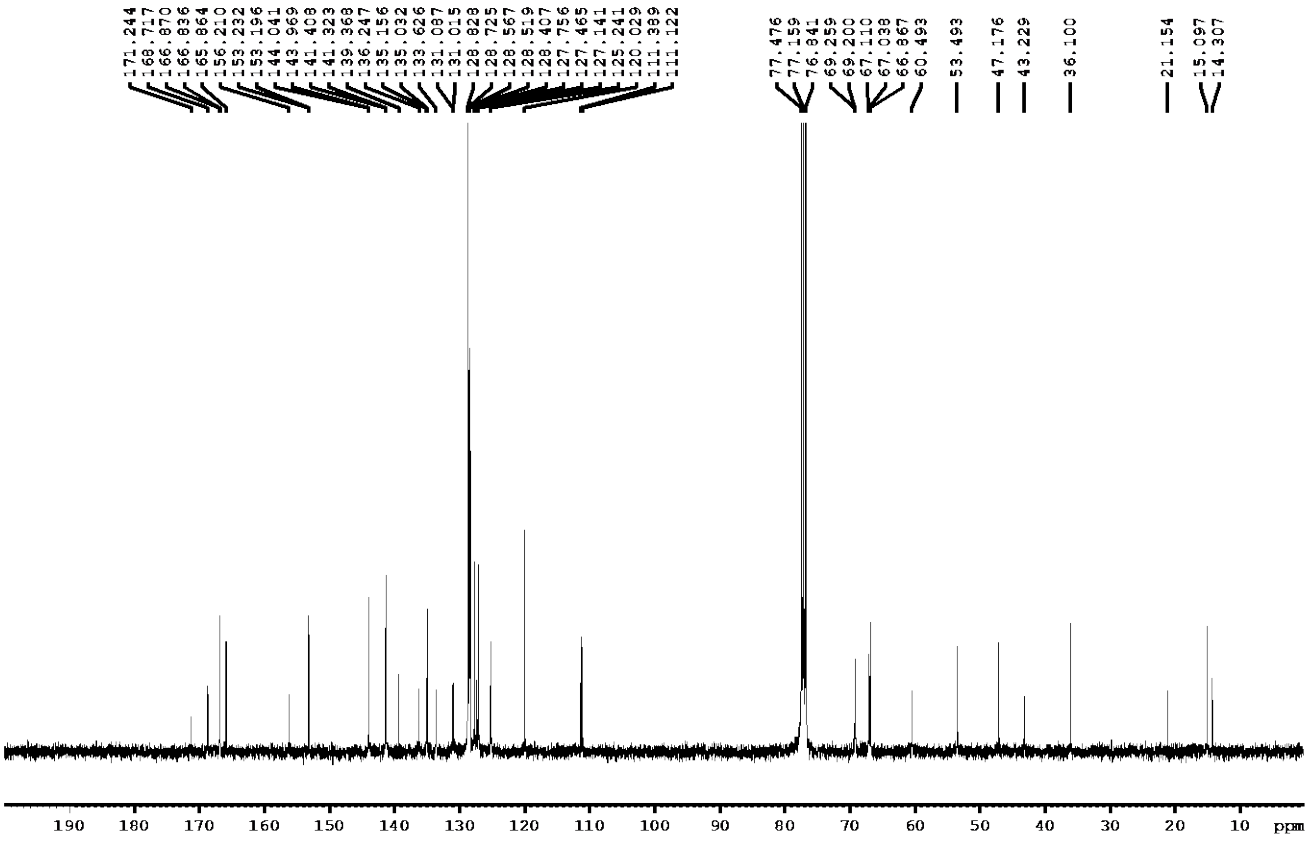
171.244
168.717
166.870
166.836
165.964
156.210
153.232
153.196
144.041
143.969
141.408
141.323
139.368
136.247
135.156
135.032
133.626
131.087
131.015
128.828
128.725
128.567
128.519
128.407
127.756
127.465
127.141
125.241
120.029
111.389
111.122
77.476
77.159
76.841
69.259
69.200
67.110
67.038
66.867
60.493
53.493
47.176
43.229
36.100
21.154
15.097
14.307
190
180
170
160
150
140
130
120
110
100
90
80
70
60
50
40
30
20
10
ppm

BIBLIOGRAPHY

1. (a) Tröger, J. *J. Prakt. Chem.* **1887**, *36*, 225–245; (b) Spielman, M.A. *J. Am. Chem. Soc.* **1935**, *57*, 583−585; (c) Wilcox, C.S.; Cowart, M.D. *Tetrahedron Lett.* **1986**, *27*, 5563−5566; (d) Cowart, M.D.; Sucholeiki, I.; Bukownik, R.R.; Wilcox, C.S. *J. Am. Chem. Soc.* **1988**, *110*, 6204−6210; (e) Wilcox, C.S. *Tetrahedron Lett.* **1985**, *26*, 5749−5752; (f) Paliwal, S.; Geib, S.; Wilcox, C.S. *J. Am. Chem. Soc.* **1994**, *116*, 4497–4498; (g) Kim, E.; Paliwal, S.; Geib, S.; Wilcox, C.S. *J. Am. Chem. Soc.* **1998**, *120*, 11192–11193.
2. (a) Hof, F.; Scofield, D.M.; Schweizer, W.B.; Diederich, F. *Angew. Chem., Int. Ed.* **2004**, *43*, 5056−5059; (b) Cornago, P.; Claramunt, R.M.; Bouissane, L.; Elguero, J. *Tetrahedron* **2008**, *64*, 3667−3673; (c) Cockroft, S.L.; Hunter, C.A. *Chem. Commun.* **2006**, *36*, 3806−3808; (d) Fischer, F. R.; Schweizer, W.B.; Diederich, F. *Chem. Commun.* **2008**, 4031−4033; (e) Fischer, F. R.; Schweizer, W.B.; Diederich, F. *Angew. Chem., Int. Ed.* **2007**, *46*, 8270−8273; (f) Fischer, F.R.; Wood, P.A.; Allen, F.H.; Diederich, F. *Proc. Natl. Acad. Sci. USA* **2008**, *105*, 3667−3673; (g) Nakamura, K.; Houk, K.N. *Org. Lett.* **1999**, *1*, 2049−2051; (h) Bhayana, B.; Wilcox, C.S. *Angew. Chem., Int. Ed.* **2007**, *46*, 6833–6836; (i) Gardarsson, H.; Schweizer, W.B.; Trapp, N.; Diederich, F. *Chem. Eur. J.* **2014**, *20*, 4608−4616.
3. (a) Carroll, W.R.; Pellechia, P.; Shimizu, K.D. *Org. Lett.* **2008**, *10*, 3547−3550; (b) Chong, Y.S.; Carroll, W.R.; Burns, W.G.; Smith, M.D.; Shimizu, K.D. *Chem. - Eur. J.* **2009**, *15*, 9117−9126; (c) Janesko, B.G.; Ams, M.R. *Theor. Chem. Acc.* **2014**, *133*, 1490−1499; (d) Hwang, J.; Li, P.; Carroll, W.R.; Smith, M.D.; Pellechia, P.J.; Shimizu, K.D. *J. Am. Chem. Soc.* **2014**, *136*, 14060−14067; (e) Hwang, J.; Dial, B. E.; Li, P.; Kozik, M.E.; Smith, M.D.; Shimizu, K.D. *Chem. Sci.* **2015**, *6*, 4358−4364; (f) Orentas, E.; Wallentin, C.J.; Bergquist, K.E.; Lund, M.; Butkus, E.; Warnmark, K. *Angew. Chem., Int. Ed.* **2011**, *50*, 2071−2074; (g) Ruńarsson, Ö.V.; Artacho, J.; Warnmark, K. *Eur. J. Org. Chem.* **2012**, 7015−7041.
4. (a) Kemp, D.S.; Li, Z.Q. *Tetrahedron Lett.* **1995**, *36*, 4175-4178; (b) Kemp, D. S.; Li, Z. Q. *Tetrahedron Lett.* **1995**, *36*, 4179–4180; (c) Alonso, E.; Lopez-Ortiz, F.; del Pozo, C.; Peralta, E.; Macias, A.; Gonzalez, J. *J. Org. Chem.* **2001**, *66*, 6333–6338.
5. (a) Espinosa, J.F.; Gellman, S.H. *Angew. Chem., Int. Ed.* **2000**, *39*, 2330–2333; (b) Newcomb, L.F.; Haque, T.S.; Gellman, S.H. *J. Am. Chem. Soc.* **1995**, *117*, 6509–6519; (c) Gardner, R. R.; Christianson, L.A.; Gellman, S.H. *J. Am. Chem. Soc.* **1997**, *119*, 5041–5042; (d) Gardner, R.R.; McKay, S.L.; Gellman, S.H. *Org. Lett.* **2000**, *2*, 2335–2338; (e) Gellman, S.H.; Dado, G. P.; Liang, G.B.; Adams, B.R. *J. Am. Chem. Soc.* **1991**, *113*, 1164–1173.
6. (a) Lam, K.S.; Khasanova, T.V.; Kemnitzer, W.E.; Maitra, S.; Hao, T.; Mee, H.T.; Liu, R.; Nowick, J.S. *J. Am. Chem. Soc.* **2002**, *124*, 4972–4973; (b) Chung, D.M.; Maitra, K.; Maitra, S.; Stigers, K.D.; Sun, Y.; Nowick, J.S. *J. Am. Chem. Soc.* **2000**, *122*, 7654–7661; (c) Brower, J.O.; Nowick, J.S. *J. Am. Chem. Soc.* **2003**, *125*, 876–877.
7. (a) Ardejani, M.S.; Powers, E.T.; Kelly, J.W. *Acc. Chem. Res.* **2017**, *50*, 1875–1882; (b) Nguyen, H.; Jager, M.; Kelly, J.W.; Gruebele, M. *J. Phys. Chem.* **2005**, *109*, 15182-15186; (c) Vagner, J.; Qu, H.; Hruby, V.J. *Curr. Opin. Chem. Biol.* **2008**, *12*, 292-296; (d) Guba, W.; Meyder, A.; Rarey, M.; Hert, J. *J. Chem. Inf. Model.* **2016**, *56*, 1-5.

8. (a) Phillips S.T.; Piersanti, G.; Bartlett, P.A. *Proc. Natl. Acad. Sci. USA* **2005**, *102*, 13737–13742; (b) Smith, C.K., Regan, L. *Acc. Chem. Res.* **1997**, *30*, 153–161; (c) Horne, W.S.; Boersma, M.D.; Windsor, M.A.; Gellman, S.H. *Angew. Chem., Int. Ed. 47*, 2853–2856; (d) Lengyel, G.A.; Horne, W.S. *J. Am. Chem. Soc.*, *134*, **2012**, 15906–15913; (e) Rana, S.; Kundu, B.; Durani, S. *Chem. Commun.* **2005**, 207–209; (f) Cooper, W.J.; Waters, M.L. *Org. Lett.* **2005**, *7*, 3825-3828.
9. Liberatore, M. A. Synthesis and NMR Studies of a *β*-Turn Mimetic Molecular Torsion Balance. Ph.D. Dissertation, University of Pittsburgh, Pittsburgh, PA, **2012**.
10. Shvo, Y.; Taylor, E.C.; Mislow, K.; Raban, M. *J. Am. Chem. Soc.* **1967**, *89*, 4910–4917.
11. (a) Theilacker, W.; Böhm, H. *Angew. Chem., Int. Ed.* **1967**, *6*, 251; (b) Mazzanti, A.; Lunazzi, L.; Minzoni, M.; Anderson, J.E. *J. Org. Chem.* **2006**, *71*, 5474–5481; (c) Kawano, N.; Okigawa, M.; Hasaka, N.; Kouno, I.; Kawahara, Y.; Fujita, Y. *J. Org. Chem.* **1981**, *46*, 389–392; (d) Hanford, W.E.; Adams, R. *Stereochemistry of Diphenyls*. **1935**, *57*, 1592–1595; (e) Meyer, W.L.; Meyer, R.B. *Communications to the Editor*, **1963**, *85*, 2170–2171; (f) Wolf, C.; Xu, H. *Tetrahedron Lett.* **2007**, *48*, 6886–6889; (g) Schurig, V.; Glausch, A.; Fluck, M. *Tetrahedron: Asymmetry* **1995**, *6*, 2161–2164; (h) Ceccacci, F.; Mancini, G.; Mencarelli, P.; Villani, C. *Tetrahedron: Asymmetry* **2003**, *14*, 3117–3122; (i) Grein, F. *J. Phys. Chem.* **2002**, *106*, 3823–3827; (j) Hall, D.M.; Harris, M.M. *J. Chem. Soc.* **1960**, 490–494; (k) Casarini, D.; Lunazzi, L.; Mancinelli, M.; Mazzanti, A.; Rosini, C. *J. Org. Chem.* **2007**, *72*, 7667–7676.
12. Petit, M.; Geib, S.J.; Curran, D.P. *Tetrahedron* **2004**, *60*, 7543–7552.
13. (a) Hruby, V.J. *Nat. Rev. Drug Disc.* **2002**, *1*, 847–851; (b) Kalyani., G.; Sharma, Vaishnav, Y.; Deshmukh, *V.I.J.P.R.D.* **2013**, *5*, 15–30.
14. (a) Driggers, E. M.; Hale, S. P.; Lee, J.; Terrett, N. K. *Nat. Rev. Drug Disc.* **2008**, *7*, 608–624; (b) White, C.J.; Yudin, A. K. *Nat. Chem.* **2011**, *3*, 509–524.
15. Ferrie, J.J.; Gruskos, J.J.; Goldwaser, M.E.; Guarracino, D.A. *Bioorg. Med. Chem. Lett.* **2013**, *23*, 989–995.
16. (a) LaPlante, S.R.; Bos, M.; Brochu, C.; Chabot, C.; Coulombe, R.; Gillard, J.R.; Jakalian, A.; Poirier, M.; Rancourt, J.; Stammers, T.; Thavonekham, B.; Beaulieu, P.L.; Kukolj, G.; Tsantrizos, Y.S. *J. Med. Chem*. **2014**, *57*, 1845–1854; (b) LaPlante, S.R.; Nar, H.; Lemke, C.T.; Jakalian, A.; Kawai, S.H. *J. Med. Chem.* **2014**, *57*, 1777.
17. Zheng, Y.; Tice, M.C.; Singh, S.B. *Bioorg. Med. Chem. Lett.* **2017**, *27*, 2825–2837.
18. Scott, D.E.; Bayly, A.R.; Abell, C.; Skidmore, J. *Nat. Rev. Drug. Discov.* **2016**, *15*, 533–550.
19. Hawkins, P.C.D. *J. Chem. Inf. Model.* **2017**, *57*, 1747–1756.
20. Czodrowski, P.; Mallinger, A.; Wienke, D.; Esdar, C.; Poschke, O.; Busch, M; Rohdich, F.; Eccles, S.A.; Ortiz-Ruiz, M.; Schneider, R.; Raynaud, F.I.; Clarke, P.A.; Musil, D.; Schwarz, D.; Dale, T.; Urbahns, K.; Blagg, J.; Schiemann, K. *J. Med. Chem.* **2016**, *59*, 9337–9349.
21. GroB, A.; Hashimoto, C.; Sticht, H.; Eichler, J. *Front. Bioeng. Biotechnol.* **2016**, *3*, 1–16.
22. Mahon, C.S.; Fulton, D.A. *Nat. Chem.* **2014**, *6*, 665–672.
23. Gopalakrishnan, R.; Frolov, A.I.; Knerr, L.; Drury, III, W.J.; Valuer, E. *J. Med. Chem.* **2016**, *59*, 9599–9621.
24. Dominelli-Whitely, N.; Brown, J.J.; Muchowska, K.B.; Mati, I.K.; Adam, C.; Hubbarb, T.A.; Elmi, A.; Brown, J.A.; Bell, I.A.W.; Cockroft, S.L. *Angew. Chem., Int. Ed.* **2017**, *129*, 7766–7770.
25. Srinivasula, S.M.; Hegde, R.; Saleh, A.; Datta, P.; Shiozaki, E.; Chai, J.; Lee, R.; Robbins, P.D.; Fernandes, T.; Shi, Y.; Alnemri, E.S. *Nature* **2001**, *410*, 112–116.

26. Cai, Q.; Sun, H.; Peng, Y.; Lu, J.; Nikolovska, Z.; McEachern, D.; Qiu, S.; Yang, C.; Miller, R.; Yi, H.; Zhang, T.; Sun, D.; Kang, S.; Guo, M.; Leopold, L.; Yang, D.; Wang, S. *J. Med. Chem. 54*, **2004**, 2714–2726.
27. Cossu, F.; Milani, M.; Mastrangelo, E.; Vachette, P.; Servida, F.; Lecis, D.; Canevari, G.; Domenico, D.; Drago, C.; Rizzo, V.; Manzoni, L; Seneci, P.; Scolastico, C.; Bolognesi, M. *Biochem. Biophys. Res. Commun.* **2009**, *378*, 162–167.
28. Monfardini, I.; Huang, J.W.; Beck, B.; Cellitti, J.F.; Pellecchia, M.; Domling, A. *J. Med. Chem.* **2011**, *54*, 890–900.
29. Huang, J.W.; Zhang, Z.; Wu, B.; Cellitti, J.F.; Zhang, X.; Dahl, R.; Shiau, C.; Welsh, K.; Emdadi, A.; Stebbins, J.L.; Reed, J.C.; Pellecchia, M. *J. Med. Chem.* **2008**, *51*, 7111–7118.
30. Sun, H.; Nikolovska-Coleska, Z.; Yang, C.; Xu, L.; Liu, M.; Tomita, Y.; Pan, H.; Yoshioka, Y.; Krajewski, K.; Roller., P.P.; Wang, S. *J. Am. Chem. Soc.* **2004**, *126*, 16686–16687.
31. Lotesta, S.D.; Marcus, A.P.; Zheng, Y. *Bioorg. Med. Chem.* **2016**, *24*, 1384–1391.
32. Wang, Y.; Wang, P.; Wang, Y.; Yang, G.; Zhang, A.; Miao, Z. *J. Med. Chem.* **2016**, *59*, 9575–9598.
33. van Marrewijk, L.M.; Polyak, S.W.; Hijnen, M.; Kuruvilla, D.; Chang, M.R.; Shin, Y.; Kamenecka, T.M.; Griffin, P.R.; Bruning, J.B. *ACS Chem. Biol.* **2016**, *11*, 273–283.
34. Olsson, R.I.; Xue, Y.; von Berg, S.; Aagaard, A.; McPheat, J.; Hansson, E.L.; Bernstrom, J.; Hansson, P.; Jirholt, J.; Grindebacke, H.; Leffler, A.; Chen, R.; Xiong, Y.; Ge, H.; Hansson, T.G.; Narjes, F. *ChemMedChem*, **2016**, *11*, 207–216.
35. (a) Medina, J.R.; Becker C.J.; Blackledge, C.W.; Duquenne, C.; Feng, Y.; Grant, S.W.; Heerding, D.; Li, W.H.; Miller, W.H.; Romeril, S.P.; Scherzer, D.; Shu, A.; Bobko, M.A.; Chadderton, A.R.; Dumble, M.; Gardiner, C.M.; Gilbert, S.; Liu, Q.; Rabindran, S.K.; Sudakin, V.; Xiang, H.; Brady, P.G.; Campobasso, N.; Ward, P.; Axten, J.M. *J. Med. Chem.* **2011**, *54*, 1871–1895; (b) Nishimura, N.; Norman, M.H.; Liu. L; Yang, K.C. Ashton, K.S.; Bartberger, M.D.; Chmait, S.; Chen, J.; Cupples, R.; Fotsch, C.; Helmering, J., Jordan, S.R.; Kunz, R.K; Pennington, LD, Poon, S.F.; Siegmund, A.; Sivits, G.; Lloyd, D.J.; Hale, C.; St. Jean, Jr. D.J. *J. Med. Chem*. **2014**, *57*, 3094–3116.
36. Angell, R.; Aston, N.M.; Bamborough, P.; Buckton, J.B. *Bioorg. Med. Chem.* **2008**, *18*, 4428–4432.
37. (a) Pennington, L.D.; Moustakas, D.T. *J. Med. Chem.* **2017**, *60*, 3552–3579; (b) Ellis, J.M.; Altman, M.D. Cash, B. *ACS Med. Chem. Lett.* **2016**, *7*, 1151–1155.
38. (a) Carpino, L.A.; Cohen, B.J.; Stephens Jr., K.E.; Sadat-Aalaee, S.Y.; Tien, J-H.; Langridge, D.C. *J. Org. Chem.* **1986**, *51*, 3732–3734; (b) Carpino, L.A.; Chao, H.G.; Beyermann, M.; Bienert, M. *J. Org. Chem.* **1991**, *56*, 2635–2642; (c) Beyermann, M.; Bienert, M.; Niedrich, H.; Carpino, L.A.; Sadat-Aalaee, D. *J. Org. Chem.* **1990**, *55*, 721–728.
39. Bo, Z.; Schafer, A.; Franke, P.; Schluter, A. D. *Org. Lett.* **2000**, *2*, 1645–1648.
40. Vutukuri, D.R.; Basu, S.; Thayumanavan, S. *J. Am. Chem. Soc.* **2004**, *126*, 15636–15637.
41. Barder, T.E.; Walker, S.D.; Martinelli, J.R.; Buchwald, S. L. *J. Am. Chem. Soc.* **2005**, *127*, 4685–4696.
42. (a) Ishiyama, T.; Murata, M.; Miyaura, N. *J. Org. Chem.* **1995**, *60*, 7508–7510; (b) CGI Pharmaceuticals, Inc. Patent WO2008/33858, **2008**.
43. (a) Hashem, A.I.; Shaban, M.E.; El-Kafrawy, A.F. *J. Chem. Soc. Pak.* **1983**, *5*, 19–21; (b) Bloomer, J.L.; Zheng, W. *Syn. Comm.* **1998**, *28*, 2087–2095; (c) Anbar, M.; Dostrovsky, I.; Samuel, D.; Yoffe, A.D. *J. Chem. Soc.* **1954**, 3603–3611.

44. (a) Fillion, E.; Fishlock, D. *J. Am. Chem. Soc*. **2005**, *127*, 13144–13145; (b) Denmark, S. E. *Tetrahedron* **2010**, *66*, 4745–59.
45. (a) Lee, K.S.; Kim, K.D.; *Bull. Korean Chem. Soc*. **2010**, 3842–3843; (b) Boovanahalli, S.K.; Kim, D.W.; Chi, D.Y. *J. Org. Chem.* **2004**, *69*, 3340–3344; (c) Hammond, G.S.; Wu, C.S. *J. Am. Chem. Soc.* **1973**, *95*, 8215–8222.
46. (a) Kuehne, M.E.; Pitner, J.B. *J. Org. Chem.* **1989**, *54*, 4553–4569; (b) Ranu, B.C.; Bhar, S. *S. Org. Prep. Proced. Int.* **1996**, *28*, 371–409; (c) Kaboudin, B.; Abedi, Y. *Synthesis* **2009**, *12*, 2025–2028; (d) Morita, T.; Okamoto, Y.; Sakurai, H. *J. Chem. Soc., Chem. Comm.* **1978**, 874–875; (e) McOmie, J.F.W.; Watts, M.L.; West, D.E. *Tetrahedron* **1968**, *24*, 2289–2292.
47. (a) Kaiser, F.; Schmalz, H. *Tetrahedron* **2003**, *59*, 7345–7355; (b) Ganieva, E.S.; Ganiev, I.M.; Grabovskii, S.A.; Kabal'nova, N.N. *Russ. Chem. Bull., Int. Ed.* **2008**, *57*, 2332–2334.
48. (a) Day, J.D.; McFadden, R.M.; Virgil, S.; Kolding, H.; Alleva, J.L.; Stolz, B. *Ang. Chem., Int. Ed.* **2011**, *50*, 6814–6818; (b) Shiohara, H.; Nakamura, T.; Kikuchi, N.; Ozawa, T.; Nagano, R.; Matsuzawa, A.; Ohnota, H.; Miyamoto, T.; Ichikawa, K.; Hashizume, K. *Bioorg. Med. Chem*. **2012**, *20*, 3622–3634; (c) William, A.D.; Lee, A.C.-H.; Goh, K.C.; Blanchard, S.; Poulsen, A.; Nagaraj, H.; Lee, C.P.; Wang, H.; Williams, M.; Sun, E.T.; Hu, C.; Jayaraman, R.; Pasha, M.K.; Ethirajulu, K.; Wood, J.M.; Dymock, B.W. *J. Med. Chem.* **2012**, *55*, 169–196; (d) Simon, L.; Muniz, F.M.; Saez, S.; Raposo, C.; Sanz, F.; Moran, J.R.; *Hel. Chim. Acta*. **2005**, *88*, 1682–1701; (e) Li, Y.; Silamkoti, A.; Kolavi, G.; Mou, L.; Gulati, S.; Air, G.M.; Brouilette, W.J. *Bioorg. Med. Chem*. **2012**, *20*, 4582–4589; (f) Sharma, U.; Verma, P.K.; Kumar, N.; Kumar, V.; Bala, M.; Singh, B. *Chem. Eur. J*. **2011**, *17*, 5903–5907; (g) Gowda, D., Maheseh, B.; Shankare, G. *Ind. Sect. J. Chem*. **2001**, *40*, 75–77.
49. (a) Le Pera, A. Leggio, A.; Ligouri, A. *Tetrahedron* **2006**, *62*, 6100–6106; (b) Prechter, A.; Heinrich, M.R. *Synthesis* **2011**, *10*, 1515–1525.
50. (a) Di Gioia, M.L.; Leggio, A.; Le Pera, A.; Liguori, A.; Napoli, A.; Siciliano, C.; Sindona, G. *J. Org. Chem*. **2003**, *68*, 7416–7421; (b) De Marco, R.; Di Gioia, M.L.; Ligouri, A.; Perri, F.; Siciliano, C.; Spinella, M. *Tetrahedron* **2011**, *67*, 9708–9714.
51. Golding, B.T.; Bleasdale, C.; McGinnis, J.; Muller, S.; Rees, H.T.; Rees, N.H.; Farmer, P.B.; Watson, W.P. *Tetrahedron* **1997**, *53*. 4063–4082.
52. (a) Katritzky, A.R.; Akutagaw, K. *Org. Prep. Proc. Int.* **1989**, *21*, 340–341; (b) Katrizky, A.R.; Rachwal, S.; Rachwal, B. *J. Chem. Soc. Perkin Trans.* **1987**, *1*, 781–809.
53. Katritzky, A.R.; Wu, J.; Wrobel, L.; Rachwal, S.; Steele, P.J. *Acta Chemica Scandinavica* **1993**, *47*, 167–175.
54. (a) Moraczewski, A. L.; Banaszynski, L. A.; From, A. M.; White, C. E.; Smith, B. D. *J. Org. Chem.* **1998**, *63*, 7258–7262; (b) Smith, B. D.; Goodenough-Lashua, D. M.; D'Souza, C. J. E.; Norton, K. J.; Schmidt, L. M.; Tung, J. C., *Tetrahedron Lett.* **2004**, *45*, 2747–2749; (c) Deetz, M. J.; Forbes, C. C.; Jonas, M.; Malerich, J. P.; Smith, B. D.; Wiest, O., *J. Org. Chem.* **2002**, *67*, 3949–3952.